AD NUMBER

AD820556

NEW LIMITATION CHANGE

TO

Approved for public release, distribution unlimited

FROM

Distribution authorized to U.S. Gov't. agencies and their contractors; Administrative/Operational Use; Sep 1967. Other requests shall be referred to Air Force Weapons Lab., Attn: WLDN, Kirtland AFB, NM 87117.

AUTHORITY

AFWL Notice

A COMPUTER-AUTOMATED ITERATIVE METHOD FOR NEUTRON FLUX SPECTRA DETERMINATION BY FOIL ACTIVATION

Volume I

A Study of the Iterative Method

W. N. McElroy S. Berg T. Crockett

R. G. Hawkins
Lt USAF

Atomics International
A Division of North American Aviation, Inc.
Canoga Park, California 91304

Contracts AF 29(601)-7196 and AF 29(601)-6780

TECHNICAL REPORT NO. AFWL-TR-67-41, Vol I

September 1967

AIR FORCE WEAPONS LABORATORY
Research and Technology Division
Air Force Systems Command
Kirtland Air Force Base
New Mexico

Research and Technology Division
AIR FORCE WEAPONS LABORATORY
Air Force Systems Command
Kirtland Air Force Base
New Mexico

A COMPUTER-AUTOMATED ITERATIVE METHOD FOR NEUTRON FLUX SPECTRA DETERMINATION BY FOIL ACTIVATION

Volume I

A Study of the Iterative Method

W. N. McElroy S. Berg T. Crockett

R. G. Hawkins
Lt USAF

Atomics International
A Division of North American Aviation, Inc.
Canoga Park, California 91304
Contracts AF 29(601)-7196 and AF 29(601)-6780

TECHNICAL REPORT NO. AFWL-TR-67-41, Vol I

FOREWORD

This report was prepared by Atomics International, Canoga Park, California, under Contracts AF 29(601)-7196 and AF 29(601)-6780. The research was performed under Program Element 6.24.05.21.4, Project 1831, Task 183108, and Program Element 7.60.08.01.D, Project 5710, Subtask 06.514, and was funded by the Air Force and the Defense Atomic Support Agency (DASA).

Portions of the experimental work involving reactor tests were accomplished under reactor physics and fuel cladding programs which were funded by the Atomic Energy Commission.

Inclusive dates of research were April 1966 to July 1967. The report was submitted 18 August 1967 by the Air Force Weapons Laboratory Project Officer, Lt Gerald P. McCarthy (WLDN). Other Project Officers for the Laboratory were Captain J. K. Morrow and Lt R. G. Hawkins (WLDN).

Results are presented which are based on interlaboratory cooperative studies. The free exchange of unpublished results and information and the assistance of R. E. Dahl, J. Ulseth, A. dePino, and J. Jackson of Battelle Northwest; J. Walker, C. Mehl, and L. Morrison of Sandia Corporation; R. Armani of Argonne National Laboratory; E. Tochilin of US Naval Radiological Defense Laboratory; W. Biggers, G. Hansen, and J. Grundl of Los Alamos Scientific Laboratory; R. Barral of Stanford University; and C. Weber, H. Morewitz, F. Fillmore, C. Bingham, S. Carpenter, H. Alter, L. Beller, and R. Tuttle of Atomics International are gratefully acknowledged. Atomics International personnel who directly assisted in this work are G. Gigas and N. M. Ewbank.

This report has been prepared in four volumes. The titles of the other three volumes are: Volume II; SAND II (Spectrum Analysis by Neutron Detectors II) and Associated Codes; Volume III, Reference Cross Section Library for SAND II; Volume IV, Reference Spectrum Library for SAND II.

This work was performed under Atomics International account numbers SO 2239 and SO 2201 and was assigned Atomics International report number AI-67-90, Volume I.

This technical report has been reviewed and is approved.

Gerald P. McCarthy
GERALD P. MCCARTHY
Lt, USAF
Project Officer

James K. Morrow
J. K. MORROW
Captain, USAF
Senior Project Engineer

Kenneth R. Hawks
CARL J. SCHRA
Major, USAF
Chief, Nuclear Power Branch

George C. Darby, Jr.
GEORGE C. DARBY, JR.
Colonel, USAF
Chief, Development Division

ABSTRACT

(Distribution Limitation Statement No. 2)

A multiple foil activation iterative method has been developed to determine neutron flux spectra. A computer code (SAND II) has been written which provides a "best fit" neutron differential flux spectrum for a given input set of infinitely dilute foil activities. The results of experimental and analytical studies for a wide variety of neutron environments strongly suggest that, in addition to determining neutron flux spectra, the multiple foil activation iterative method can be helpful in (1) the validation and improvement of calculational techniques used to predict neutron flux spectra, (2) upgrading of confidence in neutron spectrometer measurements, (3) determining the reliability of foil activity measurement methods, (4) assessing material scattering/absorption effects, and (5) examining current foil detector cross section evaluations to provide guidance for re-evaluation for these data, and eventual "unfolding" of the absolute differential form of cross sections for any foil reactions producing a detectable product.

CONTENTS

Contents (Continued)

LIST OF FIGURES

List of Figures (Continued)

LIST OF TABLES

List of Tables (Continued)

SECTION I

INTRODUCTION

The authors have previously reported an iterative perturbation method for determining neutron flux spectra by multiple foil activation (Refs. 1, 2, 3). This method required certain subjective decisions on the part of the user to generate each perturbation. A computer code SAND II* has since been developed to determine spectra by a fully automated iterative method, described in Section III. Greer and Walker (Ref. 4) have studied this same problem from a somewhat different point of view and have developed a code (SPECTRA) which gives integral results comparable to those of SAND II. Both of these methods have been subjected to extensive analytical and experimental testing, the results of which (for the SAND II code) are discussed in Sections IV and V. Both the immediate and long-range implications of this work for problems related to neutron spectral definition are considered in Section II.

The SAND II code provides a "best fit" neutron flux spectrum for a given input set of infinitely dilute† foil§ activities. The calculational procedure consists of the selection of a known flux spectrum form to serve as the initial approximation to the solution, and subsequent iteration to a form acceptable as an appropriate solution. The solution is specified either as time-integrated flux (fluence) for a pulsed environment or as flux for a steady-state type neutron environment.

The results of the analytical and experimental studies presented in Sections IV and V indicate that the multiple foil iterative method of neutron flux spectral determination can be expected to give integral neutron flux results over the energy range from 10^{-10} Mev to 18 Mev that are accurate to within ±10% to 30% at all energies, if the errors in the foil reaction cross sections and measured activities are within similar limits. (The problem of errors is

*Spectrum Analysis by Neutron Detectors II.

†Infinitely dilute means that the density of target nuclei is small enough to preclude self-absorption and scattering effects.

§The word "foils" as used in this report is meant to include all physical forms in which target nuclei of any particular element are irradiated, foils, pellets, wires, powder, etc.

given consideration throughout this Volume, and particularly in Section VI.) Differential flux spectra are also obtained which reflect true structure as well as fluctuations resulting from experimental errors. The method is such that the use of a large number of foils with overlapping energy regions of sensitivity, and subsequent examination of the solution differential spectral structure, can be used to distinguish the true structure from that which may be caused by cross section errors, activity errors, and absorption effects.

SECTION II

FLUX SPECTRAL DEFINITION

A. Review and Objectives

Radioactivation techniques are in common use for measuring neutron flux. If the neutron spectrum can be well represented as a fission spectrum, straightforward procedures are available for the interpretation of the experimental data (Ref. 5). If the form of the neutron spectrum is not known, or known only approximately, the problem of interpretation is more difficult and at present is the subject of considerable review and investigation (Refs. 6, 7).

For fast neutron flux spectra (i.e., $E > 0.1$ Mev), methods that involve the use of a set of materials with different neutron energy sensitivity limits have been proposed and studied quite extensively (Refs. 6, 8, 9, 10, 11, 12). Difficulties in interpreting the experimental data arise, however, caused by the propagation of experimental errors in the system of activation integral equations. These errors, associated with uncertainties in available cross section data and in the measured values of saturated activities, place limitations on the mathematical techniques that can successfully be used to determine neutron spectra from the foil activation data. (In the present work, realistic limits have been assigned to these errors both for the experimental and analytical studies.)

The current state of technology of neutron flux spectral definition includes problems in several areas, affecting both calculational and experimental techniques. These areas are

1. Reaction Cross Sections

Current cross section evaluations for neutron interactions used in spectral calculations and measurements by both spectrometers and the foil activation technique contain uncertainties and inaccuracies in both absolute magnitude and differential form.

2. Activity Measurements

Measurements of foil activities are hampered by incomplete knowledge of decay schemes, interfering impurities, uncertainties in half-life, nonavailability of standards for short half-life products, etc.

3. Absorption Effects

Absorption effects may be manifest as apparent errors in activities for the foil technique and as a decrease in energy resolution for spectrometers.

4. Spectrometry

Accuracy of spectrometer measurements is affected by such factors as uncertainties in cross section (such as He^3), sensitivity of electronics, calibration of efficiency, and sensitivity to secondary radiation, such as gamma rays in a neutron environment.

5. Calculation

There is a need to prove the validity of calculational techniques for neutron environments, in general, over the whole neutron energy range. The iterative foil activation method is uniquely suited to the problem of the validation of analytical methods that have been developed for the characterization of neutron flux spectra, by allowing a direct comparison with experiment (see Section V). Such validation is necessary to give confidence in the analytical calculations that will be required for locations in which the placement of foils or spectrometers is not possible or practicable, due to such considerations as high temperature, accessibility, or space limitation.

The authors strongly believe that through a marriage of the results of foil activation measurements, spectrometry and calculational techniques, significant progress can be made in resolving some of the current problems in the definition of neutron environments and subsequent studies of neutron material damage effects.

The immediate objectives of the present work relating to neutron spectral definition have been (1) to develop a computer code (SAND II) for determination of neutron flux spectra from foil activity measurements by iterative solution of a set of activity integral equations, (2) to increase knowledge of neutron flux spectral forms for a wide range of neutron environments, (3) to examine current cross section data evaluations for foil reactions used in neutron spectral determination and to provide guidance for re-evaluation for these data, (4) to determine the reliability of current foil activity measurement methods, and (5) to establish direction for future application of the foil activation technique.

Long-range objectives, toward which this program has been the first step, include the improvement of neutron flux spectral dosimetry by foil activation, upgrading of confidence in neutron spectrometer measurements, validation and improvement of calculational techniques for flux spectra, and "unfolding" of the absolute differential form of cross sections for any foil reactions producing a detectable product.

B. Foil Activation Equations

The foil method of neutron spectral measurement depends upon neutron activation of a set of foils and the subsequent determination of the radioactive decay rates (activities) of the foils. A general mathematical representation of this process must consider the differential flux as a function of both energy and time [$\varphi(E,t)$].

Let "n" be the number of neutron reaction product atoms present in a given target foil material at any time t, and "m" be the number of target atoms. The net time-rate of production of reaction product atoms is

$$\frac{dn}{dt} = m\bar{\sigma}_{mn}(t)\,\Phi(t) - n\bar{\sigma}_{n}(t)\,\Phi(t) - n\lambda_{n} \qquad (1)$$

where λ_n is the radioactive decay constant of the neutron reaction product, $\bar{\sigma}_{mn}(t)$ is the spectrum-averaged cross section for the reaction producing the "n" atoms, $\bar{\sigma}_{n}(t)$ is the total spectrum-averaged cross section for all neutron reactions that remove any of the "n" atoms and $\Phi(t)$ (often called "integral flux") is the time-differential flux defined by the equation

$$\Phi(t) \equiv \int_o^\infty \varphi(E, t)\, dE, \quad (n/cm^2\text{-sec}) \tag{2}$$

The time-rate of change of target atoms (burn-up) is

$$\frac{dm}{dt} = -m\bar{\sigma}_m(t)\, \Phi(t) \tag{3}$$

where $\bar{\sigma}_m(t)$ is the total spectrum-averaged cross section for all neutron reactions that remove any of the "m" atoms. Equation (3) has the solution

$$m = m_o\, e^{-\int_o^t \bar{\sigma}_m(t')\, \Phi(t')\, dt'} \tag{4}$$

The integration constant m_o is the initial number of target atoms or the number of target atoms at time t = 0.

In Eqs. (1), (3), and (4), the spectrum-averaged cross sections are defined by equations of the form

$$\bar{\sigma}_x(t) \equiv \frac{\int_o^\infty \sigma_x(E)\, \varphi(E, t)\, dE}{\Phi(t)} \quad , x = n,\ mn,\ \ldots \tag{5}$$

where $\sigma_x(E)$ is the energy-dependent cross section.

Combination of Eqs. (1) and (4) gives

$$\frac{dn}{dt} = m_o \bar{\sigma}_{mn}(t)\, \Phi(t)\, e^{-\int_o^t \bar{\sigma}_m(t')\, \Phi(t')\, dt'} - n\left[\lambda_n + \bar{\sigma}_n(t)\, \Phi(t)\right] \tag{6}$$

Equation (6) is an ordinary first order first degree linear differential equation which has the solution

$$n = m_o e^{\left[-\lambda_n t - \int_o^t \bar{\sigma}_n(t')\,dt'\right]} \int_o^t \bar{\sigma}_{mn}(t')\,\Phi(t') \cdot$$

$$e^{\left\{\lambda_n t' + \int_o^{t'} \left[\bar{\sigma}_n(t'') - \bar{\sigma}_m(t'')\right] dt''\right\}} dt' \qquad (7)$$

Under the restriction that there is no significant burn-up of the target or product atoms (that is, both $\bar{\sigma}_n(t)\,\Phi(t)$ and $\bar{\sigma}_m(t)\,\Phi(t) \ll \lambda_n$), Eq. (7) reduces to

$$n = m_o e^{-\lambda_n t} \int_o^t \bar{\sigma}_{mn}(t')\,\Phi(t')\,e^{\lambda_n t'}\,dt' \qquad (8)$$

Two different extremes in the flux time-behavior require consideration: (1) steady-state, and (2) pulsed. In the steady-state case,

$$\Phi(t) = \Phi \qquad (9)$$

and

$$\bar{\sigma}_{mn}(t) = \bar{\sigma}_{mn} \qquad (10)$$

That is, both flux and spectrum-averaged cross section are constant with time [see Eq. (5)]. Therefore, Eq. (8) may be rewritten as follows:

$$n = m_o \bar{\sigma}_{mn}\,\Phi\,e^{-\lambda_n t} \int_o^t e^{\lambda_n t'}\,dt' \qquad (11)$$

which, upon integration, gives

$$n = \frac{m_o \bar{\sigma}_{mn}}{\lambda_n}\,\Phi\left(1 - e^{-\lambda_n t}\right) \qquad (12)$$

The radioactive decay rate, or activity, of the product material at time t is given by

$$a(t) = \lambda_n n = m_o \bar{\sigma}_{mn} \Phi \left(1 - e^{-\lambda_n t}\right) \tag{13}$$

The saturated activity A (the activity for an infinitely long irradiation) may be expressed by rewriting Eq. (13) as follows:

$$A = \frac{a(t)}{\left(1 - e^{-\lambda_n t}\right)} = m_o \bar{\sigma}_{mn} \Phi \tag{14}$$

Equations (5), (9), (10), and (14) may be combined to give

$$A = m_o \int_o^\infty \sigma_{mn}(E)\, \varphi(E)\, dE \tag{15}$$

where

$$\varphi(E) = \varphi(E, t) \tag{16}$$

since flux is constant with time.

If a set of Eq. (15) is obtained by irradiation of several foils with different reaction energy responses, a matrix is provided from which $\varphi(E)$ may be determined. The solution of this matrix is considered in Section III.

In the case of a pulsed environment, the time behavior of $\Phi(t)$ is in general not constant, and may not be measurable. Equations (9) and (10) do not apply, therefore, and Eq. (8) cannot be simplified to Eq. (11). For a pulse, however, $\lambda_n t \ll 1$. Therefore, both exponential terms in Eq. (8) may be approximated by unity, and Eq. (8) reduces to

$$n = m_o \int_o^t \bar{\sigma}_{mn}(t')\, \Phi(t')\, dt' \tag{17}$$

Activity is given by

$$a(t) = \lambda_n n = \lambda_n m_o \int_o^t \overline{\sigma}_{mn}(t') \, \Phi(t') \, dt' \qquad (18)$$

where, as before, a(t) is the activity measured at time t (in this case at the end of the neutron burst or pulse). Equations (5) and (18) may be combined and re-written as follows:

$$a(t) = \lambda_n m_o \int_o^\infty \sigma_{mn}(E) \int_o^t \varphi(E, t') \, dt' \, dE \qquad (19)$$

Comparison of Eq. (19) for the pulsed case with Eq. (15) for the steady-state case shows that the same numerical procedure can be used to treat both cases. In the steady-state case, saturated activities are calculated from a differential flux; in the pulsed case, end-of-burst activities are calculated from a differential fluence. (For the pulsed case there is no requirement that $\varphi(E, t)$ be separable.)

The SAND II code has the option of obtaining a spectral solution as differential flux for the steady-state case, or as differential fluence for the pulsed case (see Vol. II, Section II-A-2). Except for the multiplication of the calculated integral by the decay constant for the pulsed case [see Eq. (19)], and the extrapolation to saturated input activities for the steady-state case, the problems of obtaining $\int_0^t \varphi(E, t') \, dt'$ and $\varphi(E)$ respectively, are the same.

The discussion of the SAND II iterative method in Section III is based on the equations for the steady-state case.

SECTION III
SAND II ITERATIVE METHOD

A. General Description

The SAND II code is designed to provide a "best fit" neutron flux spectrum for a given input set of infinitely dilute foil activities. As explained in Section II-B, the input activities are extrapolated to saturation in the case of a steady-state environment, i.e., reactors, and are actual time-of-removal activities in

the case of a pulsed environment; the solution spectrum is differential flux in the steady-state case and differential fluence in the pulsed case.

The code uses a discrete interval description of the neutron energy range, rather than a continuous representation by analytical functions; the energy range between 10^{-10} and 18 Mev is represented in 620 intervals (45 per decade up to 1 Mev, and 170 between 1 and 18 Mev). The solution spectrum is thus presented in tabular form at 621 points. The problem is essentially to solve for 621 unknowns (solution differential flux values) in a system of n linear activity equations, where n is the number of foils used.

The calculational procedure consists of selection of an initial approximation spectral form and iteration from that approximation to a form acceptable as an appropriate solution. The solution is, of course, not unique, since the number of equations is much smaller than the number of unknowns ($n \ll 621$); appropriateness of the solution therefore depends on a suitable choice of the initial approximation, based on all available physical information in any given case. A mathematical statement of the problem and method of solution is presented in Section III-B. Briefly, the iterative procedure consists of the following steps:

1. Activities are calculated, for each foil used, based on the current iterative spectrum and the evaluated reaction cross section library which is part of the code. (See Volume II for additional information, and Volume III for graphical and tabular presentations of the evaluated cross sections as a function of energy for the 29 foil reactions in current use.)
2. These calculated activities are compared with the measured activities to provide a correction factor for each foil.
3. A weighting function (of energy) is obtained, for each foil, based on the sensitivity function (differential cross section multiplied by differential flux) for that foil calculated at the current iteration.
4. The foil weighting functions are applied to an averaging procedure, to obtain an average correction factor at each energy, based on the comparison of measured to calculated activity for each foil and on the relative contribution of the flux at the given energy to the activity of that foil.

5. The average correction factors are then applied to the current iterative flux value at each energy, to obtain the next iterative flux spectrum.

The criterion currently incorporated into the code for achievement of an acceptable solution is based on a comparison of successive iterative differential flux values; a solution is considered to have been achieved when the difference between two successive values is smaller than a specified (as input) percent at all 621 energy points. (See Section IV-B-2.)

SAND II includes the option of selecting an initial approximation spectral form from among a library of reference forms, by searching for the spectrum for which the set of calculated activities for the foils used is most nearly consistent with the input (measured) activities. Since no physical information is incorporated into this selection method, it is emphasized that the reference spectrum library is meant to be available for use only as a last resort, in cases for which so little information is available that no meaningful selection of an initial approximation can be made on the basis of physical knowledge of the measured environment. The reference spectrum library is also an important convenience in certain analytical studies aimed at understanding the solution behavior of the iterative method, in calculating spectrum-averaged cross sections, and in calculating anticipated activities and foil energy sensitivity limits for planned irradiations. (See Volume II for additional information, and Volume IV for graphical and tabular presentations of differential flux for the 59 reference spectra in current use.)

B. Mathematical Representation

The mathematical procedure for the present method involves iterative spectral perturbation to obtain a "best fit" solution for a system of simultaneous activation integral equations obtained from Eq. (15) with certain notational additions and modifications, defined as follows:

A_i ≡ measured activity for the i^{th} foil reaction (extrapolated to saturation and infinite dilution);

$A_i^{[k]}$ ≡ calculated activity for the i^{th} foil reaction, based on the k^{th} iterative spectrum;

$\varphi^{[k]}(E)$ ≡ k^{th} iterative differential flux;

E_j = energy of the j^{th} energy point;

$\Phi_j^{[k]}$ = integral flux in the j^{th} energy interval, between E_j and E_{j+1};

$\sigma_i(E)$ = i^{th} foil reaction cross section for a specified (n,γ), (n,p), (n,α), (n,n'), (n,f), or $(n,2n)$ interaction;

$A_{i,j}^{[k]}$ = that portion of $A_i^{[k]}$ contributed by neutrons in the j^{th} energy interval, between E_j and E_{j+1};

$\sigma_r(E)$ = r^{th} foil cover removal cross section for cadmium, boron 10 or gold covered foils;

N_r = r^{th} foil cover nuclei density;

X_r = r^{th} foil cover thickness;

j = 1, 2, ... , m (energy interval index; currently, m = 620)

i = 1, 2, ... , n (foil index);

r = 1, 2, or 3 (foil cover index);

k = 1, 2, 3, ... (iteration index);

(Currently, $E_1 = 10^{-10}$ Mev and $E_{m+1} = 18$ Mev.)

Each subscripted equation below is meant to represent a set of equations on the subscript(s) as defined above.

For bare, cadmium-, boron 10-, and gold-covered foil detectors, $A_{i,j}^{[k]}$ may be given (when $E_{j+1} - E_j$ is small) by

$$A_{i,j}^{[k]} = \int_{E_j}^{E_{j+1}} \sigma_i(E)\, \varphi^{[k]}(E) \prod_{r=1}^{3} e^{-N_r X_r \bar{\sigma}_{r,j}}\, dE \qquad (20)$$

where $\bar{\sigma}_{r,j}$ is an appropriate average value for $\sigma_r(E)$ over the j^{th} energy interval. An adequate approximation for $\bar{\sigma}_{r,j}$ for the energy intervals in the SAND II code has been found to be

$$\bar{\sigma}_{r,j} \simeq \frac{\int_{E_j}^{E_{j+1}} \sigma_r(E)\, dE}{\int_{E_j}^{E_{j+1}} dE} \tag{21}$$

This approximation assumes that the foil cover interval-averaged cross section is independent of "k" and $\varphi^{[k]}(E)$; errors introduced by this assumption are negligible compared to those introduced by neglecting the complicated dependence of the scattering effect on the geometry of each particular case, which generally requires error-introducing simplifications. These errors are in turn small, in most practical cases, because of the relative magnitudes of the attentuation effects.

For purposes of calculation, it is convenient to define the foil reaction interval-averaged cross section:

$$\bar{\sigma}_{i,j}^{[k]} \equiv \frac{\int_{E_j}^{E_{j+1}} \sigma_i(E)\, \varphi^{[k]}(E)\, dE}{\int_{E_j}^{E_{j+1}} \varphi^{[k]}(E)\, dE} \tag{22}$$

Combining Eqs. (20) and (22) gives

$$A_{i,j}^{[k]} = \bar{\sigma}_{i,j}^{[k]} \int_{E_j}^{E_{j+1}} \varphi^{[k]}(E) \prod_{r=1}^{3} e^{-N_r X_r \bar{\sigma}_{r,j}}\, dE \tag{23}$$

Because of the fine structure of the evaluated cross section $\sigma_i(E)$ for many of the reactions used, the calculation of $\bar{\sigma}_{i,j}^{[k]}$ by Eqs. (22) requires, for many i, a much finer energy interval model than is used by the SAND II code. If, for calculational facility, the approximation is made that

$$\varphi^{[k]}(E) = \varphi_j^{[k]} \quad \text{for } E_j \le E \le E_{j+1} \tag{24}$$

then, from Eqs. (22) the foil interval-averaged cross section $\bar{\sigma}_{i,j}$ may be calculated by

$$\bar{\sigma}_{i,j} = \frac{\int_{E_j}^{E_{j+1}} \sigma_i(E)\, dE}{\int_{E_j}^{E_{j+1}} dE} \tag{25}$$

This calculation is k-independent and does not, therefore, require recalculation at each iteration. In fact, $\bar{\sigma}_{i,j}$ (as well as $\bar{\sigma}_{r,j}$) is calculated only once, in a separate code (CSTAPE) which performs exact linear interpolation integration over $\sigma_i(E)$ and $\sigma_r(E)$ input data points for all i (and r) and j. If integral flux in the j^{th} energy interval is defined by

$$\Phi_j^{[k]} = \int_{E_j}^{E_{j+1}} \varphi^{[k]}(E)\, dE \tag{26}$$

equations (23), (25), and (26) may be combined to give

$$A_{i,j}^{[k]} = \bar{\sigma}_{i,j}\, \Phi_j^{[k]} \prod_{r=1}^{3} e^{-N_r X_r \bar{\sigma}_{r,j}} \tag{27}$$

$A_i^{[k]}$ is now given by

$$A_i^{[k]} = \sum_{j=1}^{m} A_{i,j}^{[k]} \tag{28}$$

For describing the SAND II iterative procedure, the activity-weighting function $W_{i,j}^{[k]}$ is introduced and defined using Eqs. (27) and (28):

$$W_{i,j}^{[k]} = \frac{1}{2}\left(A_{i,j}^{[k]} + A_{i,j-1}^{[k]}\right)/A_i^{[k]} \quad , \; j = 2, \ldots m \tag{29-a}$$

$$W_{i,1}^{[k]} = A_{i,1}^{[k]}/A_i^{[k]} \tag{29-b}$$

and

$$W_{i,m+1}^{[k]} = A_{i,m}^{[k]} / A_i^{[k]} \tag{29-c}$$

The ratio of measured to calculated activity is defined as

$$R_i^{[k]} = A_i / A_i^{[k]} \tag{30}$$

Using Eqs. (29) and (30), an activity-weighted correction term $C_j^{[k]}$ (based on the logarithm of $R_i^{[k]}$ since the $R_i^{[k]}$ often differ by several orders of magnitude at the start of iteration, depending on the initial approximation spectrum) is selected:

$$C_j^{[k]} = \sum_{i=1}^{n} W_{i,j}^{[k]} \ln R_i^{[k]} \Big/ \sum_{i=1}^{n} W_{i,j}^{[k]} \tag{31}$$

for all j such that $\sum_{i=1}^{n} W_{i,j}^{[k]} \neq 0$. Iteration is then performed by:

$$\varphi_j^{[k+1]} = \varphi_j^{[k]} \exp\left\{C_j^{[k]}\right\} \tag{32}$$

For all j such that $\sum_{i=1}^{n} W_{i,j}^{[k]} = 0$, log-log interpolation is performed between the nearest lower j and the nearest higher j for which $\sum_{i=1}^{n} W_{i,j}^{[k]} \neq 0$ to obtain the next (k+1) value of differential flux; if such j cannot be found both above and below, extrapolation is performed (below or above, as required) according to one of several alternate forms:

low energy end: (1) 1/E;
(2) fission ($\sqrt{E}$) form;
(3) Godiva (E) form.

high energy end: (1) fission (Maxwellian form)
(2) fusion (14 Mev peak of arbitrary magnitude).

Iteration is repeated until a solution is obtained on the ℓ^{th} iteration. Using Eqs. (32) and re-substituting the $(k+1)^{th}$ result into the $(k+2)^{th}$, etc., the ℓ^{th} solution may be written as

$$\varphi_j^{[\ell]} = \varphi_j^{[o]} \exp\left\{\sum_{p=0}^{\ell-1} C_j^{[p]}\right\} \tag{33}$$

where $\varphi_j^{[o]}$ represents the initial input approximation.

In addition to providing a differential flux solution $\varphi^{[\ell]}(E_j) \approx \varphi_j^{[\ell]}$ at 621 energy points, the SAND II code provides an integral flux solution

$$\Phi^{[\ell]}(E_j, E_{m+1}) \equiv \sum_{s=j}^{m} \Phi_s^{[\ell]} = \int_{E_j}^{E_{m+1}} \varphi^{[\ell]}(E)\, dE \tag{34}$$

The absolute value of the solution is obtained by renormalizing $\varphi^{[\ell]}(E)$ so that

$$\Phi^{[\ell]}(E_1, E_{m+1}) = \frac{1}{n} \sum_{i=1}^{n} \left[A_i / A_i'^{[\ell]}\right] \tag{35}$$

where $A_i'^{[\ell]}$ is the normalized activity produced by unity total integral flux. Calculated values of saturated activity are provided, given by

$$A_i^{[\ell]} = \sum_{j=1}^{m} A_{i,j}^{[\ell]} \simeq \int_{E_1}^{E_{m+1}} \sigma_i(E)\, \varphi^{[\ell]}(E) \prod_{r=1}^{3} e^{-N_r X_r \sigma_r(E)}\, dE \tag{36}$$

Calculated values of foil reaction energy limits of sensitivity E_i and E_i' are also provided, defined such that some large portion α (currently 95%) of the activation of the i^{th} foil is produced by neutrons of energy $E > E_i$, and the same portion α is produced by neutrons of energy $E < E_i'$. Equation (37) implies the definition of E_i and E_i':

$$\int_{E_i}^{E_{m+1}} \sigma_i(E)\, \varphi^{[\ell]}(E) \prod_{r=1}^{3} e^{-N_r X_r \sigma_r(E)}\, dE = \int_{E_1}^{E_i'} \sigma_i(E)\, \varphi^{[\ell]}(E) \cdot$$

$$\prod_{r=1}^{3} e^{-N_r X_r \sigma_r(E)}\, dE = \alpha \int_{E_1}^{E_{m+1}} \sigma_i(E)\, \varphi^{[\ell]}(E) \prod_{r=1}^{3} e^{-N_r X_r \sigma_r(E)}\, dE \tag{37}$$

The above equations are solved by the SAND II code, which has been written in Fortran IV for the CDC 6600 computer and is documented in Volume II.

SECTION IV
ANALYTICAL STUDY OF THE ITERATIVE METHOD

A. Requirements for Solution Achievement

1. General Requirements

The unknown measured flux spectrum form satisfies (except for experimental errors) the equations

$$A_i = A_i^{[k]} \quad (i = 1, 2, \ldots, n) \tag{38}$$

where, as previously defined, the A_i's are the measured saturated activities. In principle, an exact solution ($A_i = A_i^{[k]}$ for all "i") can be obtained. Such a solution will not be unique, however, and will not necessarily be more useful than an approximate solution because of experimental errors in A_i and $\sigma_i(E)$. Gold (Ref. 9) has stated that, in general, neither an exact nor even an approximate solution is required, but that the solution should properly satisfy the set of integral equations and certain necessary conditions imposed by physical implications; he calls such a solution an appropriate solution.

Assuming that the initial approximation (k = 0) is not itself an appropriate solution, the iterative procedure is applied until Eqs. (38) are satisfied, to within appropriate limits of acceptable error. If the initial approximation spectrum is properly selected and if, in addition, the essential physical conditions have been properly considered, the ℓ^{th} iterative spectrum for which

$$A_i \simeq A_i^{[\ell]} \tag{39}$$

for all i will be an appropriate solution, such that

$$\Phi^{[\ell]}(E_j, E_{m+1}) \simeq \Phi(E_j, E_{m+1}) \tag{40}$$

for all E_j within the range of foil measurements, where

$$\Phi(E_j, E_{m+1}) = \int_{E_j}^{E_{m+1}} \varphi(E)\, dE \qquad (41)$$

and $\varphi(E)$ is the true (unknown) spectral form.

2. SAND II Requirements

The SAND II code provides a "best fit" neutron flux spectrum for a given input set of infinitely dilute saturated foil activity measurements, without interruption in the calculational procedure for manual calculation or decision processes. SAND II accepts as input information:

a. A measured set of infinitely dilute saturated activities;

b. foil covers (cadmium, boron 10 and gold) used, if any, and their thicknesses;

c. an initial spectral approximation (or the option of selection from the reference spectrum library);

d. solution acceptability criterion: the degree to which all 621 differential flux values for two successive iterations must agree in order to consider the solution appropriate;

e. discard test criterion: the number of standard deviations of the measured activity of a given foil (calculated from all foils used) from the activity calculated from the solution spectrum, above which value the foil measurement is to be discarded and the solution revised to account for its exclusion.

These input requirements and the manner in which they affect the solution have been studied for both analytical and experimental cases. The results of these studies will be considered in Section IV-B and Section V.

B. SAND II Results for Selected Test Cases

1. Summary Discussion

To determine the accuracy of the SAND II iterative procedure, test cases were studied which include different ratios of resonance to fission to fusion neutrons. The analytical tests consisted of attempts to ascertain the degree to

which SAND II is capable of obtaining integral flux and "unfolding" differential spectral structure under both ideal and non-ideal conditions – that is, with and without errors in activity and cross sections.

For different kinds of test spectra, "exact" activities were calculated using the current cross section evaluations and attenuation calculational techniques. Some of these "true" spectra were chosen from SAND II solutions for the tests considered in Section V, while others were selected on the basis of being representative of different types of environments. The "exact" activities were then considered to be "measured" activities and used (with and without added errors) as input to SAND II, along with both acceptable and unacceptable input approximations, to obtain iterative solutions.

Some of the test cases considered were selected by Biggers and Mehl so that the "true" form would be unknown to the authors until after a suitable solution had been obtained (Ref. 13, 14). This technique was valuable in studying the effectiveness of the SAND II code to use the reference spectrum library to select the initial approximation, since in some of these cases no information was provided as to the type of environment. (These cases provided the most severe tests of the "unfolding" technique, since there seldom is a real case for which no information is available.)

The results of these analytical tests were in general excellent. Given sufficient foil energy coverage, the code has proved capable of unfolding the general differential envelope, as well as many structural details, especially for the energy range above 0.1 Mev, most adequately covered by threshold detectors.

The test cases discussed, in whole or in part in Sections IV-B-2, -3, and -4, are identified as follows:*

Test 1 – Ground Test Reactor (GTR) core spectrum (reference spectrum 19, Volume IV)

Test 2 – Fusion Type Spectrum (FTS)

*Since the current low-energy detectors in the SAND II code do not have different cross section shapes (all are essentially 1/v) in the thermal region, no attempt was made to determine the shape of the thermal spectrum for these tests. The SAND II code simply established a magnitude for the input form (usually Maxwellian) in relation to the higher energy component of the spectrum. In general, therefore, the thermal components of the spectra are omitted in the discussions of both the analytical and experimental results that follow.

Test 3 – Biggers' Case 1*
Test 4 – Biggers' Case 2*
Test 5 – Biggers' Case 3*
Test 6 – Biggers' Case 4*
(Forms assumed to be unknown to authors, i. e., used SAND II code with its reference spectrum library as a "black box.")

Test 7 – Biggers and Mehl's Case 1
Test 8 – Biggers and Mehl's Case 2†
Test 9 – Biggers and Mehl's Case 4†
Forms initially unknown to authors

Test 10 – Solution spectra for the Epithermal Critical Experiment Laboratory (ECEL) fast reactor test.

Test 11 – Solution spectrum for a homogeneous Water Moderated Graphite Reflected (WMGR) water cooled reactor test.

Test 12 – Graphite Moderated and Reflected Water cooled (GMRW) reactor test.

Test 13 – Time of Flight Measurements (TFM) of the leakage spectrum from a TRIGA mockup with a 2" water reflector (Ref. 15).

2. Appropriateness of Solution and Solution Criterion

For a flux spectral determination covering the entire energy region, the number of foil reactions used will in most cases be between 10 and 20. There is, therefore, no unique exact solution to Eqs. (38), and no unique "best fit" solution iterative limit. Any reasonable iterative procedure, such as that incorporated in SAND II, may be used that fulfills certain obvious requirements of stability; for example, it must not yield a solution which diverges to infinity or produces negative fluxes. The criterion of convergence is, however, not required; it is only necessary that all solutions obtained by iterations beyond that which yields an appropriate solution remain within a fixed neighborhood of that solution, the size of the neighborhood depending on acceptable experimental error limitations.

The first solution acceptability criterion studied was based on the degree to which the pertinent foil activities calculated from the solution spectrum must agree with the input measured activities. This criterion was found to be

*These were the numbers originally used for the analysis of these cases by a partially automated iterative procedure (see Reference 3).
†The Case 3 and 5 results are not discussed in this report.

unacceptable for most test cases because of its obvious inherent lack of sensitivity to differential flux changes. A series of tests was initiated, therefore, to study this parameter as well as other aspects of the iterative procedure.

A parametric study of the formula used to calculate the weighting function, Eqs. (29), was conducted in an effort to minimize what at first appeared to be inappropriate perturbations in the solution differential flux spectrum over certain energy regions, in ill-conditioned cases which include large errors in measured foil activity and/or cross sections.

Results of this study made it clear that the difficulty (which is usually negligible and is in any case not serious from the standpoint of integral flux solution accuracy) is not one of method. The difficulty is, rather, inherent in the problems of foil coverage and activity measurement, non-uniqueness of solution, and incomplete or inaccurate evaluations of reaction cross section data. Physically unreasonable structure in solution spectra can, therefore, be minimized by careful experimental planning and execution to assure sufficient foil energy coverage and accuracy of activity measurements, by utilization of all available physical information to select an appropriate spectrum, and by the acquisition of sufficiently accurate cross section data (see the results for Tests 10, 11, and 12 in Section V-B).

The appearance of inappropriate perturbations when inaccurate cross section data are used is actually an important advantage, since it can be used to survey currently used cross section evaluations to determine which require revision and in what energy regions the revision is needed. The SAND II code could then be adapted to provide improved cross section evaluations as solutions. Because of the "best fit" approach of SAND II which provides a solution using redundant (in energy coverage) foil reactions, the solution behavior can also be examined to identify inordinately large activity measurement errors, thus providing a tool to help identify either systematic errors in determining activities or uncorrected absorption-scattering effects (see the results for Test 10 in Section V-B).

A "recycle" approach was utilized to help in the study of the appropriateness of a given iterative solution. This was done by considering the SAND II calculated values of activity for a solution spectrum to be a new set of exact

"measured" activities. The solution spectrum was then used in the recycle test as the "true" spectrum with the new set of exact "measured" activities and the same input spectral approximation (that in each case had led to the "true" spectrum) as input to SAND II.

This recycle procedure helps to identify those features of a solution spectrum which are caused by peculiarities of the iteration technique or any other aspect of the data reduction method; if no such peculiarities exist to cause erroneous spectral structure, the solution to a test using this procedure should agree with the "true" spectrum. (It is recommended that this procedure be applied to any real case in which the reality of spectral structure comes into question.) A typical test result is shown in Figure 1 for Test 12. The 100-iteration limit was chosen to test whether once a reasonable solution had been achieved, further iteration would cause the solution to diverge, or "blow up." In all cases studied, it was found that, once an appropriate solution is achieved, it remains within a quite acceptable neighborhood of that solution upon further iteration.

It was found that certain ill-conditioning can cause an apparent "blow up" (depending on the method of presentation of results). This occurs when a reaction has a response curve such that it is very dominant in a particular narrow energy region, compared to all other reactions used, and the measured activity for that reaction is in substantial error (again compared to the other reactions) on the low side. This causes negative corrections to the flux at that energy region; if the first few iterations are not sufficient to generate close agreement between the measured and calculated activities for that reaction, subsequent iterations will cause continued negative corrections to the flux at that energy region. After the first several reductions, however, which have been sufficient to remove most of the flux from that region, the continued negative corrections although perhaps substantial relatively, will have no further significant corrective effect on the calculated activity (which is produced over a much wider energy range, not so strongly affected by the negative error of that foil). If the spectrum is graphically plotted on a logarithmic display (as is usual), successive iterations will cause a successively more severe "dip" at the pertinent energy region while, actually, once the flux is "almost" zero, compared to the flux in its immediate energy vicinity, further reduction (which appears substantial on a logarithmic display) will have no significant effect.

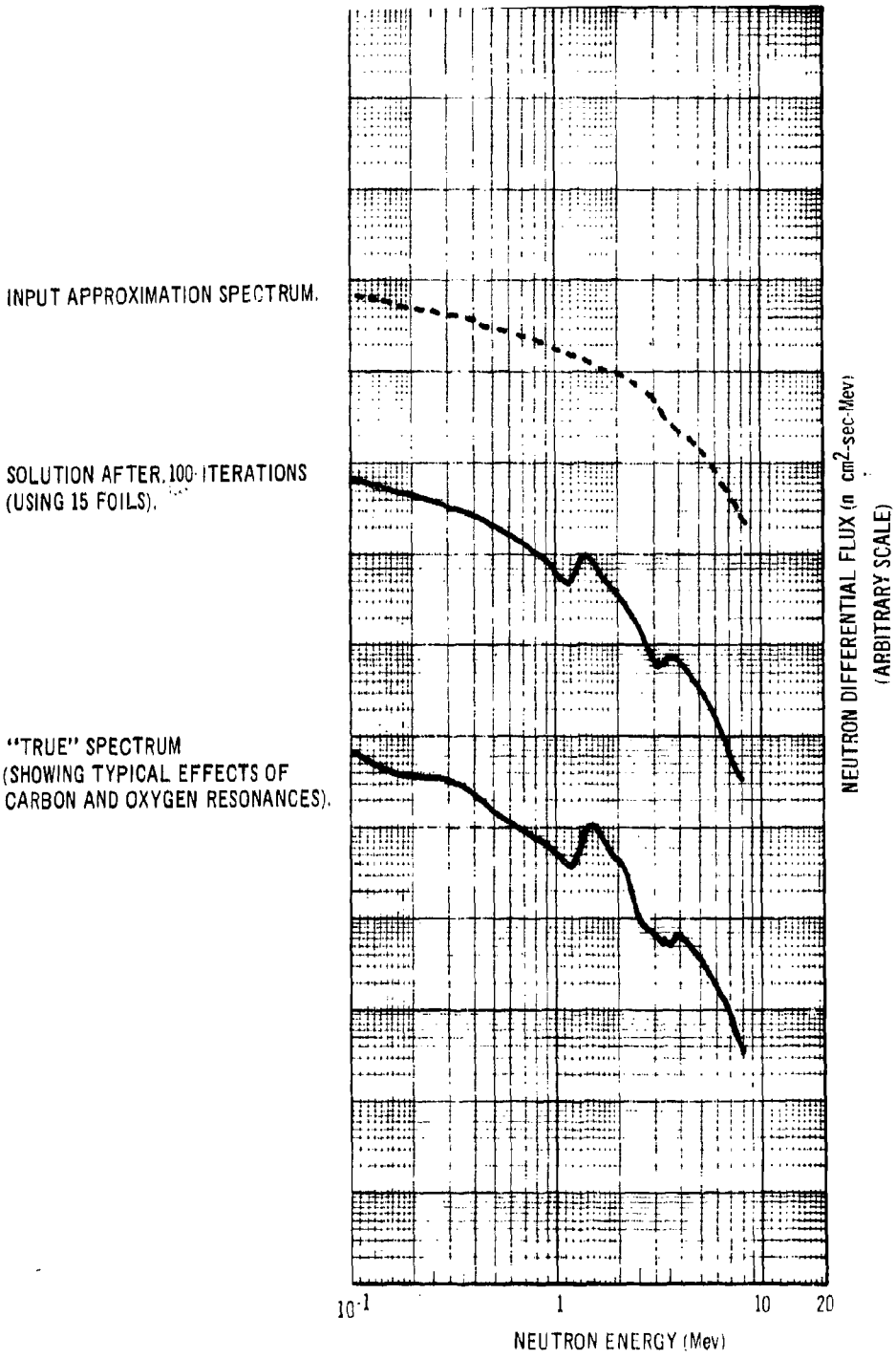

Figure 1. Capability of SAND II to Unfold Differential Neutron Flux, Test 12

It is emphasized that this apparent (on a logarithmic display) blow up can occur only in fairly ill-conditioned cases, when a set of foils is used such that one foil (1) is particularly dominant in one narrow energy region, (2) has an activity produced over a much wider energy range, over most of which it is not particularly dominant compared to the other foils used, and (3) has a large negative measured activity error.

In the resonance region, the code cannot always produce real structure in the solution spectrum when the resonance foils are used in the usual manner; conversely, the code will often produce artificial structure. This is because the very severe resonance structure in the reaction cross section functions can result in sensitivity energy ranges for the various resonance foils which are essentially separate. In some extreme cases (notably gold), 90% or more of the activity can be produced by one major cross section resonance peak. This means that initial iterative flux corrections are generally not averaged over more than one foil, and peaks and dips are readily introduced at the respective resonance energies, to make the spectrum consistent with all the measured activities. This difficulty will not be encountered in a spectrum with very little thermal and intermediate flux, since this would result in response curves shifted upward in energy from the resonance region into a region in which they are much smoother and overlap. Usually, only $1/E$ or similar behavior in the intermediate energy range will allow the problem to arise. As previously stated, the difficulty of artificial structure may in some cases be put to good advantage; examination of the solution for structure of this type is often an easy way to detect large errors in activity measurements or self-absorption effects (see Section V-B).

A very effective device for solution of the problem of artificial structure in the resonance region is the use of self-sandwiched resonance detectors. This would preferentially attenuate a large portion of the flux at the resonance energies in the outer covers, effectively smoothing the response curves for the sandwiched foils by eliminating or sharply reducing the large peaks; this in turn causes regions of foil energy overlap to be much more significant in terms of contribution to total activity. In effect, self-sandwiching causes resonance foils to behave more like integrating threshold detectors.

The results of the above studies as well as those that will be discussed in subsequent sections of this report suggest that the criterion for solution achievement should be based on a comparison of the differential spectra of successive iterations. For the current SAND II code, therefore, a particular iterative spectrum is considered to be an appropriate solution if its differential flux differs from that of the preceding iteration by less than a given percent (specified as input) at all 621 energy points between 1×10^{-10} Mev and 18 Mev.

The results of a parametric study of the required number of iterations as a function of the value of the current solution criterion (as well as of the study based on the standard percent deviation of the ratios of measured to calculated activity), for a measurement of the neutron flux spectrum in the ECEL reactor, are presented in Figure 2. (Other aspects of the ECEL test are discussed in detail in Section V-B.) Testing performed to date suggests that, in most realistic cases, a successive iteration difference of about 5 to 10% is a reasonable solution criterion, and that such a criterion is usually satisfied in fewer than thirty iterations. The actual value used, however, will depend on the confidence the user places in the accuracy of the measured activities, and on the aptness of the initial spectral approximation.

3. Foil Set Selection and Input Spectrum Sensitivity

During the development and testing of the SAND II code, studies were performed to determine the degree of input sensitivity of the current iterative procedure; that is, to what degree the solution differential flux shape is affected by the selection of the foil set and the choice of the input spectral approximation. Based on the studies completed, it appears that, if the foil set selected provides sufficient coverage, the code is less input dependent than was originally expected. In cases where foil coverage is not adequate, however, the code has been observed to be quite input sensitive in terms of the differential flux. A poor choice of input spectrum can result in foil sensitivity energy regions which, if insufficient foil overlap occurs, cannot be shifted sufficiently by iteration to approach the true solution. As suggested previously, a "recycle" technique can be used to study the input sensitivity of the iterative procedure, in those cases in which the credibility of the solution spectrum is in question.

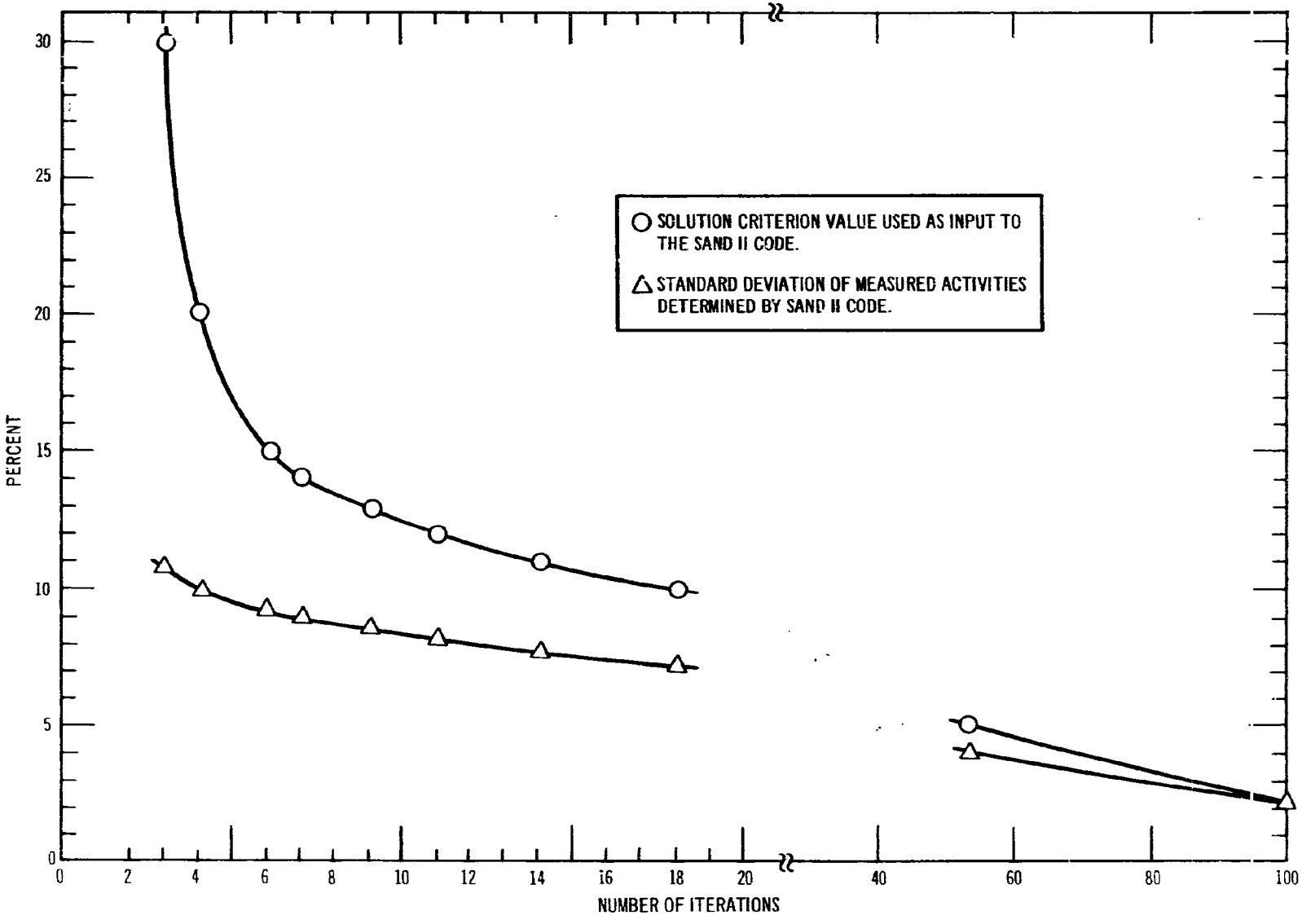

Figure 2. ECEL Parametric Study of the Number of Iterations versus the Solution Criterion Value and Standard Deviation of Measured Activities

The dependence of the SAND II solution spectrum on the selection of a suitable foil set and an initial spectral approximation can best be illustrated by presenting several examples. The SAND II solution spectrum will not agree with the "true" spectrum below the energy range of the lowest detector (about 10^{-6} Mev for most of the tests except Test 7, for which it is about 10^{-2} Mev because of the sharp spectral cutoff at about 10^{-4} Mev); the complete spectrum is retained in Tests 7, 8, and 9 simply for completeness.

First, several cases were studied in which a large number (~25 of the 29 available reactions) of foils were used, and no information was provided on the errors associated with the measurement of the foil activities and/or the type of neutron environment being measured. The only available information was that, in two of five cases (three of which are discussed here as Tests 7, 8, and 9), foil activity probable errors are 10%; in one case (Test 7), an initial input spectral form was provided (shown by the dashed curve in Figure 3).

The SAND II results for these three cases, and the "true" spectral forms, are given in Figures 3, 4, and 5 respectively. The reference spectrum library was used to select an initial approximation for Tests 8 and 9. For Test 9, the library search technique was modified to include two separate reference library searches, one for the low energy (resonance) and one for the high energy (threshold) foil detectors. The two spectra selected were then combined to provide a hybrid input approximation. (The application of this technique can significantly increase the confidence in the final SAND II solution when the reference spectrum library is used, since it results in an initial approximation with a reduced standard deviation of activity ratios.) The mutually independent selection of two regions of the initial approximation spectrum is justified for spectra in which the resonance foils and threshold foils form essentially independent sets – that is, their sensitivity curves do not substantially overlap in energy.

In general, the differential flux results are reasonably correct for these three tests, even though the foil coverage (and overlap) was rather poor in certain energy regions. This lack of proper foil coverage might seem surprising in view of the large number of foils used for these tests. It must be emphasized, however, that the SAND II energy range spans more than eleven decades; also, the 25 foil reactions used do not necessarily have energy response functions

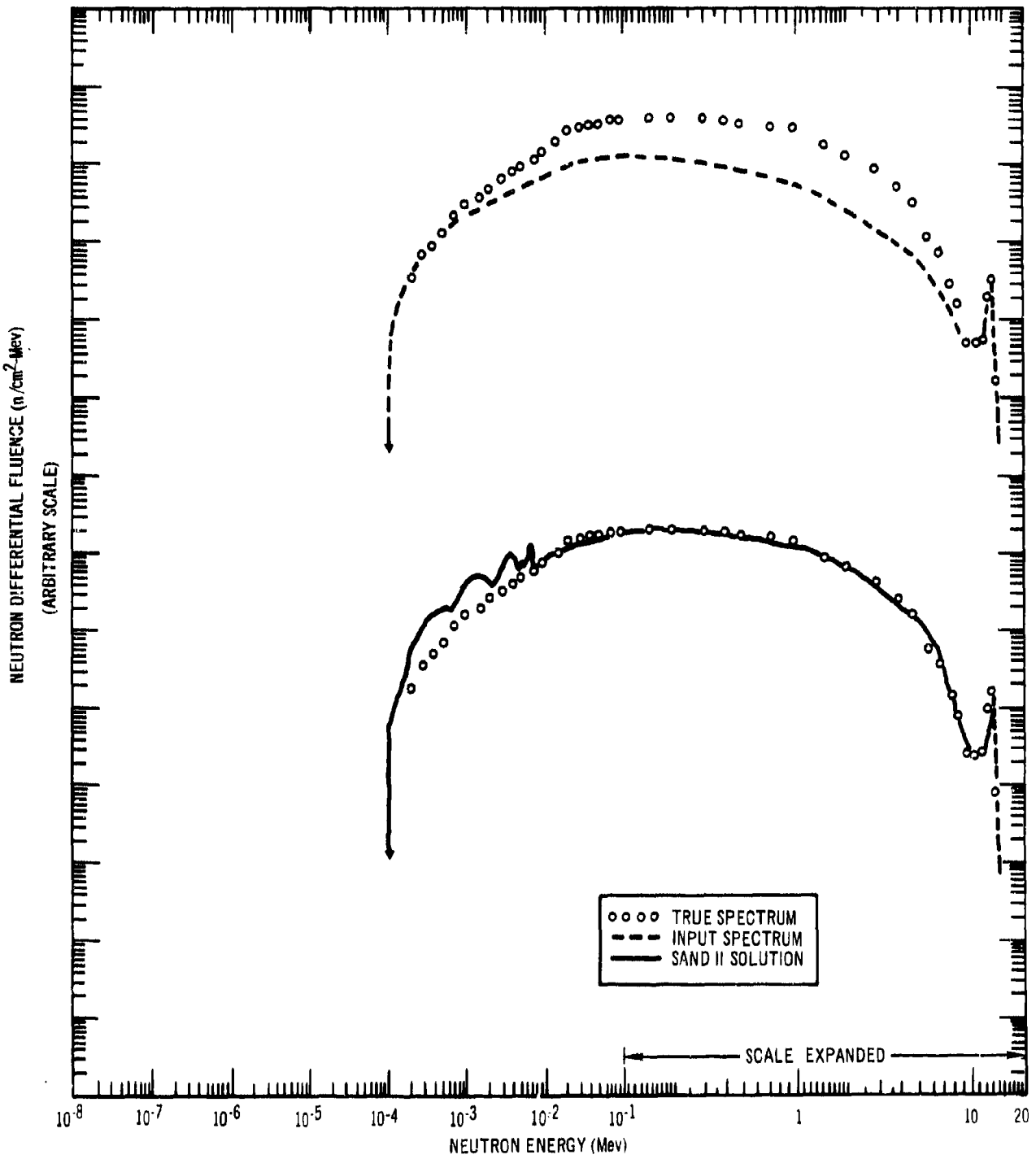

Figure 3. SAND II Differential Fluence Result for Test 7

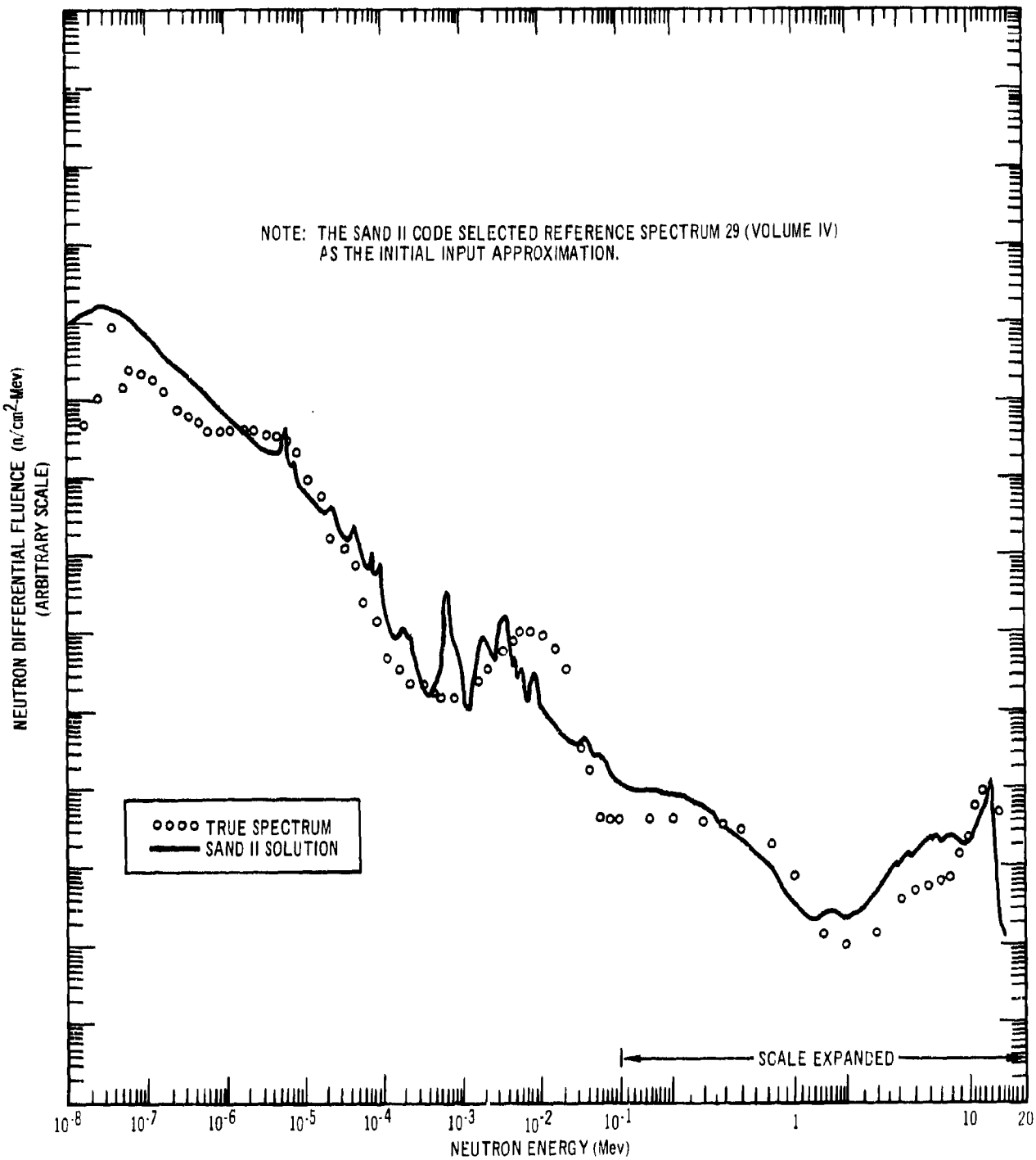

Figure 4. SAND II Differential Fluence Result for Test 8

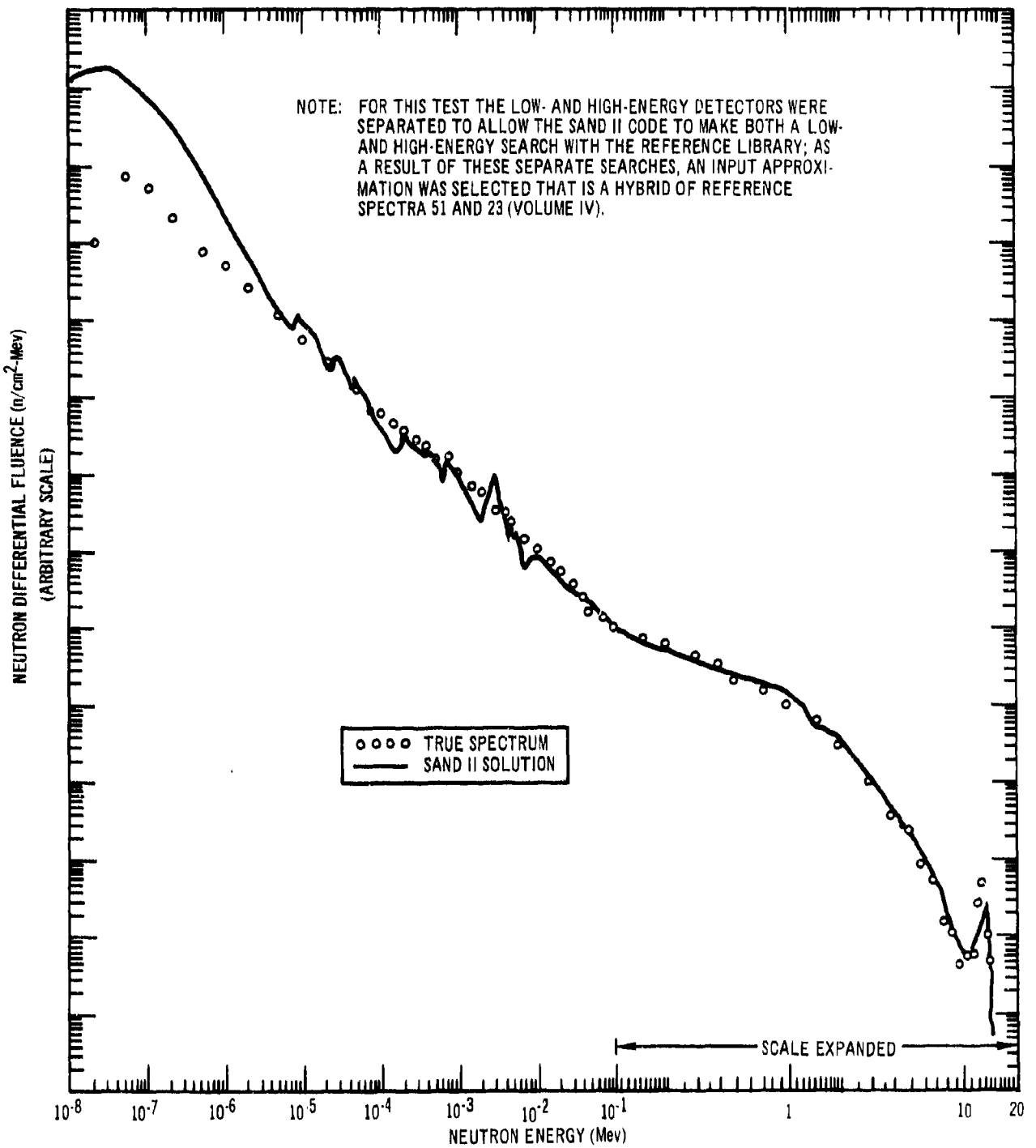

Figure 5. SAND II Differential Fluence Result for Test 9

suitable for obtaining a proper solution in all cases especially if selected with little or no knowledge of the environment.

SAND II integral flux results for similar cases (Tests 3, 4, 5, and 6) will be discussed in more detail in Section IV-B-4 for a smaller set of 14 foil detectors that have been found suitable for measurements in a number of fission- and fusion-type environments.

The next pertinent examples consider only the high energy region of the neutron spectrum, above ~0.1 Mev. The iterative results of two "recycle" studies, Tests 11 and 13, are presented in Figure 6. The same set of 13 foil detectors was used for Test 13A and Test 11. Test 13B used the same set of 15 foils that was used for Test 12, Figure 1. The 13-foil set included sulfur, while the 15-foil set did not. (The individual foils used for these tests are listed in Tables XIV and XVIII of Section V.)

In Figure 6, the "true" spectrum and SAND II results for each test are represented by the solid lines and the input approximation by the dashed line. Tests 11 and 13 again demonstrate that the iterative method is capable of unfolding differential structure, but both the relative hardness of the spectrum (which will affect the energy response range of individual foils), and the particular foil set selected, will affect the final shape of the solution differential flux spectrum. (The effect on the integral flux is significantly less.) In this regard, it is noted that the general envelope of the solution differential flux is more correct in Test 12, Figure 1, than in either Tests 11 or 13. This is at least in part due to the fact that in Test 12 the solution spectrum is softer and more (fifteen) foil detectors were used. The fine structure superimposed on the solution envelope between 2.5 and 5 Mev for Test 11 is due mainly to similar fine structure in the cross section of the S^{32} (n, p)P^{32} reaction (see Volume III). It is most pronounced in this test because of the relative softness of the spectrum and the particular foil set used. Conversely, the effect of sulfur is only slightly evident in Test 13A where the spectrum is much harder. The sulfur cross section fine structure is predominantly in the low energy region of its sensitivity range; therefore, a softer environment causing increased low-region sensitivity and therefore more dominant low-end iterative weighting (see Eqs. (29)), will result in a stronger reflection of this structure in the solution spectrum than will a harder environment.

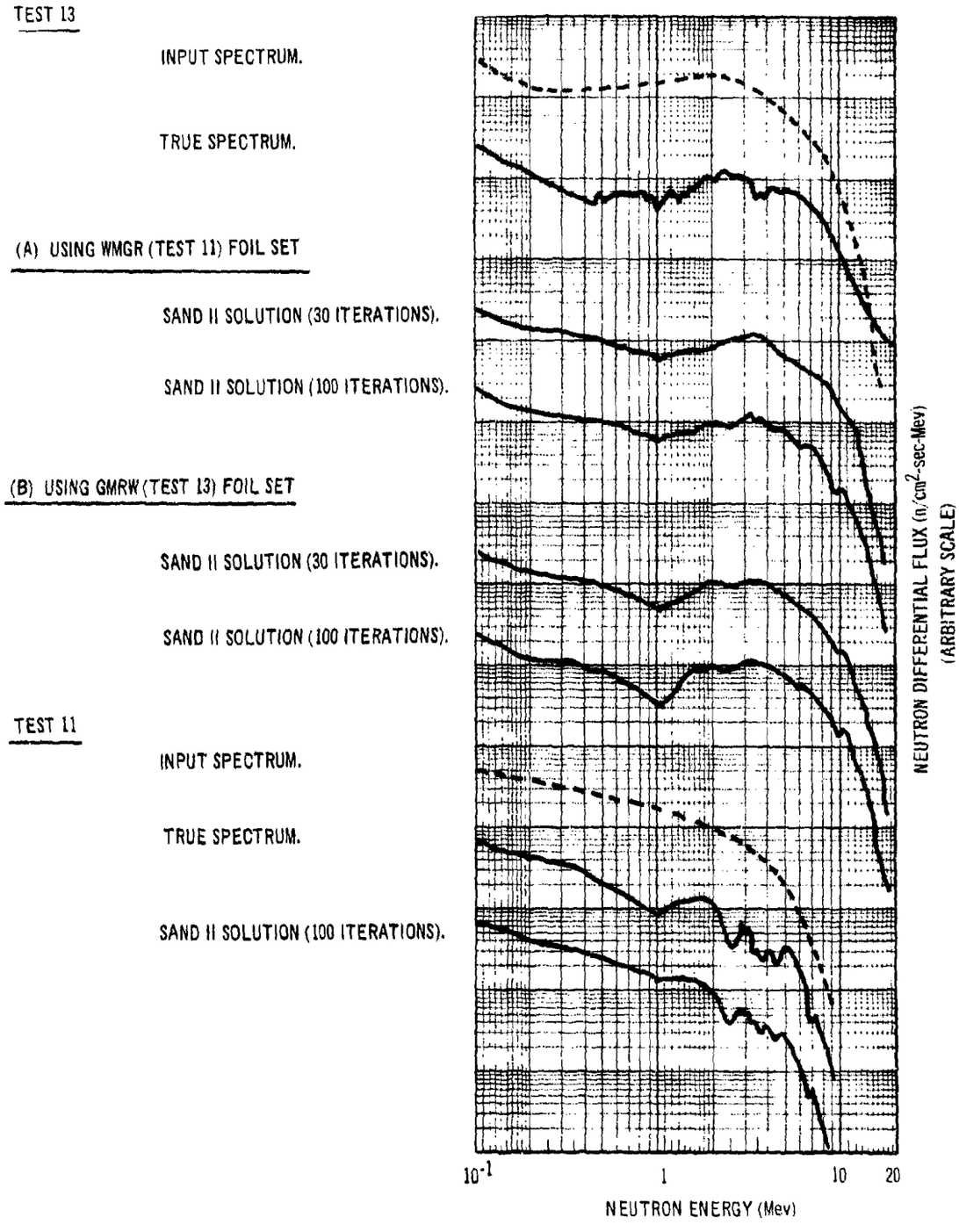

Figure 6. SAND II Recycle Study Differential Flux Results

These examples serve to illustrate the dependence of the input sensitivity of the iterative solution on the choice of foil sets and initial spectral approximation. A final example illustrates a case in which all the high energy foils were utilized and three different input spectral approximations were selected. Figure 7 presents the iterative results for Test 2. An assumed fusion form was selected as the "true" spectrum for this test; the three different input approximations (the three dashed lines) were used to obtain the three solutions (three solid lines) shown. This test makes apparent the capability of the SAND II code to generate a reasonable solution with a poor input approximation in certain cases when there is adequate foil coverage.

4. Integral Flux Comparison

As indicated previously, the thermal component of the flux has been omitted in the discussion of differential flux results throughout this report, because currently available low energy detectors do not have sufficiently different response functions to allow spectral unfolding. The thermal component of the integral flux spectra will not be considered either, since all that is currently possible is to establish the magnitude of the flux in this region.

It is worth mentioning, however, that there are foil reactions that have only one predominant resonance in the few electron volt region. Combinations of such foils (both bare and cadmium-covered) present a variety of absorption cross sections, which could be used to determine the shape of the differential flux in the thermal region. Fulmer and Ruane (Ref. 16) have recently reported on the use of such a group of detectors for determining spectra in this region. The incorporation of such reactions as $Dy^{164}(n,\gamma)Dy^{165}$, $Eu^{151}(n,\gamma)Eu^{152}$, $Lu^{176}(n,\gamma)Lu^{177}$, and $In^{115}(n,\gamma)In^{116}$ into the SAND II cross section library could permit the unfolding of spectra for the very low energy region.

To determine the accuracy of the SAND II integral flux results, several test cases were studied. Test 1 involved a known spectrum for the Ground Test Reactor (reference spectrum 19), a set of foil activities with and without errors, and the use of a previously determined input approximation spectrum. (This was a repeat of a test that had been studied before and was reported in reference 2.) The SAND II results are presented in Table I and Figure 8 for the first part of this test, which involved the assumption that there were no errors in measured activities or cross sections.

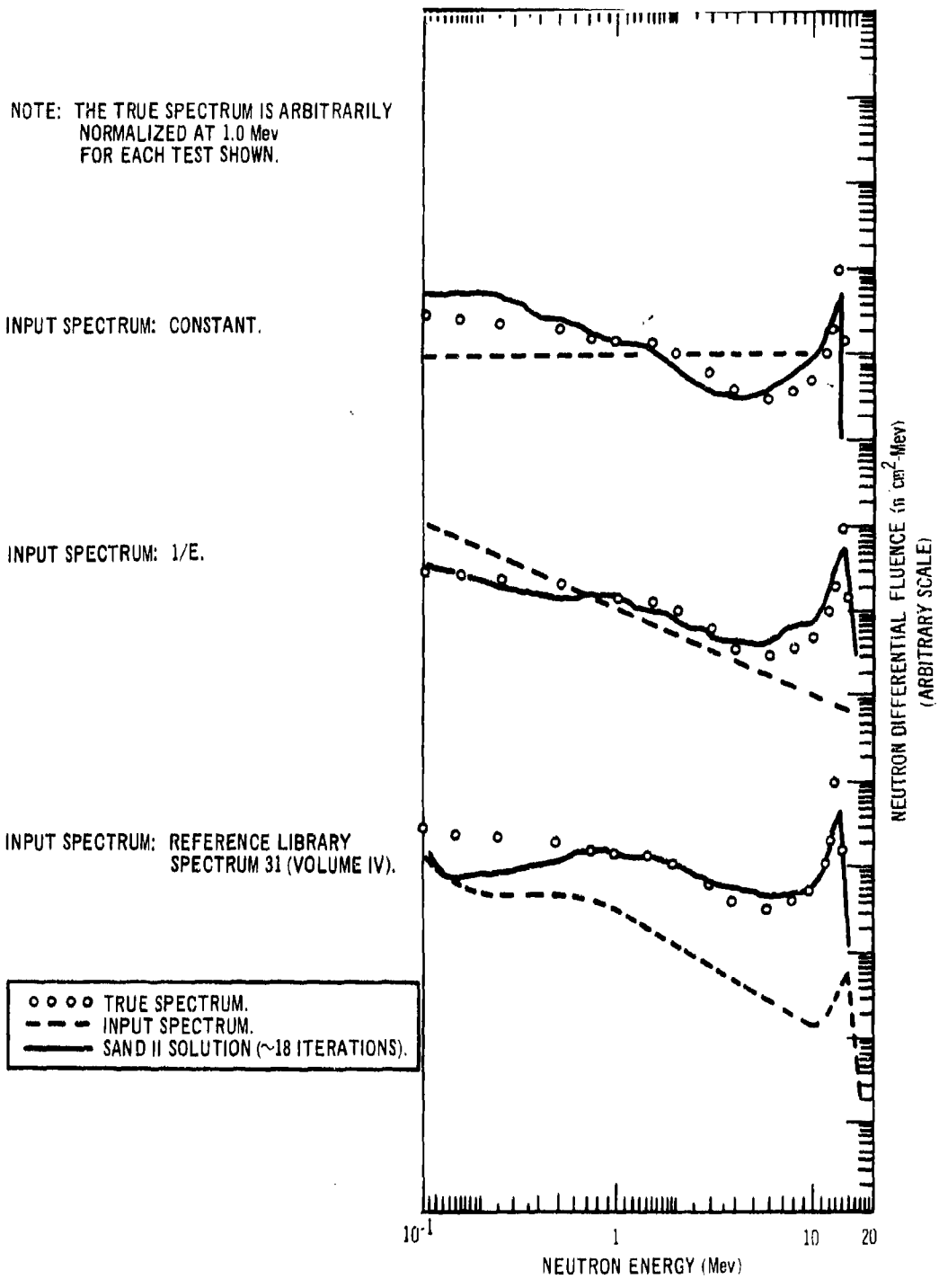

Figure 7. SAND II Differential Fluence Result with Different Input Approximations for Test 2

Table I

SAND II SOLUTION RESULTS OBTAINED AFTER 5 ITERATIONS
FOR TEST 1 WITH NO ACTIVITY ERRORS

Foil Reaction	Saturated* Measured Activity (dps/nucleus)	Saturated† Calculated Activity (dps/nucleus)	Nominal 5% Activity Limits (Mev)		% Deviation of Measured From Calculated Activity
			Lower	Upper	
Na^{23} (n,γ) Na^{24} Cd§	2.777×10^{-27}	2.778×10^{-27}	5.0×10^{-7}	3.2×10^{-3}	-0.03
Au^{197} (n,γ) Au^{198} Cd	1.455×10^{-23}	1.455×10^{-23}	4.0×10^{-6}	6.6×10^{-6}	0.00
Co^{59} (n,γ) Co^{60} Cd	6.486×10^{-25}	6.486×10^{-25}	8.0×10^{-7}	1.6×10^{-4}	0.00
Cu^{63} (n,γ) Cu^{64} Cd	4.715×10^{-26}	4.713×10^{-26}	6.2×10^{-7}	0.022	+0.03
In^{115} (n,n') In^{115m}	2.165×10^{-26}	2.176×10^{-26}	1.2	5.7	-0.51
Ni^{58} (n,p) Co^{58}	1.553×10^{-26}	1.555×10^{-26}	2.2	8.0	-0.11
Fe^{54} (n,p) Mn^{54}	1.378×10^{-26}	1.379×10^{-26}	2.1	8.1	-0.11
S^{32} (n,p) P^{32}	8.354×10^{-27}	8.408×10^{-27}	2.5	8.1	-0.64
Mg^{24} (n,p) Na^{24}	2.944×10^{-28}	2.965×10^{-28}	6.6	12.1	-0.72
Al^{27} (n,α) Na^{24}	1.396×10^{-28}	1.401×10^{-28}	6.7	12.4	-0.32
Cl^{35} (n,α) P^{32}	1.925×10^{-27}	1.889×10^{-27}	3.2	8.6	+1.90
I^{127} (n,2n) I^{126}	2.066×10^{-28}	2.055×10^{-28}	10.1	14.6	+0.52
			Standard Deviation of Measured Activities		0.69%

*Values inputted to SAND II
†Values calculated by SAND II after 5 iterations
§Means foil detector is covered with cadmium

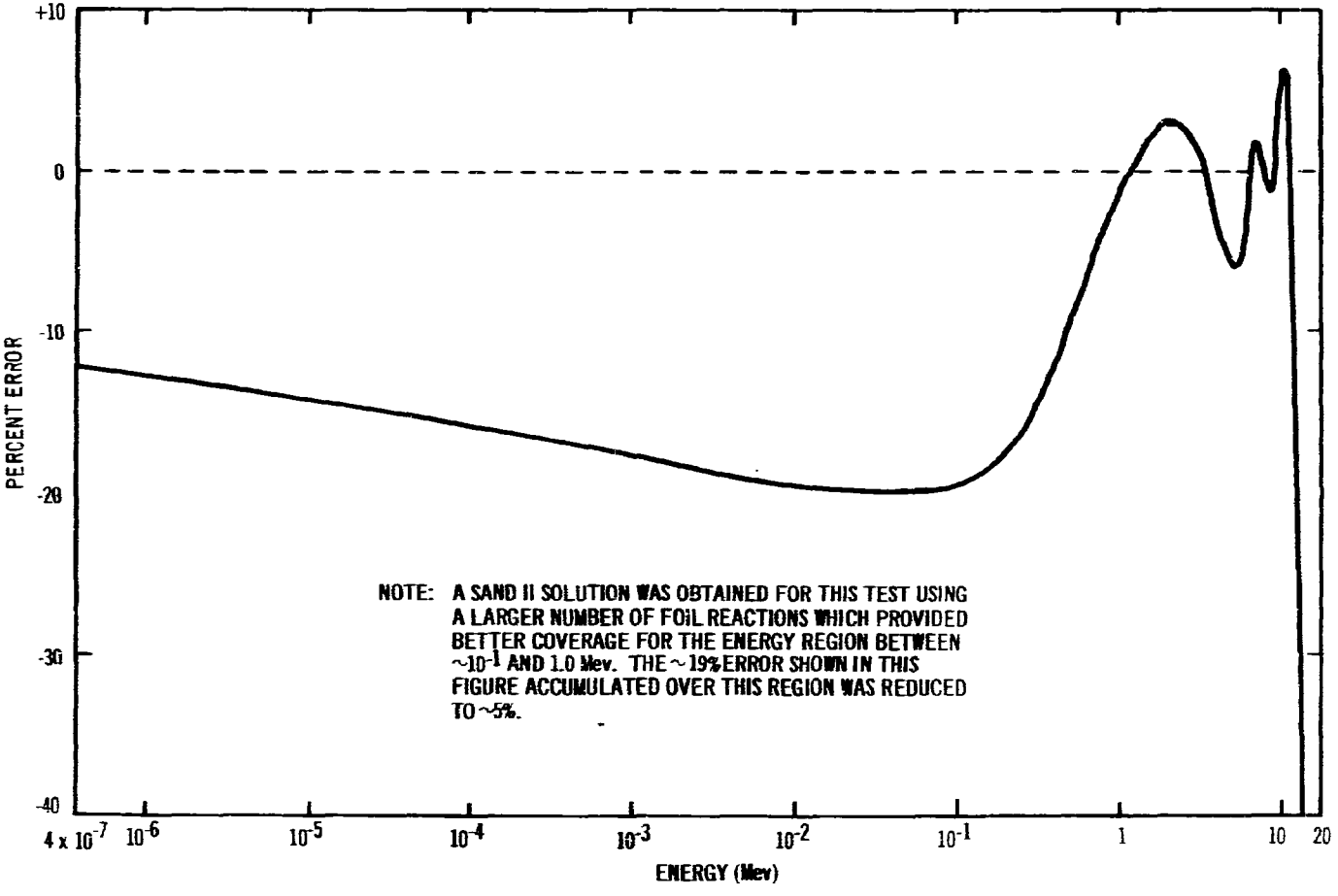

Figure 8. SAND II 5th Iterative and True Test Spectrum Integral Flux Comparison for the Ground Test Reactor (GTR) Core Flux Spectrum Test 1 with no Activity Errors

The results for Test 1 were intended to be representative of a typical well-moderated reactor test where the user of the SAND II code might have some pre-knowledge of the anticipated overall form of the unknown spectrum. It was assumed, therefore, as might be in an actual case, that a 1/E + fission spectrum (reference library spectrum 7) is a reasonable input approximation based on the available physical knowledge about the reactor environment. (More typically, a good input approximation might be available as a result of reactor physics calculations.)

The results for Test 1 are good, considering that the foil set selected did not provide proper foil coverage for the regions $\sim 10^{-1}$ to 1 Mev and ~15 to 18 Mev (see Table I), where negative accumulated errors up to and greater than ~19% appear in Figure 8. These large negative errors are a result of a lack of proper foil coverage, which yields a solution that is largely a reflection of the input approximation in these regions. For those regions where there is adequate foil coverage, however, the integral flux solution is accurate to within ±10% based on a relative comparison; i.e., neglecting the ~19% error accumulated between 10^{-1} and 1 Mev. Similar results are given in Table II and Figure 9 for the second part of this test, where activity errors were introduced, selected at random from a set of percent error values with an assumed normal distribution and a standard deviation of 15%. In Figure 9, the manner in which the integral flux solution reflects the magnitude and the direction of the errors listed in Table II is apparent. In this case, the integral flux solution is within ~ ±20% at most energies. (Experimental results for environments similar to that of Test 1, where the initial input spectra were based on reactor physics calculations, are discussed in Section V-B.)

A cooperative study was conducted involving work performed at Atomics International and the Los Alamos Scientific Laboratory. For the initial step of the study, the evaluated cross section data presented in reference 17 were used by Biggers of Los Alamos Scientific Laboratory to calculate, for each of four selected spectra, the activities of a set of 14 foils selected from the 29 reactions listed in Volume III. The calculated saturated activities of the selected foils for each of the four test cases were then altered in a random manner to simulate experimental errors, and were used as "measured" activities for the test cases.

Table II

SAND II SOLUTION RESULTS OBTAINED AFTER 3 ITERATIONS
FOR TEST 1 WITH RANDOM ACTIVITY ERRORS*

Foil Reaction	Assigned† Errors %	Saturated Measured Activity (dps/nucleus)	Saturated Calculated Activity (dps/nucleus)	Nominal 5% Activity Limits (Mev)		% Deviation of Measured From Calculated Activity
				Lower	Upper	
Na^{23} (n,γ) Na^{24} Cd§	-15.0	2.360×10^{-27}	2.459×10^{-27}	5.0×10^{-7}	3.2×10^{-3}	- 4.02
Au^{197}(n,γ) Au^{198} Cd	+10.5	1.608×10^{-23}	1.606×10^{-23}	4.4×10^{-6}	6.0×10^{-6}	+ 0.14
Co^{59} (n,γ) Co^{60} Cd	+16.5	7.556×10^{-25}	7.505×10^{-25}	9.8×10^{-7}	1.4×10^{-4}	+ 0.68
Cu^{63} (n,γ) Cu^{64} Cd	+10.5	5.210×10^{-26}	5.134×10^{-26}	6.8×10^{-7}	0.026	+ 1.48
In^{115} (n,n') In^{115m}	+22.5	2.652×10^{-26}	2.447×10^{-26}	1.1	5.4	+ 8.38
Ni^{58} (n, p) Co^{58}	-22.5	1.204×10^{-26}	1.491×10^{-26}	2.1	8.0	-19.23
Fe^{54} (n, p) Mn^{54}	0.0	1.378×10^{-26}	1.334×10^{-26}	1.9	8.1	+ 3.34
S^{32} (n, p) P^{32}	- 1.5	8.229×10^{-27}	7.931×10^{-27}	2.4	8.1	+ 3.76
Mg^{24} (n, p) Na^{24}	+12.0	3.297×10^{-28}	2.873×10^{-28}	6.6	12.2	+14.78
Al^{27} (n,α) Na^{24}	-18.0	1.145×10^{-28}	1.352×10^{-28}	6.7	12.5	-15.30
Cl^{35} (n,α) P^{32}	- 7.5	1.781×10^{-27}	1.730×10^{-27}	3.2	8.7	+ 2.95
I^{127} (n, 2n) I^{126}	+ 4.5	2.159×10^{-28}	2.095×10^{-28}	10.1	14.7	+ 3.06
			Standard Deviation of Measured Activities			9.32%

*Errors selected at random from a set of percent error values with an assumed normal distribution and a standard deviation of 15%.
†The input values of saturated measured activities listed in Table I were either increased or decreased by this percentage for this second SAND II run.
§Means foil detector is covered with cadmium.

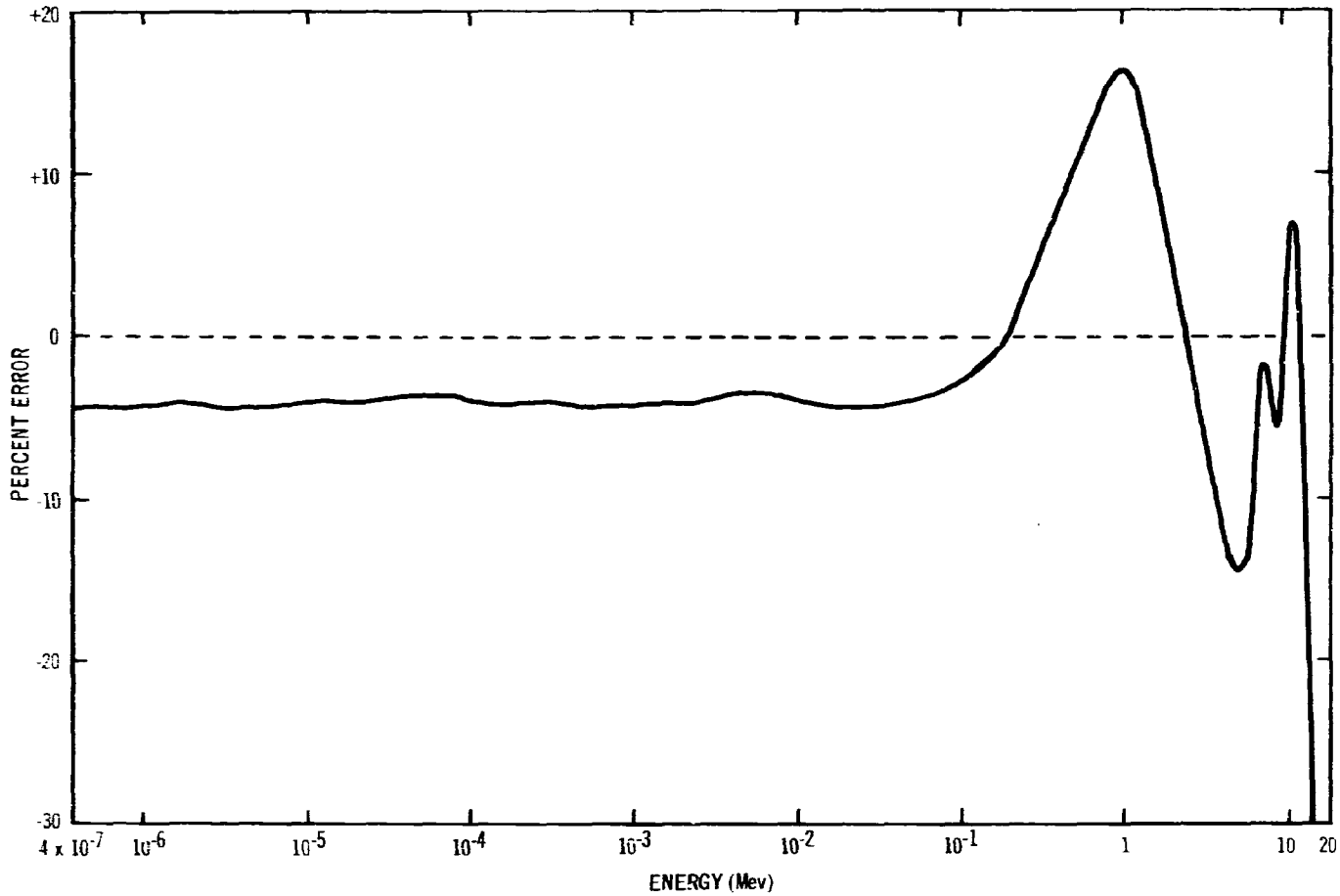

Figure 9. SAND II 3rd Iterative and True Test Spectrum Integral Flux Comparison for the Ground Test Reactor Core Flux Spectrum, Test 1 with Random Activity Errors

The selection of a best set of foil detectors depends on having adequate knowledge about the anticipated form of an unknown spectrum. Without such knowledge, a selected set may not contain foils with suitable energy sensitivity limits for the unknown spectrum. Since the forms of the 4 test spectra were originally not known, the set of 14 foil reactions used was based on a set that had previously been found suitable for both fission and fusion type environments.

These four cases were used to test the capability of the SAND II code to select a proper input approximation from the current reference library. The results presented, therefore, are representative of the type of solution that might be obtained when the SAND II code is used in a "black box" fashion.

Biggers had selected four spectra with different ratios of resonance to fast to fusion neutrons, identified as Tests 3, 4, 5, and 6. He had used the cross section data of reference 17 to calculate the saturated activities of the 14 foils, for each of the four test cases. These calculations utilized a group structure with four energy groups per decade (group energy limits within each decade: 1, 2, 4, 7) below 1.0 Mev, and 0.5 Mev intervals above 1.0 Mev. Group-averaged cross sections based on uniform flux weighting within each group* were used to calculate the contribution of each group to the saturated activity of each foil. The results were summed for each foil and a random error was introduced into each of the 14 saturated activity values. The activities and assigned values of error as provided by Biggers for the 4 test cases are given in Table III.

For these tests, the solution criterion and foil discard values were assigned extreme values so that no foils would be discarded and the iteration would proceed to an assigned limit of 30 cycles. Although this procedure is unrealistic from an experimental standpoint, it does make the effect of experimental errors (those assigned in Table III) more pronounced for studying the iterative process.

In a completely "black box" fashion, the SAND II code selected the initial spectral approximation, performed the numerical steps of iteration, and provided a solution. The detector results for Tests 3, 4, 5, and 6 are presented in Tables IV, V, VI and VII respectively. An integral flux comparison was made of the SAND II solutions with the "true" spectra for all cases, and the results are

*This is a substantially more coarse approximation than that used in SAND II, where the energy interval division is much finer (see Section III-A).

Table III

INPUT CALCULATED SATURATED FOIL ACTIVITIES
FOR BIGGERS' TEST SPECTRA

Foil Detector	Test 3 Value Used (dps/nucleus)	Assigned % Experimental Error	Test 4 Value Used (dps/nucleus)	Assigned % Experimental Error	Test 5 Value Used (dps/nucleus)	Assigned % Experimental Error	Test 6 Value Used (dps/nucleus)	Assigned % Experimental Error
Au^{197} (n,γ)	1.178×10^{-21}	0	2.244×10^{-22}	-10	2.764×10^{-21}	-21.8	3.460×10^{-20}	-13.1
Cc^{59} (n,γ)	3.329×10^{-23}	0	1.764×10^{-23}	+10	1.176×10^{-22}	+17.8	1.579×10^{-21}	+17.6
Na^{23} (n,γ)	1.154×10^{-24}	0	9.412×10^{-25}	+10	4.687×10^{-24}	+35.4	7.122×10^{-24}	-12.8
Cu^{63} (n,γ)	8.405×10^{-23}	0	5.159×10^{-23}	+10	2.544×10^{-22}	+ 0.9	1.320×10^{-22}	+17.7
In^{115} (n,n′)	3.564×10^{-23}	0	3.836×10^{-22}	-10	1.534×10^{-22}	+43.5	1.931×10^{-23}	-13.1
S^{32} (n,p)	1.495×10^{-23}	0	4.057×10^{-22}	-10	5.124×10^{-23}	+14.2	9.896×10^{-24}	+17.9
Ni^{58} (n,p)	2.766×10^{-23}	0	8.452×10^{-22}	+10	1.068×10^{-22}	+28.7	1.785×10^{-23}	+17.6
Fe^{54} (n,p)	2.525×10^{-23}	0	6.644×10^{-22}	-10	9.636×10^{-23}	+27.2	1.616×10^{-23}	+17.7
Cl^{35} (n,α)	4.181×10^{-24}	0	1.475×10^{-22}	-10	1.372×10^{-23}	+ 9.4	4.038×10^{-24}	-13.2
Al^{27} (n,p)	2.239×10^{-24}	0	9.024×10^{-23}	-10	6.426×10^{-24}	- 4.3	5.135×10^{-25}	-13.1
Mg^{24} (n,p)	3.336×10^{-24}	0	1.880×10^{-22}	+10	1.483×10^{-23}	+48.2	2.171×10^{-24}	+17.7
Al^{27} (n,α)	1.904×10^{-24}	0	1.016×10^{-22}	+10	6.359×10^{-24}	+11.3	1.612×10^{-24}	-12.9
I^{127} (n,2n)	1.496×10^{-23}	0	8.193×10^{-22}	+10	1.008×10^{-23}	-77.5	8.004×10^{-24}	-13.2
Zr^{90} (n,2n)	5.423×10^{-24}	0	3.863×10^{-22}	+10	1.500×10^{-23}	- 7.8	2.540×10^{-24}	+17.6

Table IV

SAND II SOLUTION RESULTS OBTAINED AFTER 30 ITERATIONS FOR TEST 3

Foil Reaction	Saturated Measured Activity (dps/nucleus)	Saturated Calculated Activity (dps/nucleus)	Nominal 5% Activity Limits (Mev)		% Deviation of Measured From Calculated Activity
			Lower	Upper	
Na^{23} (n,γ) Na^{24} Cd*	1.154×10^{-24}	1.156×10^{-24}	4.4×10^{-4}	0.14	- 0.18
Au^{197} (n,γ) Au^{198} Cd*	1.178×10^{-21}	1.178×10^{-21}	2.0×10^{-4}	0.03	0.02
Co^{59} (n,γ) Co^{60} Cd*	3.329×10^{-23}	3.336×10^{-23}	1.2×10^{-4}	0.014	- 0.20
Cu^{63} (n,γ) Cu^{64} Cd*	8.405×10^{-23}	8.415×10^{-23}	5.6×10^{-4}	0.07	- 0.12
In^{115} (n,n') In^{115m}	3.564×10^{-23}	3.533×10^{-23}	1.1	8.1	0.88
Ni^{58} (n, p) Co^{58}	2.766×10^{-23}	2.809×10^{-23}	2.2	14.1	- 1.53
Fe^{54} (n, p) Mn^{54}	2.525×10^{-23}	2.518×10^{-23}	2.0	14.2	0.29
S^{32} (n, p) P^{32}	1.495×10^{-23}	1.533×10^{-23}	2.6	14.2	- 2.49
Al^{27} (n, p) Mg^{27}	2.239×10^{-24}	2.227×10^{-24}	4.0	14.6	0.52
Mg^{24} (n, p) Na^{24}	3.336×10^{-24}	3.188×10^{-24}	7.4	14.8	4.65
Al^{27} (n,α) Na^{24}	1.904×10^{-24}	1.764×10^{-24}	7.7	14.8	7.92
Cl^{35} (n,α) P^{32}	4.181×10^{-24}	4.238×10^{-24}	3.4	14.5	- 1.34
I^{127} (n, 2n) I^{126}	1.496×10^{-23}	1.420×10^{-23}	12.2	14.9	5.36
Zr^{90} (n, 2n) Zr^{89}	5.423×10^{-24}	6.289×10^{-24}	13.3	15.0	-13.78
Standard Deviation of Measured Activities					4.92%

*Means foil detector is covered with cadmium.

Table V

SAND II SOLUTION RESULTS OBTAINED AFTER 30 ITERATIONS FOR TEST 4

Foil Reaction	Saturated Measured Activity (dps/nucleus)	Saturated Calculated Activity (dps/nucleus)	Nominal 5% Activity Limits (Mev)		% Deviation of Measured From Calculated Activity
			Lower	Upper	
Na^{23} (n,γ) Na^{24} Cd*	9.412×10^{-25}	9.425×10^{-25}	2.0×10^{-3}	14.7	- 0.13
Au^{197} (n,γ) Au^{198} Cd*	2.244×10^{-22}	2.245×10^{-22}	3.0×10^{-4}	9.1	- 0.04
Co^{59} (n,γ) Co^{60} Cd*	1.764×10^{-23}	1.766×10^{-23}	1.2×10^{-4}	2.2	- 0.13
Cu^{63} (n,γ) Cu^{64} Cd*	5.159×10^{-23}	5.167×10^{-23}	5.6×10^{-4}	7.4	- 0.15
In^{115} (n, n′) In^{115m}	3.836×10^{-22}	3.896×10^{-22}	1.5	14.3	- 1.55
Ni^{58} (n, p) Co^{58}	8.452×10^{-22}	7.368×10^{-22}	3.2	14.7	14.71
Fe^{54} (n, p) Mn^{54}	6.644×10^{-22}	6.798×10^{-22}	3.1	14.8	- 2.27
S^{32} (n, p) P^{32}	4.057×10^{-22}	4.358×10^{-22}	3.3	14.8	- 6.91
Al^{27} (n, p) Mg^{27}	9.024×10^{-23}	9.714×10^{-23}	5.4	14.9	- 7.10
Mg^{24} (n, p) Na^{24}	1.880×10^{-22}	1.758×10^{-22}	8.2	15.0	6.91
Al^{27} (n, α) Na^{24}	1.016×10^{-22}	1.023×10^{-22}	8.9	15.0	- 0.72
Cl^{35} (n, α) P^{32}	1.475×10^{-22}	1.488×10^{-22}	4.1	14.9	- 0.85
I^{127} (n, 2n) I^{126}	8.193×10^{-22}	8.672×10^{-22}	11.6	15.0	- 5.52
Zr^{90} (n, 2n) Zr^{89}	3.863×10^{-22}	3.723×10^{-22}	13.1	15.1	3.76
		Standard Deviation of Measured Activities			5.65%

*Means foil detector is covered with cadmium.

Table VI

SAND II SOLUTION RESULTS OBTAINED AFTER 30 ITERATIONS FOR TEST 5

Foil Reaction	Saturated Measured Activity (dps/nucleus)	Saturated Calculated Activity (dps/nucleus)	Nominal 5% Activity Limits (Mev)		% Deviation of Measured From Calculated Activity
			Lower	Upper	
Na^{23} (n,γ) Na^{24} Cd^{*}	4.687×10^{-24}	4.798×10^{-24}	6.4×10^{-4}	0.14	- 2.31
Au^{197} (n,γ) Au^{198} Cd^{*}	2.764×10^{-21}	2.829×10^{-21}	2.6×10^{-4}	0.072	- 2.31
Co^{59} (n,γ) Co^{60} Cd^{*}	1.176×10^{-22}	1.204×10^{-22}	1.2×10^{-4}	0.014	- 2.31
Cu^{63} (n,γ) Cu^{64} Cd^{*}	2.544×10^{-22}	2.604×10^{-22}	5.6×10^{-4}	0.094	- 2.31
In^{115} (n,n′) In^{115m}	1.534×10^{-22}	1.576×10^{-22}	1.1	8.6	- 2.68
Ni^{58} (n, p) Co^{58}	1.068×10^{-22}	1.039×10^{-22}	2.0	10.1	2.75
Fe^{54} (n, p) Mn^{54}	9.636×10^{-23}	9.780×10^{-23}	1.9	10.2	- 1.48
S^{32} (n, p) P^{32}	5.124×10^{-23}	5.328×10^{-23}	2.4	13.8	- 3.83
Al^{27} (n, p) Mg^{27}	6.426×10^{-24}	9.170×10^{-24}	5.1	14.5	-29.93
Mg^{24} (n, p) Na^{24}	1.483×10^{-23}	1.228×10^{-23}	7.5	14.8	20.81
Al^{27} (n,α) Na^{24}	6.359×10^{-24}	5.436×10^{-24}	7.6	14.9	16.97
Cl^{35} (n,α) P^{32}	1.372×10^{-23}	1.435×10^{-23}	3.6	14.5	- 4.37
I^{127} (n, 2n) I^{126}	1.008×10^{-23}	1.760×10^{-23}	13.5	15.2	-42.72
Zr^{90} (n, 2n) Zr^{89}	1.500×10^{-23}	9.758×10^{-24}	13.8	15.3	53.72
				Standard Deviation of Measured Activities	22.19%

*Means foil detector is covered with cadmium.

Table VII

SAND II SOLUTION RESULTS OBTAINED AFTER 30 ITERATIONS FOR TEST 6

Foil Reaction	Saturated Measured Activity (dps/nucleus)	Saturated Calculated Activity (dps/nucleus)	Nominal 5% Activity Limits (Mev)		% Deviation of Measured From Calculated Activity
			Lower	Upper	
Na^{23} (n,γ) Na^{24} Cd*	7.122×10^{-24}	7.375×10^{-24}	5.0×10^{-7}	3.2×10^{-3}	- 3.43
Au^{197} (n,γ) Au^{198} Cd*	3.460×10^{-20}	3.583×10^{-20}	4.0×10^{-6}	7.6×10^{-6}	- 3.43
Co^{59} (n,γ) Co^{60} Cd*	1.579×10^{-21}	1.635×10^{-21}	7.8×10^{-7}	1.6×10^{-4}	- 3.44
Cu^{63} (n,γ) Cu^{64} Cd*	1.320×10^{-22}	1.367×10^{-22}	6.4×10^{-7}	0.016	- 3.43
In^{115} (n,n′) In^{115m}	1.931×10^{-23}	2.026×10^{-23}	1.1	10.1	- 4.68
Ni^{58} (n, p) Co^{58}	1.785×10^{-23}	1.828×10^{-23}	2.4	13.3	- 2.37
Fe^{54} (n, p) Mn^{54}	1.616×10^{-23}	1.590×10^{-23}	2.2	13.6	1.66
S^{32} (n, p) P^{32}	9.896×10^{-24}	1.082×10^{-23}	2.7	13.5	- 8.53
Al^{27} (n, p) Mg^{27}	5.135×10^{-25}	1.283×10^{-24}	3.8	15.3	-59.98
Mg^{24} (n, p) Na^{24}	2.171×10^{-24}	1.913×10^{-24}	9.0	16.0	13.46
Al^{27} (n, α) Na^{24}	1.612×10^{-24}	1.116×10^{-24}	9.5	16.0	44.44
Cl^{35} (n, α) P^{32}	4.038×10^{-24}	2.796×10^{-24}	3.4	15.0	44.42
I^{127} (n, 2n) I^{126}	8.004×10^{-24}	8.451×10^{-24}	11.0	16.7	- 5.29
Zr^{90} (n, 2n) Zr^{89}	2.540×10^{-24}	2.803×10^{-24}	12.8	17.6	- 9.40
			Standard Deviation of Measured Activities		24.79%

*Means foil detector is covered with cadmium.

given in Tables VIII, IX, X, and XI. The results for Test 3 are also displayed graphically in Figure 10 for comparison and further discussion.

For Test 3, and as explained in reference 3, no solution could be obtained with the SAND I code "by-hand" procedure below 1 Mev, because the foil set selected was not suitable for this spectrum.* With SAND II, however, a satisfactory solution was obtained and, in fact, the value of total flux obtained is seen to be very accurate (less than 1/4% error). The relatively large error (nearly 20%) in the region about 10^{-3} Mev probably results from an assumed fission form in the low energy range for the input approximation, while the true spectrum had zero flux below 10^{-3} Mev (the arbitrary low limit of the calculation by Biggers). The "blowup" of the solution in the region above approximately 14 Mev results from the same kind of pathology in the true spectrum, which was assigned zero flux above 15.5 Mev. This type of behavior was not found in other tests, where there were no assigned sharp flux cutoff points. No provision is included in SAND II for coping with spectra having a sudden cutoff limit.

The effect of experimental errors on the solution was amplified in these tests by setting the solution criterion value very low, <0.1%, so that iteration would continue to the specified limit of 30 cycles; this allows the integral solution to develop more structure to become more nearly exact.† The effect of these errors on the solution is clearly seen in a comparison of the results in Table XI for the energy region between 4 and 8 Mev with the results for the individual foils, Tables III and VII, for Test 6. The $Al^{27}(n, p)$ assigned value of error (-13.1%) is obviously in error itself. The deviation of measured from calculated activity for this one reaction is -59.98%, which is 2.42 standard deviations. Based on a reasonable foil discard criterion of 1.96 standard deviations (95% confidence level assuming normally distributed errors), this foil would have been discarded in a normal SAND II run (see Section IV-A-2). In a

*The SAND I iterative procedure involved graphical plotting of integral flux points and differentiation by a "by-hand" best fit integral flux curve.

†Exactness in this sense refers to the degree of consistency of the input "measured" activities, or the degree to which the ratios of measured to calculated activities for the spectrum in question agree; exactness is not necessarily meant to infer correctness.

Table VIII

TEST 3 – COMPARISON OF THE SAND II 30th ITERATION ABSOLUTE INTEGRAL FLUX RESULTS WITH THE TRUE TEST SPECTRUM

Neutron* Energy (Mev)	Integral Neutron Flux		Ratio SAND II/TTS
	True Test Spectrum (TTS)	SAND II Spectrum	
4×10^{-7}	-	3.171×10^{4}	-
1×10^{-4}	-	3.169×10^{4}	-
1×10^{-3}	3.282×10^{4}†	2.840×10^{4}	0.865
1×10^{-2}	2.167×10^{4}	2.300×10^{4}	1.061
1×10^{-1}	1.786×10^{4}	1.509×10^{4}	0.845
1.0	9.343×10^{3}	9.354×10^{3}	1.001
1.5	6.963×10^{3}	7.032×10^{3}	1.010
2.0	5.063×10^{3}	5.155×10^{3}	1.018
3.0	3.055×10^{3}	3.138×10^{3}	1.027
4.0	2.172×10^{3}	2.176×10^{3}	1.002
5.0	1.578×10^{3}	1.676×10^{3}	1.062
6.0	1.280×10^{3}	1.349×10^{3}	1.054
7.0	1.112×10^{3}	1.122×10^{3}	1.009
8.0	9.935×10^{2}	9.228×10^{2}	0.920
9.0	9.122×10^{2}	7.866×10^{2}	0.862
10.0	8.306×10^{2}	7.158×10^{2}	0.862
11.0	7.548×10^{2}	6.804×10^{2}	0.901
12.0	6.589×10^{2}	6.504×10^{2}	0.986
13.0	5.273×10^{2}	5.927×10^{2}	1.124
14.0	2.503×10^{2}	3.063×10^{2}	1.224
15.5	0	1.971×10^{1}	-

*Not all of the "true" spectrum's energy points are listed.
†The "true" differential flux was set equal to zero below 10^{-3} Mev.

Table IX

TEST 4 – COMPARISON OF THE SAND II 30th ITERATION ABSOLUTE INTEGRAL FLUX RESULTS WITH THE TRUE TEST SPECTRUM

Neutron* Energy (Mev)	Integral Neutron Flux		Ratio SAND II/TTS
	True Test Spectrum (TTS)	SAND II Spectrum	
4×10^{-7}	-	1.325×10^{5}	-
1×10^{-4}	-	1.325×10^{5}	-
1×10^{-3}	1.570×10^{5}†	1.322×10^{5}	0.842
4×10^{-3}	1.565×10^{5}	1.316×10^{5}	0.841
1×10^{-2}	1.555×10^{5}	1.306×10^{5}	0.840
4×10^{-2}	1.541×10^{5}	1.294×10^{5}	0.840
1×10^{-1}	1.521×10^{5}	1.289×10^{5}	0.847
4×10^{-1}	1.431×10^{5}	1.284×10^{5}	0.897
1.0	1.251×10^{5}	1.218×10^{5}	0.947
1.5	1.201×10^{5}	1.121×10^{5}	0.933
2.0	1.126×10^{5}	1.039×10^{5}	0.923
3.0	8.920×10^{4}	9.036×10^{4}	1.013
4.0	8.525×10^{4}	7.902×10^{4}	0.927
5.0	7.550×10^{4}	7.000×10^{4}	0.927
6.0	6.600×10^{4}	6.300×10^{4}	0.955
7.0	5.830×10^{4}	5.791×10^{4}	0.993
8.0	5.430×10^{4}	5.369×10^{4}	0.989
9.0	4.755×10^{4}	4.983×10^{4}	1.048
10.0	4.155×10^{4}	4.626×10^{4}	1.114
11.0	3.775×10^{4}	4.259×10^{4}	1.128
12.0	3.435×10^{4}	3.864×10^{4}	1.125
13.0	3.135×10^{4}	3.275×10^{4}	1.045
14.0	2.020×10^{4}	2.009×10^{4}	0.995
15.0	2.900×10^{3}	2.494×10^{3}	0.860

*Not all of the true spectrum's energy points are listed.
†The "true" differential flux was set equal to zero below 10^{-3} Mev.

Table X

TEST 5 – COMPARISON OF THE SAND II 30th ITERATION ABSOLUTE INTEGRAL FLUX RESULTS WITH THE TRUE TEST SPECTRUM

Neutron* Energy (Mev)	Integral Neutron Flux		Ratio† SAND II/TTS
	True Test Spectrum (TTS)	SAND II Spectrum	
4×10^{-7}	-	1.112×10^{5}	-
1×10^{-4}	-	1.111×10^{5}	-
1×10^{-3}	9.846×10^{4}	1.041×10^{5}	1.057
1×10^{-2}	6.501×10^{4}	8.784×10^{4}	1.352
1×10^{-1}	5.358×10^{4}	6.678×10^{4}	1.247
1.0	2.803×10^{4}	4.372×10^{4}	1.560
1.5	2.089×10^{4}	2.999×10^{4}	1.437
2.0	1.519×10^{4}	1.865×10^{4}	1.228
3.0	9.165×10^{3}	9.558×10^{3}	1.043
4.0	6.516×10^{3}	7.386×10^{3}	1.134
5.0	4.734×10^{3}	6.606×10^{3}	1.395
6.0	3.840×10^{3}	6.300×10^{3}	1.641
7.0	3.336×10^{3}	5.789×10^{3}	1.736
8.0	2.981×10^{3}	4.307×10^{3}	1.445
9.0	2.737×10^{3}	2.045×10^{3}	0.747
10.0	2.492×10^{3}	8.592×10^{2}	0.345
11.0	2.264×10^{3}	7.914×10^{2}	0.350
12.0	1.977×10^{3}	7.896×10^{2}	0.400
13.0	1.582×10^{3}	7.866×10^{2}	0.497
14.0	7.509×10^{2}	6.378×10^{2}	0.907
15.0	0	1.070×10^{2}	-

*Not all of the "true" spectrum's energy points are listed.

†The assigned errors in individual foil "measurements" (listed in Table III) and energy regions of greatest sensitivity (listed in Table VI) are not exactly consistent with the regions of maximum error in the solution spectrum. This is because the inordinately large assigned errors resulted in substantial shifts in energy regions of sensitivity, which in effect created large flux depressions and peaks with resultant "gaps" in the foil energy coverage. Large errors in measured activity have essentially the same kind of effect arithmetically as a poor initial approximation; the phenomenon of shifts in energy regions of sensitivity caused by a poor initial approximation is discussed in Volume II, Section II-D-3.

Table XI

TEST 6 – COMPARISON OF THE SAND II 30th ITERATION ABSOLUTE INTEGRAL FLUX RESULTS WITH THE TRUE TEST SPECTRUM

Neutron* Energy (Mev)	Integral Neutron Flux		Ratio SAND II/TTS
	True Test Spectrum (TTS)	SAND II Spectrum	
4×10^{-7}	3.238×10^{4}	2.914×10^{4}	0.900
1×10^{-6}	3.150×10^{4}	2.771×10^{4}	0.880
1×10^{-5}	2.882×10^{4}	2.419×10^{4}	0.839
1×10^{-4}	2.547×10^{4}	2.075×10^{4}	0.815
1×10^{-3}	2.127×10^{4}	1.732×10^{4}	0.814
4×10^{-3}	1.814×10^{4}	1.515×10^{4}	0.835
1×10^{-2}	1.600×10^{4}	1.355×10^{4}	0.847
4×10^{-2}	1.351×10^{4}	1.108×10^{4}	0.820
1×10^{-1}	1.192×10^{4}	9.456×10^{3}	0.793
4×10^{-1}	8.324×10^{3}	7.020×10^{3}	0.843
1.0	4.054×10^{3}	5.036×10^{3}	1.242
1.5	3.307×10^{3}	4.048×10^{3}	1.224
2.0	3.117×10^{3}	3.274×10^{3}	1.050
3.0	2.204×10^{3}	2.273×10^{3}	1.031
4.0	2.013×10^{3}	1.480×10^{3}	0.735
5.0	1.466×10^{3}	7.566×10^{2}	0.516
6.0	1.180×10^{3}	6.642×10^{2}	0.563
7.0	9.184×10^{2}	6.360×10^{2}	0.693
8.0	7.044×10^{2}	6.144×10^{2}	0.872
9.0	6.331×10^{2}	5.861×10^{2}	0.926
10.0	5.756×10^{2}	5.428×10^{2}	0.943
11.0	5.110×10^{2}	4.677×10^{2}	0.915
12.0	4.412×10^{2}	3.489×10^{2}	0.791
13.0	3.135×10^{2}	2.096×10^{2}	0.669
14.0	7.580×10^{1}	1.260×10^{2}	1.662
15.0	0	7.464×10^{1}	-

*Not all of the "true" spectrum's energy points are listed.

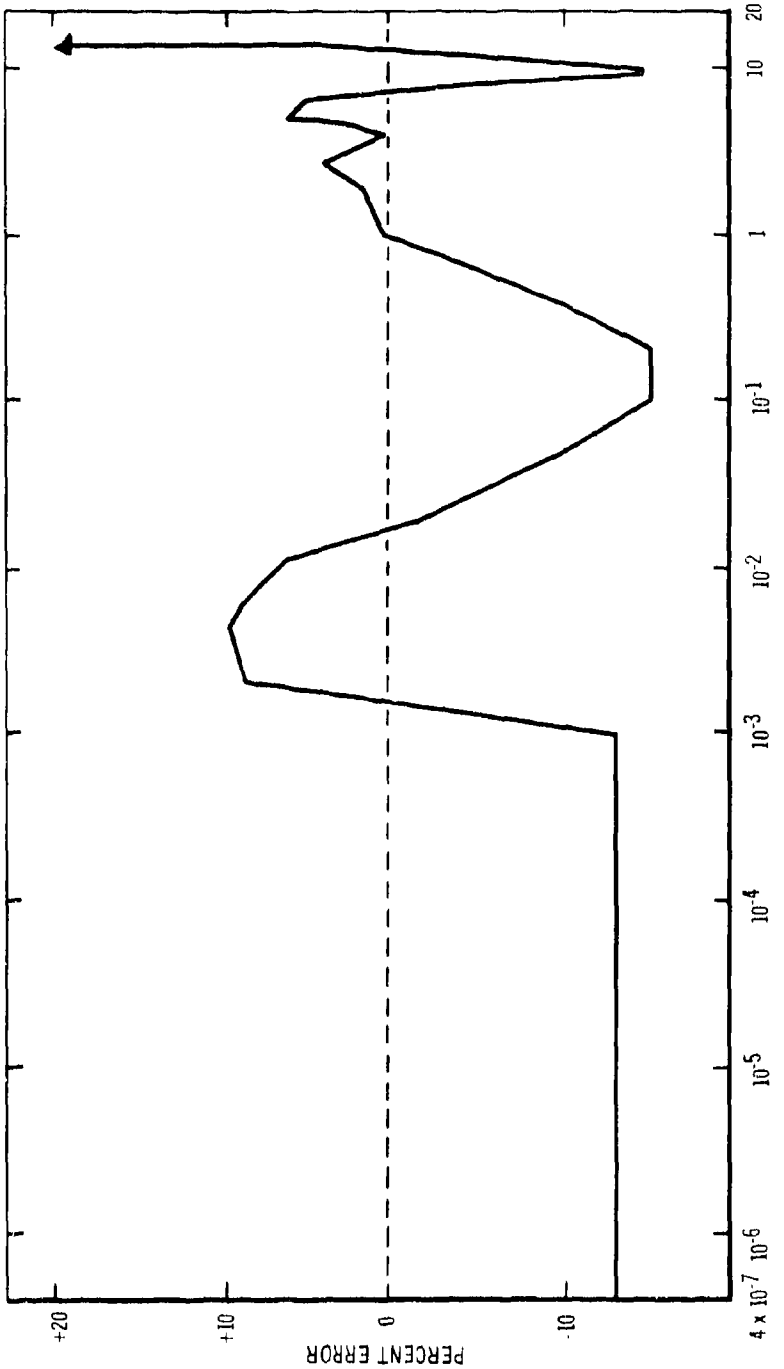

Figure 10. SAND II 30th Iterative and True Test Spectrum Integral Flux Comparison for Test 3

subsequent SAND II run for Test 6, the Al^{27} (n, p) reaction was removed and a new integral solution was obtained, which had deviations more consistent with the errors listed in Table III. The low ratios of the SAND II to true integral flux values, shown in Table XI between 4 and 8 Mev, are thus due mainly to a large inadvertent error in the value of activity for the Al^{27} (n, p) reaction,* beyond the intentional error listed in Table III.

The detector results given in Tables V and VI, and the integral flux results in Tables IX and X for Tests 4 and 5 respectively, are analogous in most respects to those of Tests 3 and 6, and require no further discussion.

Tests 1 through 13, as well as others not reported here, have helped to substantiate the expected capability of the SAND II code to yield integral flux results (by about the 5th to 30th cycle of iteration) that are accurate to within 10 to 30% at all energy points over the range of 10^{-10} to 18 Mev, if the absolute errors in measured activity and foil reaction cross sections are within similar limits and the set of foil reactions has been properly selected for the spectrum being measured.

SECTION V
INTERPRETATION OF EXPERIMENTAL DATA USING THE SAND II CODE

A. Foil Activation Measurements

1. Foil Set Selection

For the tests discussed in Section V-B, the choice of foil material was dictated primarily by the half-life of the product nuclide and the accuracy with which the reaction cross section was known. Another important factor was the degree of gamma heating and/or fission heating which the foil would experience. Table XII is a compilation of all the foil detectors used, along with pertinent nuclear data.

In general, all non-fissionable foils were made ~1/2 inch diameter and then were packaged together so that the axial length of one completely assembled

*In reference 3, Figure 3, the negative displacement of the integral flux point for the Al^{27}(n, p) reaction is also consistent with this conclusion, which had not been noted in the previous study.

Table XII

FOIL DETECTOR NUCLEAR AND PHYSICAL PROPERTIES

Foil Form	Foil Reaction	Product Nuclide's Half-Life
U^{238}	$U^{238}(n,\gamma)U^{239}$	*
	$U^{238}(n,f)$ F.P.	*
Th^{232}	$Th^{232}(n,f)$ F.P.	*
U^{235}	$U^{235}(n,f)$ F.P.	*
Np^{237}	$Np^{237}(n,f)$ F.P.	*
NaCl (30 to 187 mil foils)	$Na^{23}(n,\gamma)Na^{24}$	15.00 hours
	$Cl^{35}(n,\alpha)P^{32}$	14.41 days
Au (1/2 and 2 mil foils)	$Au^{197}(n,\gamma)Au^{198}$	2.698 days
0.130% Au-Al (20 mil wire)	$Au^{197}(n,\gamma)Au^{198}$	2.698 days
Co (40 mil wire)	$Co^{59}(n,\gamma)Co^{60}$	5.242 years
0.483% Co-Al (30 mil wire)	$Co^{59}(n,\gamma)Co^{60}$	5.242 years
0.457% Co-Al (5 mil foil)	$Co^{59}(n,\gamma)Co^{60}$	5.242 years
80% Mn - 20% Cu (2 mil foil)	$Mn^{55}(n,\gamma)Mn^{56}$	2.58 hours
	$Cu^{63}(n,\gamma)Cu^{64}$	12.84 hours
Cu (0.7 to 5 mil foils)	$Cu^{63}(n,\gamma)Cu^{64}$	12.84 hours
In (10 mil foil)	$In^{115}(n,n')In^{115m}$	4.51 hours
Fe (5 mil foil and ≤ 20 mil wire)	$Fe^{54}(n,p)Mn^{54}$	313.5 days
	$Fe^{56}(n,p)Mn^{56}$	2.58 hours
S (187 mil foil)	$S^{32}(n,p)P^{32}$	14.41 days
Ni (10 mil foil)	$Ni^{58}(n,p)Co^{58}$	71.7 days
	$Ni^{58}(n,2n)Ni^{57}$	36.7 hours
Al (7 and 30 mil foils)	$Al^{27}(n,\alpha)Na^{24}$	15.00 hours
Mg (5 mil foil)	$Mn^{24}(n,p)Na^{24}$	15.00 hours
KI (70 to 150 mil foils)	$I^{127}(n,2n)I^{126}$	13.1 days
NH_4I (187 mil foil)	$I^{127}(n,2n)I^{126}$	13.1 days
Zr (5 mil foil)	$Zr^{90}(n,2n)Zr^{89}$	78.4 hours

*These reactions were analyzed by fission product (Mo^{99}) and/or fission track counting (except for the $U^{238}(n,\gamma)$ reaction which was analyzed by Np^{239} counting) by Armani (Ref. 18) and Tochilin (Ref. 19) respectively.

set was about 1/2 to 1 inch. The individual foils were separated by 1.3 mil aluminum spacers to prevent cross contamination during handling. The entire foil set was wrapped in aluminum foil and irradiated bare, cadmium-covered, and/or boron-covered as required. In some instances, such as for the resonance detectors, individual foils were prepared and irradiated separately in order to study the self-shielding effect of the entire package (or a specific foil material). In this regard the use of thick, thin, and alloyed resonance foil materials helped considerably in the analysis of data. (Experience gained from these tests has shown that it is not practical to use alloys and/or backing material in cases where the diluent and/or backing materials have reaction product nuclides longer lived than the reaction product nuclide of interest, such as indium with aluminum backing.) The fission detectors were always contained in separate packages that were placed adjacent to (or in the same location as, if separate irradiations were made) the non-fissionable foils. In some cases involving low flux levels, it was necessary to wrap the iron and cobalt-aluminum wires around the outside of the assembled package to increase the total quantity of foil material without causing serious self-absorption-scattering effects.

An initial irradiation using most of the foil materials uncovered some problems with the foil detectors that might not have become evident in subsequent tests. Examination of these foils revealed that cross contamination of the foil materials had occurred during manufacture and that some of the certified assay values for the alloys were inaccurate. The correct values for these alloys determined by subsequent chemical analyses are given in Table XII.

2. Foil Activity Measurement Techniques*

Comparable capability for measuring the foil activities exists at each of the laboratory sites [ANL (Ref. 18), USNRDL (Ref. 19), Sandia (Ref. 20), BNW (Ref. 21), and Stanford (Ref. 22)] involved in this program, as evidenced by the excellent agreement of results obtained for the measurement of foils common to most laboratories. Each laboratory measured particular foils or foil sets. Most of the sets were measured by Atomics International.

*Only the methods employed at Atomics International are discussed, but they are representative, in a general sense, of currently used techniques.

A 4π gamma ionization chamber is the primary instrument at AI for the calibration of gamma-emitting nuclides. Cross calibration of the chamber's response with the National Bureau of Standards has been effected for all available nuclides. The daily response of the 4π GIC is checked against an NBS Ra^{226} standard. Table XIII reports results of an interlaboratory comparison conducted by the ASTM Committee E-10, Sub V, on Neutron Dosimetry (Ref. 23). Similar results have been reported by Yoshikawa and Zimmer (Ref. 24).

Table XIII

ASTM INTERLABORATORY CALIBRATION RESULTS FOR SELECTED FOIL REACTIONS*

Laboratory	Reaction Product		
	Co^{58}	Co^{60}	Mn^{54}
Argonne National Laboratory	0.996 0.989	0.983 0.979	1.024 1.023
IIT Research Institute	0.960† 0.957†	0.996 0.971	1.037 0.999
Idaho - NRT	0.986 1.000	1.000 0.996	1.034 1.004
Atomics International	0.982 0.982	1.000 1.017	0.997 1.000
U. S. Naval Radiological Defense Laboratory	1.015 1.015	1.015 1.010	1.024 1.014
Pratt and Whitney	1.000 0.993	0.922 0.917	1.019 0.992
Euratom	1.04 (0.997)§	0.996	
	1.05 (1.003)§	0.994	

*The values given are the ratio of the reported activity by the participating laboratories to that measured by the reference laboratory for two separate foils; Battelle Northwest (R. Dahl) served as the reference laboratory and provided the irradiated foils which had been measured by W. Zimmer at Iso-Chem Corporation.

†These values were obtained assuming a decay scheme somewhat different from that used by the other laboratories; if the same decay scheme had been used, these values would have been about 2% higher.

§Remeasured

Normally the set of calibrated gamma spectrometer standards is maintained at approximately 40 nuclides with many shorter lived nuclides being produced and calibrated as needed. These standards serve as both gamma energy and quantitative activity standards for the spectrometer.

At AI, a 4π gamma re-entrant high pressure (40 atmospheres) ionization chamber, a 2π proportional flow counter, and a 400 channel gamma spectrometer (with associated readout equipment) utilizing both a 3 in. x 3 in. NaI(Tl) well crystal and a 3 in. x 3 in. NaI(Tl) end window crystal, were involved in making the measurements for these tests.

Since some of the foil detectors were alloys (for reasons discussed in Section V-A-1), the gamma spectrometer was used to measure the separate activities of the components. The half-lives were followed to ascertain that no impurities were present to contribute errors to the measurement. In some foils the reaction product nuclide's half-life was long and did not afford a means with which to check the nuclide purity. The foil material Co-Al (see Table XII), after a reasonable decay period, was essentially free of the Na^{24} activity from the Al (n,α) reaction and was chemically free of other starting material impurities, yet was still nuclidically impure. Cobalt-59, which is 100% abundant, still has three reactions, $Co^{59}(n,\gamma)Co^{60}$; $Co^{59}(n,p)Fe^{59}$, and $Co^{59}(n,2n)Co^{58}$; the product nuclides' gamma ray energies from the last two are similar enough to interfere with the 1.17 Mev and 1.33 Mev photopeaks commonly used for the measurement of Co^{60}. To avoid errors caused by either over- or under-corrections for these extraneous activities, the 2.50 Mev coincidence sum peak, which is well removed from interference from these nuclides, was utilized for some of the measurements.

Selection of Zn as a foil detector posed a similar problem due to the γ-energy and half-life similarities of the reaction product nuclides from the $Zn^{64}(n,p)Cu^{64}$ and $Zn^{68}(n,\gamma)Zn^{69m}$ reactions. Zinc 69m emits a gamma ray with an energy of 0.44 Mev and has a half-life of 13.9 hours, whereas Cu^{64} emits a positron and has a half-life of 12.8 hours. (The 1.34 Mev gamma ray from Cu^{64} is not useful because of the relatively low number of gammas per disintegration.) When the positron from Cu^{64} is annihilated two gamma photons of 0.51 Mev are emitted. By using a NaI(Tl) well crystal, the sum peak at 1.02 Mev

due to the gamma photon pair from the positron annihilation can be used in the determination of Cu^{64} activity, thus avoiding the interference at 0.51 Mev caused by the 0.44 Mev gamma ray from Zn^{69m}.

This technique involving the measurement of positron annihilation radiation must be used with care to assure that no other positron-emitting nuclide is present to interfere. Such interference may be difficult to resolve, especially if the half-lives of the two positron-emitters are similar. In zinc, the $Zn^{64}(n,\gamma)Zn^{65}$ produces a positron-emitting nuclide, although in this case it may be corrected for easily because of the very different half-lives (12.9 hours for Cu^{64} and 243 days for Zn^{65}).

In certain foils, it may be impossible to distinguish an error-contributing impurity because a reaction product from the impurity is the same as the product of the pertinent reaction. For example, the $Fe^{56}(n,p)Mn^{56}$ activity measured in an iron foil may have interference from the $Mn^{55}(n,\gamma)Mn^{56}$ reaction caused by the presence of manganese as an impurity; in this case, manganese quantities of only several hundredths of one percent may yield Mn^{56} of the same order of magnitude as that produced by the reaction of interest. In one of the experiments discussed in Section V-B-2 (ECEL test), this problem was made evident by a comparison of the results of bare foil and boron 10-covered foil irradiations; the measured Mn^{56} activity was a factor of two higher for the bare iron foil than for the one in a boron 10 cover. (The $Mn^{55}(n,\gamma)Mn^{56}$ reaction cross section is most significant in the resonance region and below; flux in this region was essentially removed by the boron 10 cover.)

In some tests the high cross section of $In^{115}(n,\gamma)In^{116m}$ necessitated a 24-hour cooling period before attempting the $In^{115}(n,n')In^{115m}$ determination. Indium 114 produced by the $In^{113}(n,\gamma)In^{114m}$ reaction, because of its relatively long half-life and the ~5 half-life delay imposed by In^{116m}, was approximately an order of magnitude greater in activity than the In^{115m}. This three-way decay permitted approximately an 8-hour period (starting 24 hours after time of removal) in which to determine the In^{115m} activity and to verify the half-life. In spectra that were harder, a delay of 10 hours eliminated the In^{116m} interference, allowing the $In^{115}(n,n')In^{115m}$ measurement to be made before In^{114m} interfered appreciably.

Pure beta-emitting nuclides were determined by measuring either a sublimed or evaporated aliquot (on a platinum disk) in a 2π proportional flow counter. Other means of measurement exist, but this technique is quite adequate for beta energies greater than $\sim$ 0.3 Mev. As in the previous cases discussed, nuclide purity is a concern and now a much more serious problem than it had been in γ-spectrometric measurements. For example, the $Cl^{35}(n, \alpha)P^{32}$ reaction has interference from $Cl^{35}(n, p)S^{35}$, and the $S^{32}(n, p)P^{32}$ reaction has interference from $S^{33}(n, p)P^{33}$; all four product nuclides are pure beta emitters. The P^{32} activity was determined in both cases using an aluminum absorber to remove the contribution of the weaker betas (0.168 Mev from S^{35} and 0.25 Mev from P^{33}) to the count rate, and subsequently correcting the count rate for the attenuation of the P^{32} betas (1.71 Mev) by the absorber.

This discussion does not exhaust the possible difficulties that might be encountered in foil activity measurement. It is clear that, when reactions are used with which there is little or no previous experience, or when neutron environments are encountered which might produce unforeseen effects, the materials used and the reactions measured must be carefully examined to determine whether any problems such as those discussed here may be in effect, before any conclusions are drawn regarding the accuracy of the actual activity measurements or cross section evaluations.

It is interesting from a practical point of view to observe that the type of agreement achieved in the ASTM interlaboratory comparison, Table XIII, was never achieved in the current tests. There are reasons for this, however; the ASTM study only involved the re-counting of foils that had been previously counted by the reference laboratory (BNW). For the tests discussed in this report, Section V-B, the results are based on the counting of different foils by different laboratories; i.e., each laboratory provided its own sealed foil set that was irradiated and returned for counting. Since multiple irradiations were also performed in some cases, the assigned values of error reflected errors due to changes in flux level and exposure times. Consequently the values of errors (one standard deviation) listed in Tables XIV, XVI, XVIII, XX, XXI, XXII, XXIII, XXIV, and XXV are realistic, in the sense that they indicate what currently can be achieved (with a reasonable effort) in cases where the multiple foil technique has been utilized.

B. SAND II Foil Activation Data Reduction

1. Summary Discussion

The SAND II code has been used to determine experimentally the neutron flux spectra in different types of neutron environment. In each environment, a set of foil detectors, utilizing both low and high energy neutron reactions, was irradiated. Measured foil activities for each foil set (extrapolated to saturation, except in one pulsed case, in which time-of-removal values were required) were used as input to the code to obtain an appropriate solution flux spectrum for each environment.

One of the goals of the present work was to compare the results of the foil activation method with spectrometer measurements, multigroup diffusion and transport calculations, and Monte Carlo calculations. Emphasis was placed on attempting to correlate the effect of scattering and absorption (in materials such as carbon, oxygen, beryllium, iron, aluminum, chromium, and other elements present in a given environment) with structure that appeared in the SAND II iterative solution spectra. This required that a distinction be made between possible "true" structure and that resulting from foil activity, foil self-absorption, and foil cross section measurement errors.

As a convenience in the analysis of the experimental data, the thirtieth iterative results are used as the solution for the first five cases studied. For the sixth case, SAND II results are reported that were achieved using solution and foil discard criteria of 10% and 1.96 (95% confidence level), respectively.

For the experimental cases studies, the foil irradiations were performed using the following facilities:

a. WMGR, at the center of a homogeneous Water Moderated and Graphite Reflected water cooled reactor;

b. GMRA, at the center of a large graphite central region in a Graphite Moderated and Reflected Air cooled reactor;

c. GMRW, in a test location in a Graphite Moderated and Reflected Water cooled reactor;

d. SMFS, in a collimated beam from a Slightly Moderated Fission Source;

e. BRGM, in the leakage spectrum from a Beryllium oxide Reflected Graphite Moderated gas cooled reactor;

f. ECEL, in the central core region of the Epithermal Critical Experiment Laboratory fast critical assembly, Core 14-13.

In the SMFS beam, two tests were conducted in somewhat different locations (expected to yield qualitatively similar results, except for differences in side- and back-scattering effects). In both the GMRW and BRGM tests, there were significant amounts of foreign materials; in the GMRW, the foils used were surrounded by approximately 1/4 inch each of stainless steel, aluminum and water, and in the BRGM the foils were separated from the source by approximately 1/2 inch of Hastelloy C. The core region of the ECEL was made up of repeating 2" x 2" (by ~ 1/8 to 1/4" thick) squares of carbon, aluminum, stainless steel, uranium 238, and uranium 235 (Ref. 25). (Because of this arrangement of materials, the ECEL core region could be considered to be homogeneous for reactor physics calculations.)

It is clear from the study and analysis of these six test cases that most materials present in a given neutron environment have certain identifiable effects on the flux — that the total cross sections of all the materials in an environment are, in a rough qualitative way, mirrored in the neutron spectrum. Some examples of this may be seen in Fig. 11. All the structural features of the calculated spectra shown, as well as most of those of the measured spectra, are quite readily identifiable with structure in the total cross sections of the materials known to be present. The spectra shown in Fig. 11 will be used for comparison in discussing the test results presented in Section V-B-2.

2. Iterative Results

The SAND II foil activation results, integral flux comparison, and differential flux comparison for the WMGR, GMRA, and GMRW tests are presented in: Tables XIV, XVI, and XVIII; Tables XV, XVII, XIX; and Figs. 12, 13, and 14, respectively. In each figure, the dashed curve is the theoretical calculation (used as the input approximation) and the solid curve is the 30th iteration solution. In the lower part of each curve, pertinent representative spectra shown in Fig. 11 are reproduced (as dotted circle curves) to help establish the credibility of some of the differential structure generated in the iterative solution.

HETEROGENEOUS LIGHTWATER MODERATED AND COOLED THERMAL REACTOR [PROTON RECOIL EMULSION (Ref. 26)] ·

DEEP PENETRATION IN H_2O [CALCULATION (Ref. 27)]

TRIGA MARK III LEAKAGE SPECTRUM, 2 in. H_2O REFLECTOR [SPECTROMETRY (Ref. 15)]

SWIMMING POOL REACTOR, CLOSE TO CORE. [SPECTROMETRY (Ref. 28)]

DEEP PENETRATION IN HYDROGEN [CALCULATION (Ref. 27)]

DEEP PENETRATION IN $(CH)_x$ [CALCULATION (Ref. 27)]

SCATTERED BY CARBON AT 70° [SPECTROMETRY (Ref. 29)] ·

DEEP PENETRATION IN CARBON [CALCULATION (Ref. 27)] ·

DEEP PENETRATION IN BERYLLIUM [CALCULATION (Ref. 27)] ·

SCATTERED BY ALUMINUM AT 70° [SPECTROMETRY (Ref. 29)] ·

SCATTERED BY STEEL AT 1[illegible] SPECTROMETRY (Ref. 29)] ·

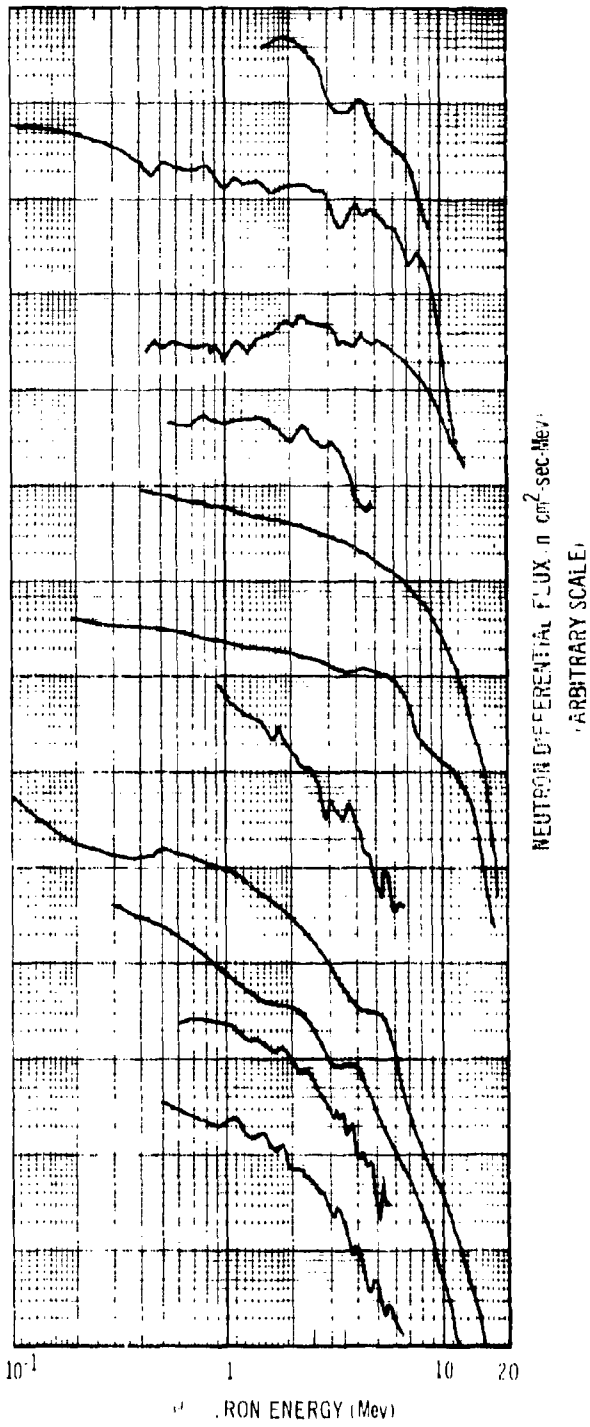

Figure 11. Representative Neutron Flux Spectra for Different Environments, Showing Depression Effects of Material Cross Sections

Table XIV

WMGR TEST

SAND II THIRTIETH ITERATION RATIOS OF MEASURED TO CALCULATED ACTIVITIES

Foil[a] Reaction	Saturated[b] Measured Activity (Dps/Nucleus)	Saturated Calculated Activity (Dps/Nucleus)	Ratio Meas./Calc. Activities
Na^{23} (n, γ) Na^{24}	$4.21 \times 10^{-26} \pm 5\%$	4.233×10^{-26}	0.995
Mn^{55} (n, γ) Mn^{56}	$2.02 \times 10^{-24} \pm 7\%$	2.031×10^{-24}	0.995
Cu^{63} (n, γ) Cu^{64}	$7.12 \times 10^{-25} \pm 12\%$	7.158×10^{-25}	0.995
Co^{59} (n, γ) Co^{60}	$1.01 \times 10^{-23} \pm 3\%$	1.015×10^{-23}	0.995
Au^{197} (n, γ) Au^{198}	$2.20 \times 10^{-22} \pm 10\%$	2.212×10^{-22}	0.995
Au^{115} (n, n') In^{115m}	$2.65 \times 10^{-25} \pm 10\%$	2.763×10^{-25}	0.959
Fe^{54} (n, p) Mn^{54}	$2.04 \times 10^{-25} \pm 15\%$	1.687×10^{-25}	1.21
Ni^{58} (n, p) Co^{58}	$2.14 \times 10^{-25} \pm 3\%$	2.012×10^{-25}	1.06
S^{32} (n, p) P^{32}	$7.50 \times 10^{-26} \pm 5\%$	1.011×10^{-25}	0.742
Cl^{35} (n, α) P^{32}	$2.92 \times 10^{-26} \pm 5\%$	2.747×10^{-26}	1.06
Al^{27} (n, α) Na^{24}	$1.36 \times 10^{-27} \pm 5\%$	1.254×10^{-27}	1.09
Mg^{24} (n, p) Na^{24}	$2.60 \times 10^{-27} \pm 5\%$	2.834×10^{-27}	0.918
I^{127} (n, 2n) I^{126}	$1.94 \times 10^{-27} \pm 10\%$	1.964×10^{-27}	0.988

Standard Percent Deviation of the Ratios = 10.6

(a) The foils were irradiated inside a ~ 40 mil cadmium-covered capsule.

(b) All measurements made at Atomics International. Experimental errors listed are one standard deviation.

Table XV

WMGR TEST

SAND II THIRTIETH ITERATION NORMALIZED INTEGRAL NEUTRON FLUX COMPARISON

Energy (Mev)	Theoretical (Ref. 30)	Experimental (30th Iteration)	Ratio Exp. / Theo.
4.14×10^{-7}	1.000	1.000	1.000
1.13×10^{-6}	0.968	0.961	0.99
3.06×10^{-6}	0.936	0.920	0.98
8.32×10^{-6}	0.903	0.881	0.98
2.26×10^{-5}	0.869	0.840	0.97
6.14×10^{-5}	0.835	0.801	0.96
4.54×10^{-4}	0.763	0.725	0.95
3.36×10^{-3}	0.690	0.644	0.93
1.7×10^{-2}	0.626	0.572	0.91
1.0×10^{-1}	0.540	0.475	0.88
4.0×10^{-1}	0.420	0.348	0.83
9.0×10^{-1}	0.302	0.282	0.93
1.4	0.223	0.250	1.12
3.0	7.54×10^{-2}	9.33×10^{-2}	1.24
4.0	3.85×10^{-2}	6.37×10^{-2}	1.65
5.0	1.91×10^{-2}	3.84×10^{-2}	2.01
6.0	9.23×10^{-3}	1.32×10^{-2}	1.43
7.0	4.38×10^{-3}	5.96×10^{-3}	1.36
8.0	2.05×10^{-3}	2.85×10^{-3}	1.39
9.0	9.47×10^{-4}	1.66×10^{-3}	1.75
10.0	4.32×10^{-4}	8.60×10^{-4}	1.99
11.0	1.95×10^{-4}	3.78×10^{-4}	1.94
12.0	8.72×10^{-5}	1.83×10^{-4}	2.09
13.0	3.84×10^{-5}	8.11×10^{-5}	2.11
14.0	1.66×10^{-5}	3.57×10^{-5}	2.15
15.0	6.92×10^{-6}	1.51×10^{-5}	2.18
16.0	2.66×10^{-6}	5.82×10^{-6}	2.19
17.0	8.04×10^{-7}	1.76×10^{-6}	2.18

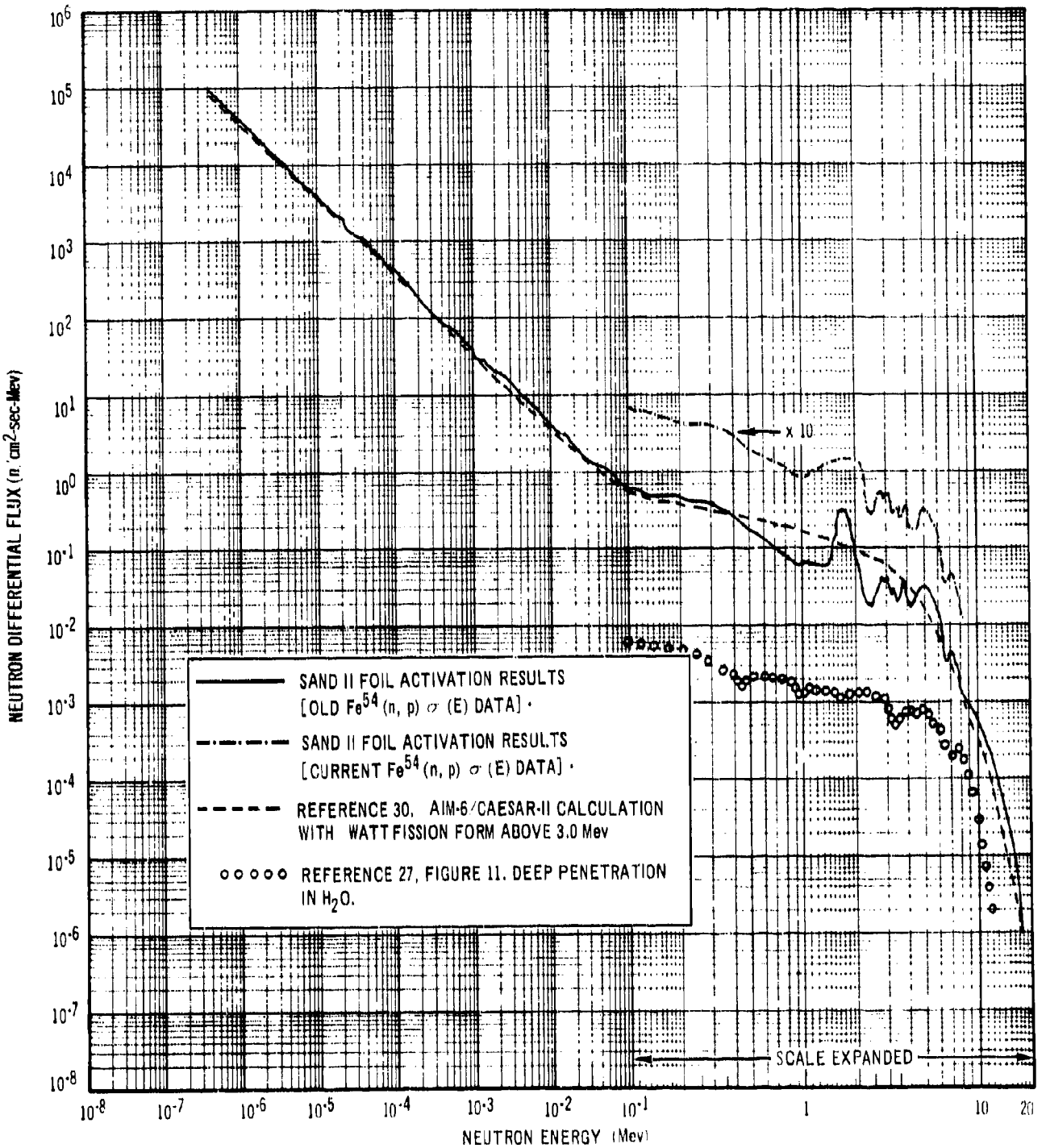

Figure 12. SAND II Differential Flux Results for the WMGR Test

Table XVI

GMRA TEST

SAND II THIRTIETH ITERATION RATIOS OF MEASURED TO CALCULATED ACTIVITIES

Foil[a] Reaction	Saturated[b] Measured Activity (Dps/Nucleus)	Saturated Calculated Activity (Dps/Nucleus)	Ratio Meas./Calc. Activities
Na^{23} (n, γ) Na^{24}	$3.26 \times 10^{-27} \pm 5\%$	3.276×10^{-27}	0.995
Mn^{55} (n, γ) Mn^{56}	$1.63 \times 10^{-25} \pm 7\%$	1.638×10^{-25}	0.995
Cu^{63} (n, γ) Cu^{64}	$6.00 \times 10^{-26} \pm 10\%$	6.029×10^{-26}	0.995
Co^{59} (n, γ) Co^{60}	$1.15 \times 10^{-24} \pm 20\%$	1.156×10^{-24}	0.995
Au^{197} (n, γ) Au^{198}	$1.90 \times 10^{-23} \pm 7\%$	1.909×10^{-23}	0.995
In^{115} (n, n') In^{115m}	$1.75 \times 10^{-27} \pm 10\%$	1.801×10^{-27}	0.972
Ni^{58} (n, p) Co^{58}	$9.62 \times 10^{-28} \pm 3\%$	8.004×10^{-28}	1.20
S^{32} (n, p) P^{32}	$2.88 \times 10^{-28} \pm 5\%$	3.737×10^{-28}	0.771
Cl^{35} (n, α) P^{32}	$1.09 \times 10^{-28} \pm 5\%$	9.985×10^{-29}	1.09
Al^{27} (n, α) Na^{24}	$4.69 \times 10^{-30} \pm 10\%$	4.677×10^{-30}	1.00
Mg^{24} (n, p) Na^{24}	$1.13 \times 10^{-29} \pm 10\%$	1.147×10^{-29}	0.985

Standard Percent Deviation of the Ratios = 10.2

(a) The foils were irradiated inside a ~ 60 mil cadmium-covered rotating capsule that provided identical exposures for all foils, which were located in a plane at the same radial distance.

(b) All measurements made at Atomics International. Experimental errors listed are one standard deviation.

Table XVII

GMRA TEST

SAND II THIRTIETH ITERATION NORMALIZED INTEGRAL NEUTRON FLUX COMPARISON

Energy (Mev)	Theoretical (Ref. 31)	Experimental (b) (30th Iteration)	Ratio Exp. / Theo.
4.14×10^{-7}	1.000	1.000	1.00
1.13×10^{-6}	0.027	0.968	1.04
3.06×10^{-6}	0.853	0.905	1.06
8.32×10^{-6}	0.780	0.834	1.07
2.26×10^{-5}	0.706	0.758	1.07
6.14×10^{-5}	0.635	0.682	1.07
4.54×10^{-4}	0.494	0.532	1.08
3.36×10^{-3}	0.362	0.390	1.08
1.7×10^{-2}	0.265	0.273	1.03
1.0×10^{-1}	0.171	0.156	0.91
4.0×10^{-1}	0.107	7.00×10^{-2}	0.65
9.0×10^{-1}	5.12×10^{-2}	4.27×10^{-2}	0.83
1.4	3.17×10^{-2}	2.78×10^{-2}	0.88
3.0	3.96×10^{-3}	6.25×10^{-3}	1.58
4.0	2.02×10^{-3}	4.37×10^{-3}	2.16
5.0	1.00×10^{-3}	2.62×10^{-3}	2.62
6.0	4.85×10^{-4}	1.00×10^{-3}	2.06
7.0	2.30×10^{-4}	4.57×10^{-4}	1.99
8.0	1.08×10^{-4}	1.96×10^{-4}	1.81
9.0	4.97×10^{-5}	8.55×10^{-5}	1.72
10.0	2.27×10^{-5}	3.67×10^{-5}	1.62
11.0	1.03×10^{-5}	1.59×10^{-5}	1.54
12.0	4.58×10^{-6}	6.88×10^{-6}	1.50
13.0	1.79×10^{-6}	2.93×10^{-6}	1.64
14.0	8.72×10^{-7}	1.24×10^{-6}	1.42
15.0	3.64×10^{-7}	5.05×10^{-7}	1.39
16.0	1.40×10^{-7}	1.89×10^{-7}	1.35
17.0	4.22×10^{-8}	5.56×10^{-8}	1.32

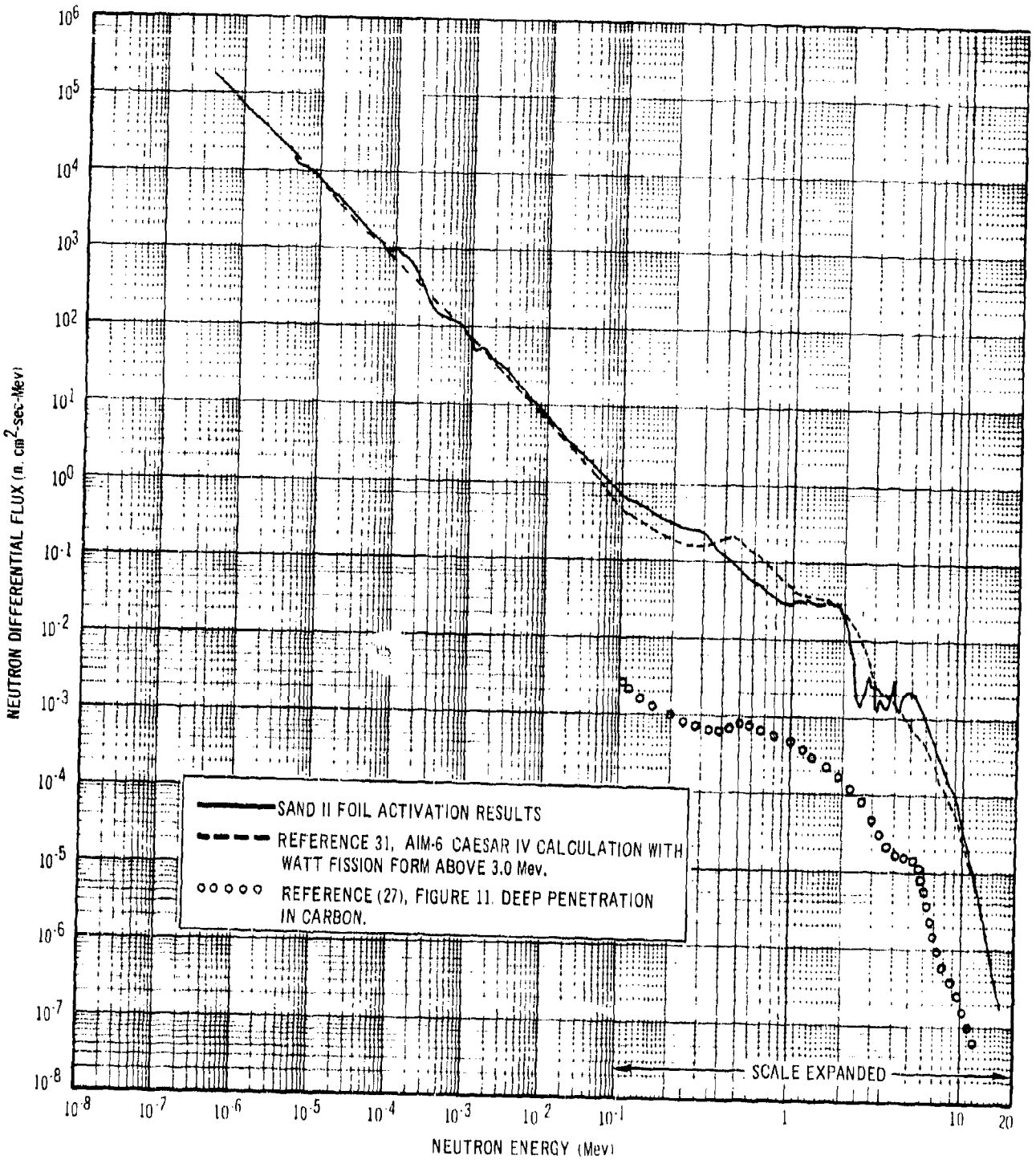

Figure 13. SAND II Differential Flux Results for the GMRA Test

Table XVIII

GMRW TEST

SAND II THIRTIETH ITERATION RATIOS OF MEASURED TO CALCULATED ACTIVITIES

Foil[a] Reaction	Saturated[b] Measured Activity (Dps/Nucleus)	Saturated Calculated Activity (Dps/Nucleus)	Ratio Meas./Calc. Activities
Au^{197} (n, γ) Au^{198}	$4.40 \times 10^{-23} \pm 6\%$	4.413×10^{-23}	0.997
Co^{59} (n, γ) Co^{60}	$2.17 \times 10^{-24} \pm 12\%$	2.177×10^{-24}	0.997
U^{238} (n, γ) Np^{239}	$9.42 \times 10^{-24} \pm 10\%$	9.449×10^{-24}	0.997
U^{235} (n, f) F.P.[c]	$8.84 \times 10^{-24} \pm 5\%$	-	-
Mn^{55} (n, γ) Mn^{56}	$4.12 \times 10^{-25} \pm 5\%$	4.133×10^{-25}	0.997
Na^{23} (n, γ) Na^{24}	$9.03 \times 10^{-27} \pm 5\%$	9.057×10^{-27}	0.997
Cu^{63} (n, γ) Cu^{64}	$1.36 \times 10^{-25} \pm 5\%$	1.364×10^{-25}	0.997
In^{115} (n, n') In^{115m}	$1.37 \times 10^{-26} \pm 5\%$	1.411×10^{-26}	0.971
U^{238} (n, f) F.P.	$2.32 \times 10^{-26} \pm 5\%$	2.372×10^{-26}	0.978
Th^{232} (n, f) F.P.	$6.11 \times 10^{-27} \pm 5\%$	5.441×10^{-27}	1.12
Fe^{54} (n, p) Mn^{54}	$3.42 \times 10^{-27} \pm 9\%$	4.368×10^{-27}	0.783
Ni^{58} (n, p) Co^{58}	$5.98 \times 10^{-27} \pm 4\%$	5.868×10^{-27}	1.02
Cl^{35} (n, α) P^{32}	$7.22 \times 10^{-28} \pm 5\%$	6.242×10^{-28}	1.16
Al^{27} (n, α) Na^{24}	$2.91 \times 10^{-29} \pm 5\%$	2.871×10^{-29}	1.01
Mg^{24} (n, p) Na^{24}	$6.29 \times 10^{-29} \pm 5\%$	6.426×10^{-29}	0.979
I^{127} (n, 2n) I^{126}	$6.67 \times 10^{-29} \pm 5\%$	6.703×10^{-29}	0.995

Standard Percent Deviation of the Ratios = 7.98

(a) The foils were irradiated inside an ~ 40 mil cadmium-covered capsule.

(b) Measurements made at Atomics International, Argonne National Laboratory (Ref. 18), Battelle Northwest (Ref. 21), and Sandia Corporation (Ref. 20). Experimental errors listed are one standard deviation.

(c) This reaction was not used to obtain the iterative solution since a correction for self-absorption has yet to be determined experimentally.

Table XIX

GMRW TEST

SAND II THIRTIETH ITERATION NORMALIZED INTEGRAL NEUTRON FLUX COMPARISON

Energy (Mev)	Theoretical (Ref. 32)	Experimental (30th Iteration)	Exp. /Theo.
1.30×10^{-4}	0.779	0.704	0.90
4.54×10^{-4}	0.721	0.637	0.88
5.53×10^{-3}	0.605	0.464	0.77
1.50×10^{-2}	0.563	0.406	0.72
4.09×10^{-2}	0.518	0.345	0.67
1.10×10^{-1}	0.463	0.278	0.60
2.35×10^{-1}	0.405	0.210	0.52
4.98×10^{-1}	0.328	0.141	0.43
1.05	0.221	0.104	0.47
1.35	0.184	8.28×10^{-2}	0.45
1.74	0.144	4.79×10^{-2}	0.33
2.23	0.105	2.86×10^{-2}	0.27
2.87	6.72×10^{-2}	1.64×10^{-2}	0.24
3.68	4.08×10^{-2}	1.09×10^{-2}	0.27
4.72	2.14×10^{-2}	5.03×10^{-3}	0.24
6.07	7.83×10^{-3}	1.69×10^{-3}	0.22
8.0	1.78×10^{-3}	4.07×10^{-4}	0.23
9.0	8.20×10^{-4}	2.59×10^{-4}	0.32
10.0	3.74×10^{-4}	1.72×10^{-4}	0.46
11.0	1.69×10^{-4}	9.54×10^{-5}	0.56
12.0	7.54×10^{-5}	4.74×10^{-5}	0.63
13.0	3.32×10^{-5}	2.29×10^{-5}	0.69
14.0	1.44×10^{-5}	1.08×10^{-5}	0.75
15.0	6.00×10^{-6}	4.88×10^{-6}	0.81
16.0	2.30×10^{-6}	2.02×10^{-6}	0.88
17.0	6.96×10^{-7}	6.53×10^{-7}	0.94

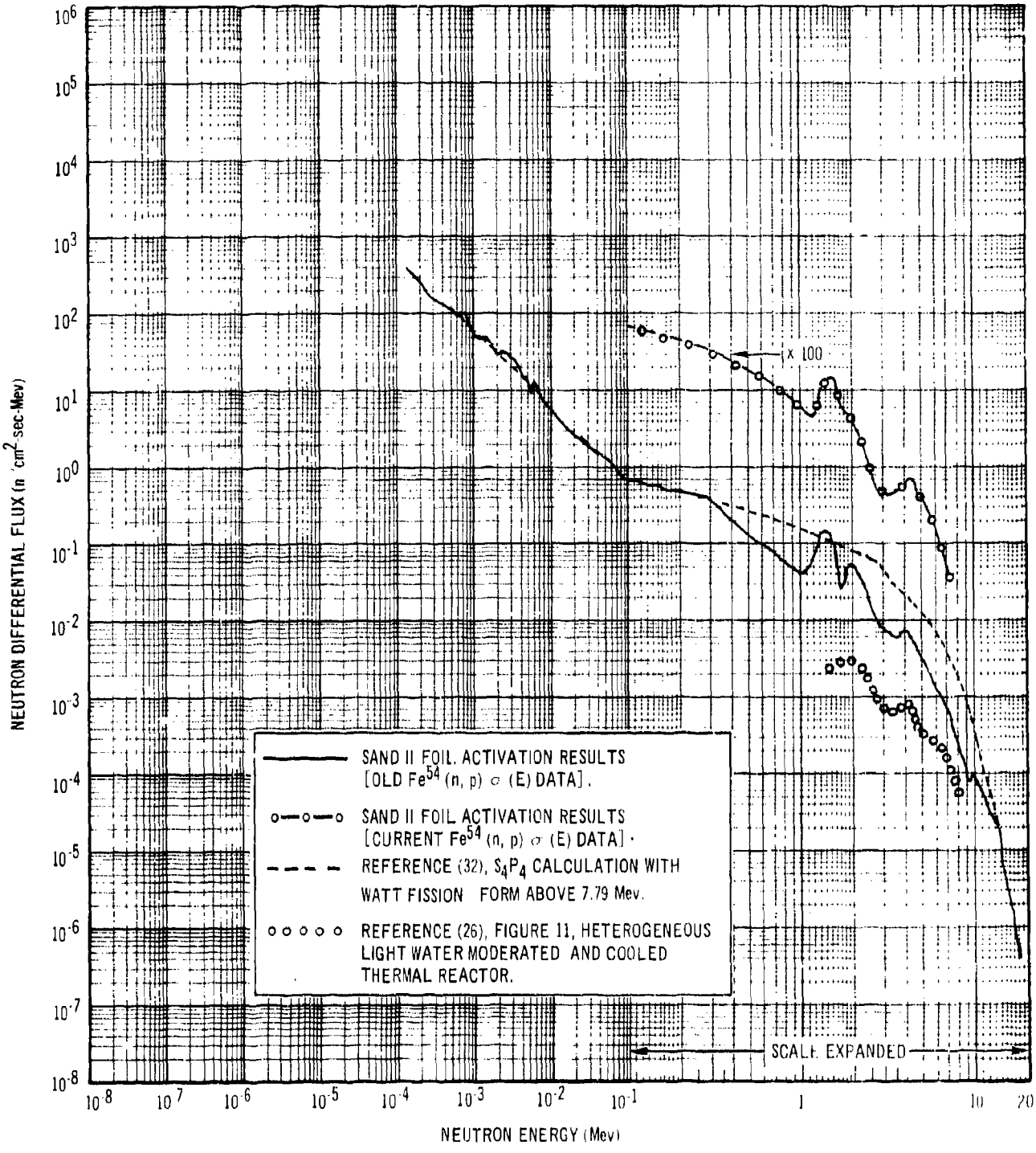

Figure 14. SAND II Differential Flux Results for the GMRW Test

It is not expected that any of the spectra from Fig. 11 would agree in structure exactly with the solution spectra for these test cases, but the interactions among the effects of the presence of water, carbon and other absorbing/scattering materials should produce structure which has some recognizable characteristics.

Some of the fine structure detail (superimposed on the solution envelope) in Figs. 12*, 13, and 14* can be associated with the properties of certain foil detectors. In Figs. 12 and 14, for example, the peak and dip, respectively, at ~ 1.7 Mev are known to be due, at least in part, to errors in the evaluated cross section for the $Fe^{54}(n,p)Mn^{54}$ reaction. This type of effect is discussed in more detail in the presentation of the ECEL test results.

The integral flux comparisons in Tables XV, XVII, and XIX show rather substantial disagreement between the theoretical and SAND II results over certain energy regions. (In all three cases, the results have been arbitrarily normalized at the low end of the energy region.) The theoretical results would not be expected to be particularly accurate, however, in any of these cases, since all three facilities have nuclear and/or structural features (heterogeneity) that require certain simplifying assumptions to make the physical model mathematically tractable.

The spectral results for the SMFS and BRGM tests (limited to the energy region between approximately 0.1 and 10 Mev) are shown by the solid curves in Figs. 15 and 16, respectively. In the lower part of Fig. 16, spectra are reproduced from Fig. 11 that show the type of flux depressions caused by carbon, oxygen, and beryllium.

For the SMFS test, previous time-of-flight results for a similar neutron source were available and were used as the input approximation, represented by the dashed curve in Fig. 15. The results obtained for two slightly different locations in the beam with different side- and back-scattering effects are shown and are identified as Tests A and B. The foil sets and covers used for Tests A and B were different; in particular, the fission foils in Test A had a boron 10 cover, and the $Fe^{54}(n,p)Mn^{54}$ reaction was omitted. This was a fortunate

*The solid and dashed curves in each figure are pertinent to this discussion; the upper curves will be discussed in Section V-B-4.

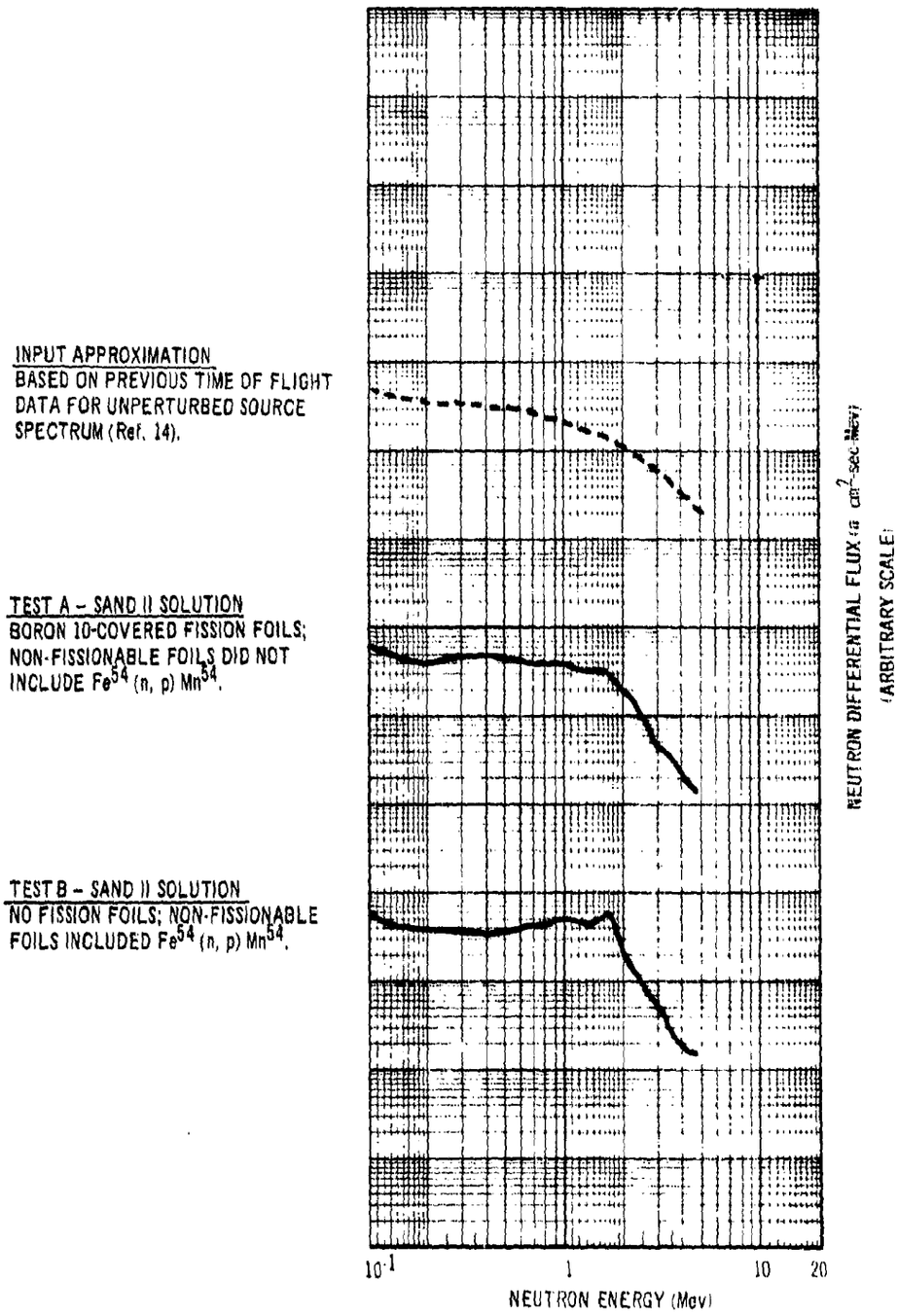

Figure 15. SAND II Differential Flux Results for the SMFS Test

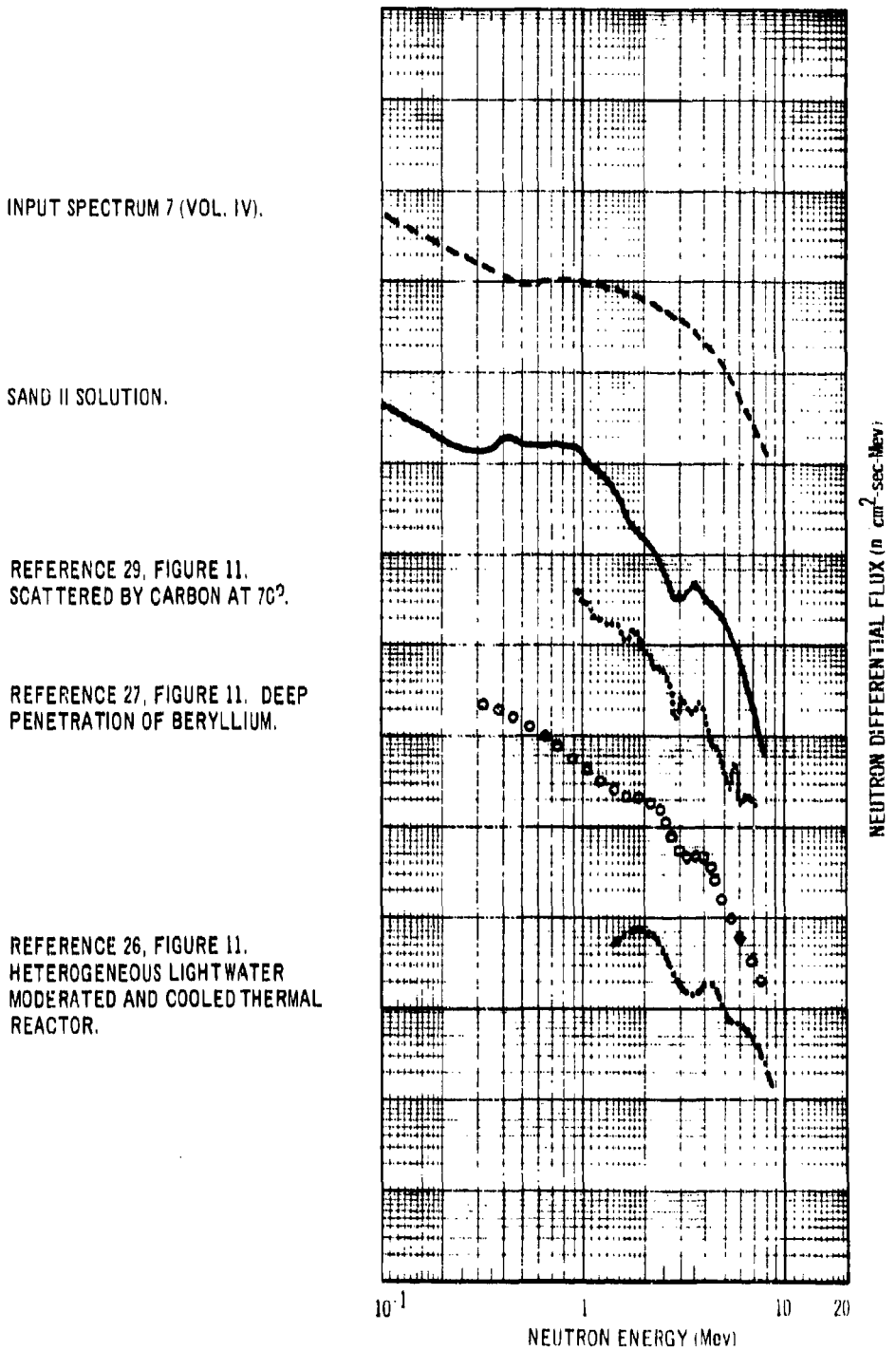

Figure 16. SAND II Differential Flux Results for the BRGM Test

omission; the most important difference between the iterative solutions for these two tests appears at ~ 1.7 Mev in the form of a spectral peak for Test B, which helped to identify suspected errors in the evaluated cross section for the $Fe^{54}(n, p)Mn^{54}$ reaction; re-evaluation of the cross section data for this reaction is discussed in Section V-B-4.

The foil reactions, measured and SAND II calculated values of activity, and ratios of these activities for Tests A and B are given in Tables XX and XXI, respectively. Since a pulsed source was used for this test, it also provides an example of the time-integrated mode of operation for SAND II using the time-of-removal (end of pulse) values of measured activity as input (See Section II-B).

In addition to the time-of-flight data, comparisons were made for the SMFS test with the results of a Monte Carlo calculation performed by Biggers (Ref. 14). Neither the time-of-flight nor the Monte Carlo calculations included any corrections for the scattering effect of adjacent materials in the SMFS beam, and exact agreement between these and the iterative results should not, therefore, be expected. The agreement among these various integral flux results (on an absolute basis) was found to be within approximately 30% over the energy region from 10^{-2} to 15 Mev. In another absolute comparison of multiple foil iterative results with Monte Carlo results for a different beam type measurement, agreement of approximately 20% was found (Ref. 33). These and other results (in particular, the ECEL test) have helped to increase confidence in the reliability of the iterative method and the evaluated cross section data currently in use.

For the BRGM test, Fig. 16, which involved measurements of a leakage spectrum, no reliable information was available on the form of the unknown spectrum. It was known, however, that it would be a fission spectrum degraded by the graphite moderator and beryllium oxide reflector of the reactor. A 1/E + fission form (reference spectrum 7, Volume IV) was therefore specified as the input approximation; this choice was supported by a preliminary comparison of the BRGM measured and spectrum 7 calculated values of saturated activities. The input approximation and the SAND II solution spectrum are shown in Fig. 16 by the dashed and solid curves, respectively; the foil activity results are given in Table XXII.

The slight dip in the solution spectrum at ~ 1.7 Mev can be associated with a low value of measured activity and/or possible cross section errors for the

Table XX

SMFS TEST A

SAND II THIRTIETH ITERATION RATIOS OF MEASURED TO CALCULATED ACTIVITIES

Foil Reaction[a]	Measured[b] Activity (Dps/Nucleus)	Calculated Activity (Dps/Nucleus)	Ratio Meas./Calc. Activities
Na^{23} (n, γ) Na^{24}	$2.10 \times 10^{-32} \pm 15\%$	2.099×10^{-32}	1.000
Au^{197} (n, γ) Au^{198}	$7.96 \times 10^{-30} \pm 10\%$	7.961×10^{-30}	1.000
Pu^{239} (n, f) F.P.	$3.03 \times 10^{-24} \pm 7\%$	3.042×10^{-24}	0.996
U^{238} (n, f) F.P.	$4.66 \times 10^{-25} \pm 7\%$	4.580×10^{-25}	1.018
S^{32} (n, p) P^{32}	$4.83 \times 10^{-32} \pm 6\%$	4.785×10^{-32}	1.009
Ni^{58} (n, p) Co^{58}	$1.68 \times 10^{-32} \pm 7\%$	1.739×10^{-32}	0.966
Mg^{24} (n, p) Na^{24}	$3.25 \times 10^{-31} \pm 12\%$	3.294×10^{-31}	0.987
Al^{27} (n, α) Na^{24}	$1.92 \times 10^{-31} \pm 12\%$	1.849×10^{-31}	1.039

Standard Percent Deviation of the Ratios = 2.08%

(a) The resonance (n, γ) foils were irradiated inside an ~ 40 mil cadmium cover. The fission foils were irradiated inside ~ 40 mil cadmium placed inside a boron carbide spherical cover ~ 1 cm thick. The other foils were bare.

(b) All measurements made at Sandia Corporation (Ref. 20). Experimental errors listed are one standard deviation.

Table XXI

SMFS TEST B

SAND II THIRTIETH ITERATION RATIOS OF MEASURED TO CALCULATED ACTIVITIES

Foil Reaction[a]	Measured[b] Activity (Dps/Nucleus)	Calculated Activity (Dps/Nucleus)	Ratio Meas./Calc. Activities
Cu^{63} (n, γ) Cu^{64}	1.63×10^{-30} ± 10%	1.632×10^{-30}	0.999
Au^{197} (n, γ) Au^{198}	2.20×10^{-29} ± 5%	2.204×10^{-29}	0.998
Co^{59} (n, γ) Co^{60}	3.41×10^{-33} ± 10%	3.416×10^{-33}	0.998
Na^{23} (n, γ) Na^{24}	2.59×10^{-32} ± 5%	2.594×10^{-32}	0.999
In^{115} (n, n′) In^{115m}	6.97×10^{-30} ± 10%	7.073×10^{-30}	0.985
Fe^{54} (n, p) Mn^{54}	2.68×10^{-33} ± 10%	2.342×10^{-33}(c)	1.145
Ni^{58} (n, p) Co^{58}	1.12×10^{-32} ± 5%	1.204×10^{-32}(d)	0.930
S^{32} (n, p) P^{32}	3.16×10^{-32} ± 6%	3.270×10^{-32}	0.966
Zn^{64} (n, p) Cu^{64}	6.62×10^{-31} ± 10%	6.517×10^{-31}	1.016
Cl^{35} (n, α) P^{32}	8.95×10^{-33} ± 10%	9.523×10^{-33}	0.940
Al^{27} (n, α) Na^{24}	1.48×10^{-31} ± 12%	1.436×10^{-31}	1.031
Mg^{24} (n, p) Na^{24}	2.54×10^{-31} ± 12%	2.517×10^{-31}	1.009

Standard Percent Deviation of the Ratios = 6.09%

(a) The resonance (n, γ) foils were all irradiated inside an ~ 20 mil cadmium cover, except for the Cu which was irradiated bare. The other foils were bare.

(b) Measurements made at Atomics International and Sandia Corporation, (Ref. 20). Experimental errors listed are one standard deviation.

Table XXII

BRGM TEST

SAND II THIRTIETH ITERATION RATIOS OF MEASURED TO CALCULATED ACTIVITIES

Foil Reaction(a)	Saturated[(b)] Measured Activity (Dps/Nucleus)	Saturated Calculated Activity (Dps/Nucleus)	Ratio Meas./Calc. Activities
$Au^{197}(n,\gamma)\ Au^{198}$	$1.62 \times 10^{-21} \pm 3\%$	1.621×10^{-21}	0.999
$Co^{59}\ (n,\gamma)\ Co^{60}$	$7.30 \times 10^{-23} \pm 10\%$	7.304×10^{-23}	0.999
$Na^{23}\ (n,\gamma)\ Na^{24}$	$2.77 \times 10^{-25} \pm 4\%$	2.772×10^{-25}	0.999
$Cu^{63}\ (n,\gamma)\ Cu^{64}$	$5.24 \times 10^{-24} \pm 3\%$	5.244×10^{-24}	0.999
$In^{115}\ (n,n')In^{115m}$	$3.55 \times 10^{-25} \pm 5\%$	3.494×10^{-25}	1.016
$Ni^{58}\ (n,p)\ Co^{58}$	$1.08 \times 10^{-25} \pm 3\%$	1.170×10^{-25}	0.923
$Fe^{54}\ (n,p)\ Mn^{54}$	$9.45 \times 10^{-26} \pm 5\%$	9.531×10^{-26}	0.992
$S^{32}\ (n,p)\ P^{32}$	$6.22 \times 10^{-26} \pm 3\%$	6.291×10^{-26}	0.989
$Al^{27}\ (n,\alpha)\ Na^{24}$	$3.07 \times 10^{-28} \pm 12\%$	3.078×10^{-28}	0.998
$Cl^{35}\ (n,\alpha)\ P^{32}$	$1.57 \times 10^{-26} \pm 10\%$	1.446×10^{-26}	1.086
$I^{127}\ (n,2n)\ I^{126}$	$7.62 \times 10^{-28} \pm 25\%$	7.620×10^{-28}	1.000

Standard Percent Deviation of the Ratios = 3.7%

(a) All foils were irradiated inside an ~ 20 mil cadmium cover.

(b) Measurements made at IIT Research Institute, (Ref. 22). Experimental errors listed are quoted limits of error.

$Fe^{54}(n,p)Mn^{54}$ reaction, which in this test as in the GMRW test (Fig. 14) is manifest as a spectral depression. In addition to errors, low values of measured activity for the $Fe^{54}(n,p)Mn^{54}$ reaction can be attributed to flux depressions resulting from materials (such as the ~ 1/2" of aluminum and stainless steel for the GMRW test and ~ 1/2" Hastelloy "C" for the BRGM test) present in an environment (see Fig. 11). Some experimental results on the flux depression effect of aluminum and stainless steel are presented in the discussion of the ECEL test (Section V-B-3).

The curves presented at the bottom of Fig. 16 are three of those shown in Fig. 11, and are included to help establish the credibility of some features of the solution spectrum. It is noted that the major depression in the solution spectrum in the vicinity of approximately 3 Mev is shifted to the left and broadened compared with the results of the GMRW test (Fig. 14); this shift is just as might be expected to result from the presence of beryllium oxide, since beryllium has a major resonance at about 4.7 Mev.

The ECEL test results will be discussed in more detail than the previous tests, since these results demonstrate most of the ways in which the iterative technique can be used to extract various types of information from foil activity measurements.

The ECEL Core 14-13 absolute value of integral flux as determined by the iterative method was about a factor of three lower than that estimated on the basis of calculations and a calibrated power monitor; with lower than expected foil activities, considerable effort had to be expended by the participating laboratories to obtain satisfactory activity measurements. Nevertheless, the overall consistency of the measurements was excellent. In general, the determination of the absolute value of total integral flux is not a trivial problem. It is noted that the multiple foil activation method is rather unique in this regard and can be used as a method of absolute calibration for most neutron environments.

For the WMGR, GMRA, and GMRW tests, there are definite limits on the reliability of the reactor physics spectral calculations, because of geometrical and non-homogeneity considerations. Because of the homogeneous and symmetrical nature of the ECEL core region, however, it would be expected that theoretical predictions would agree better with measurements for an experiment

performed in this facility. This was indeed found to be the case, for the relative integral flux agreement in the ECEL test is within 20% over the entire energy region, compared with factors of 2 or more in some of the previous tests (see Tables XV, XVII, and XIX). Prior to the ECEL test, only in beam type tests had agreement been obtained with theory to within 20%.

The preliminary* foil activity and differential flux results using the SAND II code with 12, 11, and 9 foil reactions for the +Y Cd-covered, -Y Bare, and +Y B 10-covered locations, respectively, for the ECEL test are presented in Tables XXIII, XXIV, XXV, and Figs. 17, 18 and 19. Values of 10% and 1.96 were used for the solution and foil discard criteria for all three SAND II runs. Two-inch-square voids were created approximately 4 inches from the core center along the x, y, and z axes. The two voids on the y axis were designated as the +Y and -Y locations. A description of the ECEL facility, which is of the split-table honeycomb type, has been given by Mountford and Morewitz (Ref. 25).

Tuttle (Ref. 30) (using the CAESAR IV diffusion code with 18-group and 35-group structures) and Dahl (Ref. 32) (using the S-XIII transport code and 18 groups) made one-dimensional spherical geometry reactor physics calculations for the ECEL core 14-13. (These calculations did not distinguish between the +Y and -Y locations.) Dahl obtained two results using different sets of cross section evaluations. Tuttle's and Dahl's results are given in Table XXVI. Tuttle's 18-group results were used to generate an input spectral approximation for the SAND II runs shown by the dashed curves in Figs. 17 and 19.

Tuttle (Ref. 30) also used the AILMOE code to calculate a spectrum with detailed structure for core 14-13. It was suggested that the results of these calculations be used only to indicate where some detailed structure might appear in the spectrum between about 10^{-3} and 3.6 Mev,† and that the previous CAESAR IV (either the 18-group or subsequent 35-group)§ results be relied upon for the correct overall distribution of the neutron flux. The AILMOE code results are

*At the time that this report was prepared, not all of the experimental foil activation data had been completely analyzed.

†Below 10^{-3} Mev and above 3.6 Mev, the AILMOE code assumes an E form and a fission form, respectively.

§Different sets of cross sections were used for the two calculations.

Table XXIII

SAND II SOLUTION RESULTS OBTAINED AFTER 20 ITERATIONS FOR THE ECEL TEST, +Y Cd-COVERED LOCATION

Foil Reaction	Saturated[c] Measured Activity (dps/nucleus)	Saturated Calculated Activity (dps/nucleus)	Nominal 5% Activity Limits (Mev)		% Deviation of Measured From Calculated Activity
			Lower	Upper	
U^{238} (n, γ) U^{239} Cd[a]	$7.792 \times 10^{-16} \pm 2\%$	7.761×10^{-16}	2.2×10^{-5}	0.38	0.40
Au^{197} (n, γ) Au^{198} Cd	$3.145 \times 10^{-15} \pm 10\%$	2.963×10^{-15}	4.8×10^{-6}	0.066	6.13
Au^{197} (n, γ) Au^{198} Au[b]	$2.069 \times 10^{-15} \pm 10\%$	2.314×10^{-15}	4.8×10^{-6}	0.1	-10.58
Co^{59} (n, γ) Co^{60} Cd	$1.114 \times 10^{-15} \pm 7\%$	1.115×10^{-15}	1.2×10^{-4}	1.6×10^{-4}	-0.10
Cu^{63} (n, γ) Cu^{64} Cd	$1.522 \times 10^{-16} \pm 3\%$	1.525×10^{-16}	5.6×10^{-4}	0.18	-0.21
U^{235} (n, f) F. P. Cd	$4.030 \times 10^{-15} \pm 3\%$	3.852×10^{-15}	5.0×10^{-5}	1.4	4.61
U^{238} (n, f) F. P. Cd	$6.670 \times 10^{-17} \pm 3\%$	7.376×10^{-17}	1.4	5.5	-9.57
Th^{232} (n, f) F. P. Cd	$1.780 \times 10^{-17} \pm 8\%$	1.627×10^{-17}	1.4	6.4	9.42
Ni^{58} (n, p) Co^{58} Cd	$1.574 \times 10^{-17} \pm 3\%$	1.571×10^{-17}	1.7	7.5	0.20
Fe^{54} (n, p) Mn^{54} Cd	$1.260 \times 10^{-17} \pm 7\%$	1.233×10^{-17}	1.7	7.5	2.17
S^{32} (n, p) P^{32} Cd	$7.348 \times 10^{-18} \pm 10\%$	7.523×10^{-18}	2.3	7.7	-2.33
I^{127} (n, 2n) I^{126} Cd	$1.401 \times 10^{-19} \pm 10\%$	1.403×10^{-19}	10.1	14.9	-0.15
Standard Deviation of Measured Activities					5.73%

(a) Refers to cadmium cover, 40 mils in this case.
(b) Refers to a gold-covered, 0.5 mils in this case, sandwich detector.
(c) Measurements made at Atomics International, Argonne National Laboratory (Ref. 18), Battelle Northwest (Ref. 21), and Sandia Corporation (Ref. 20). Experimental errors listed are one standard deviation.

Table XXIV

SAND II SOLUTION RESULTS OBTAINED AFTER 7 ITERATIONS FOR THE ECEL TEST, -Y BARE LOCATION

Foil Reaction	Saturated[a] Measured Activity (dps/nucleus)	Saturated Calculated Activity (dps/nucleus)	Nominal 5% Activity Limits (Mev)		%Deviation of Measured From Calculated Activity
			Lower	Upper	
U^{238} (n, γ) U^{239}	$8.926 \times 10^{-16} \pm 2\%$	9.226×10^{-16}	2.2×10^{-5}	0.24	-3.25
Au^{197} (n, γ) Au^{198}	$3.373 \times 10^{-15} \pm 10\%$	3.227×10^{-15}	4.8×10^{-6}	0.044	4.54
Co^{59} (n, γ) Co^{60}	$1.122 \times 10^{-15} \pm 7\%$	1.120×10^{-15}	1.2×10^{-4}	1.8×10^{-4}	0.14
Cu^{63} (n, γ) Cu^{64}	$1.569 \times 10^{-16} \pm 3\%$	1.563×10^{-16}	5.6×10^{-4}	0.16	0.38
U^{235} (n, f) F. P.	$4.120 \times 10^{-15} \pm 3\%$	4.213×10^{-15}	5.2×10^{-5}	1.1	-2.21
U^{238} (n, f) F. P.	$6.660 \times 10^{-17} \pm 3\%$	6.971×10^{-17}	1.4	5.6	-4.46
Th^{232} (n, f) F. P.	$1.610 \times 10^{-17} \pm 8\%$	1.522×10^{-17}	1.4	6.4	5.77
Ni^{58} (n, p) Co^{58}	$1.576 \times 10^{-17} \pm 3\%$	1.532×10^{-17}	1.7	7.4	2.89
Fe^{54} (n, p) Mn^{54}	$1.233 \times 10^{-17} \pm 7\%$	1.199×10^{-17}	1.7	7.5	2.82
S^{32} (n, p) P^{32}	$6.919 \times 10^{-18} \pm 10\%$	7.407×10^{-18}	2.3	7.6	-6.59
I^{127} (n, 2n) I^{126}	$1.363 \times 10^{-19} \pm 10\%$	1.363×10^{-19}	10.1	14.9	-0.03
Standard Deviation of Measured Activities					3.86 %

(a) Measurements made at Atomics International, Argonne National Laboratory (Ref. 18), Battelle Northwest (Ref. 21), and Sandia Corporation (Ref. 20). Experimental errors listed one standard deviation.

Table XXV

SAND II SOLUTION RESULTS OBTAINED AFTER 18 ITERATIONS FOR THE ECEL TEST, +Y BORON 10-COVERED LOCATION

Foil Reaction	Saturated[(a)] Measured Activity (dps/nucleus)	Saturated Calculated Activity (dps/nucleus)	Nominal 5% Activity Limits (Mev)		% Deviation of Measured From Calculated Activity
			Lower	Upper	
$Au^{197}(n,\gamma)\,Au^{198}$ B[(b)]	$3.002 \times 10^{-16} \pm 5\%$	3.321×10^{-16}	2.2×10^{-3}	0.62	-9.61
$Co^{59}(n,\gamma)\,Co^{60}$ B	$2.354 \times 10^{-17} \pm 10\%$	2.343×10^{-17}	1.6×10^{-4}	0.38	0.48
U^{235} (n,f) F. P. B	$1.550 \times 10^{-15} \pm 5\%$	1.384×10^{-15}	4.2×10^{-3}	1.9	12.02
Np^{237}(n,f) F. P. B	$3.423 \times 10^{-16} \pm 5\%$	3.532×10^{-16}	0.4	3.8	-3.04
U^{238} (n,f) F. P. B	$5.000 \times 10^{-17} \pm 5\%$	5.134×10^{-17}	1.4	5.8	-2.62
Th^{232}(n,f) F. P. B	$1.125 \times 10^{-17} \pm 5\%$	1.117×10^{-17}	1.4	6.6	0.71
Fe^{54} (n,p) Mn^{54} B	$1.040 \times 10^{-17} \pm 7\%$	9.500×10^{-18}	1.7	7.4	9.47
S^{32} (n,p) P^{32} B	$5.334 \times 10^{-18} \pm 15\%$	5.749×10^{-18}	2.3	7.6	-7.21
I^{127} (n,2n) I^{126} B	$7.250 \times 10^{-20} \pm 25\%$	7.265×10^{-20}	10.0	14.9	-0.20
Standard Deviation of Measured Activities					7.03%

(a) Measurements made at Atomics International and U. S. Naval Radiological Defense Laboratory (Ref. 19). Experimental errors listed are one standard deviation.

(b) Refers to a boron carbide spherical cover with the following physical properties:

Outer diameter-equatorial	= 1.882"	Inner diameter	= 1.033"
Outer diameter-polar	= 2.00 "	Wall thickness	= 0.430"
Weight (grams)	= 114.527	Boron 10 enrichment	= 92.3%

Recipe used to make sphere: boron = 1.000 gm; carbon = 0.299 gm; aluminum = 0.013 gm.

Final density = ~ 2.37 gm/cc.

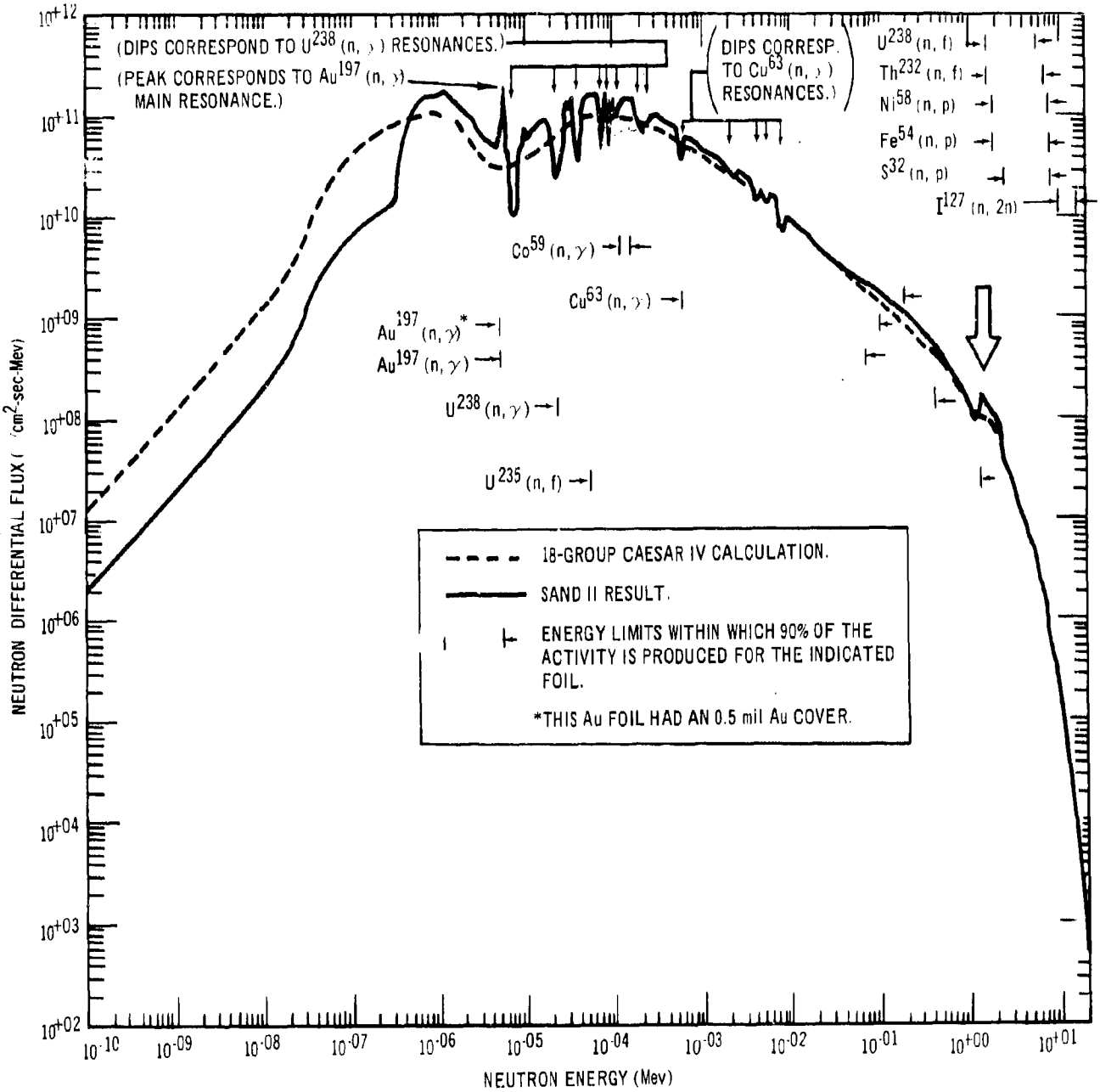

Figure 17. SAND II Solution Spectrum After 20 Iterations for ECEL +Y Cd-Covered Location

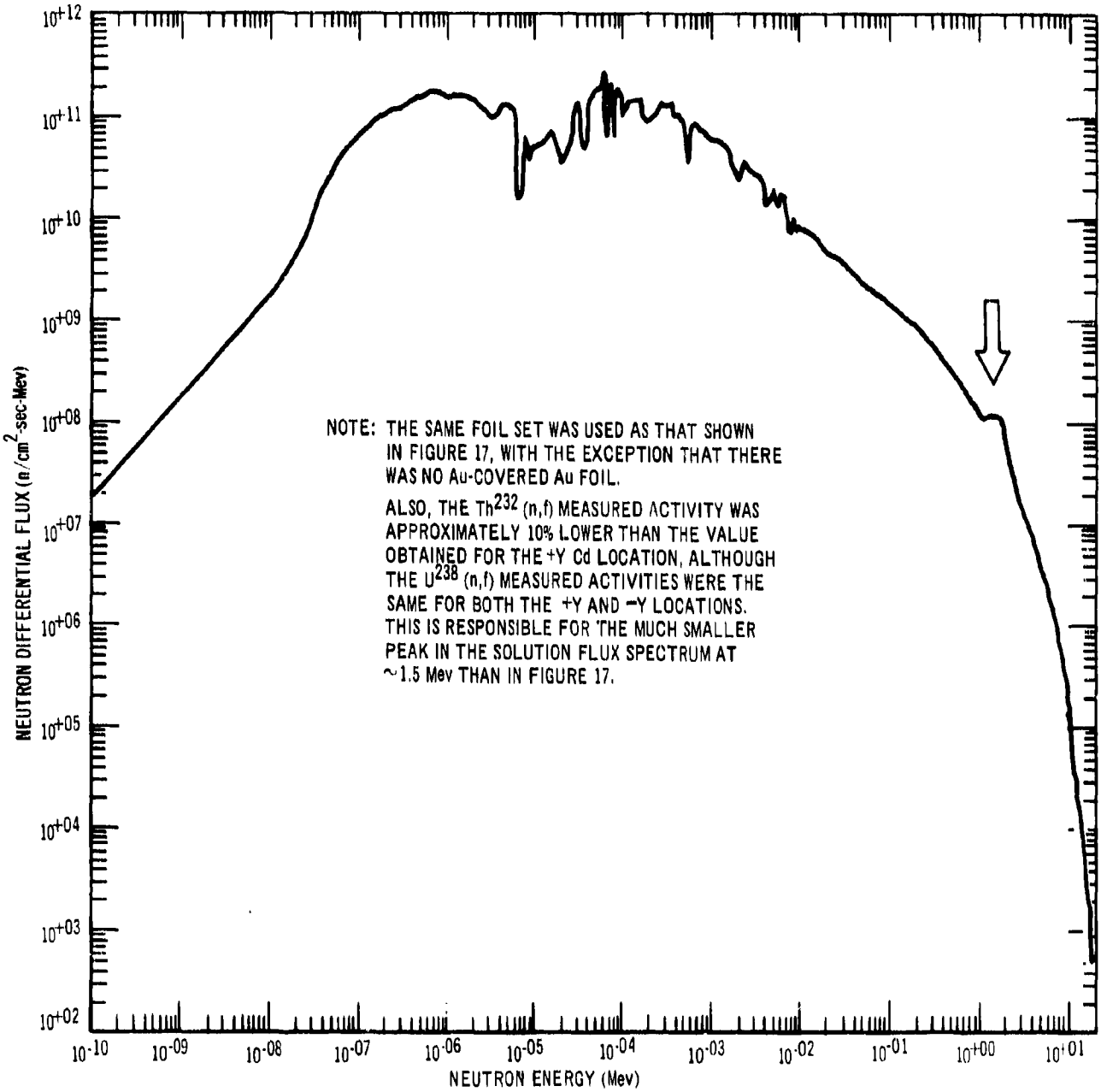

Figure 18. SAND II Solution Spectrum After 7 Iterations for ECEL Test, -Y Bare Location

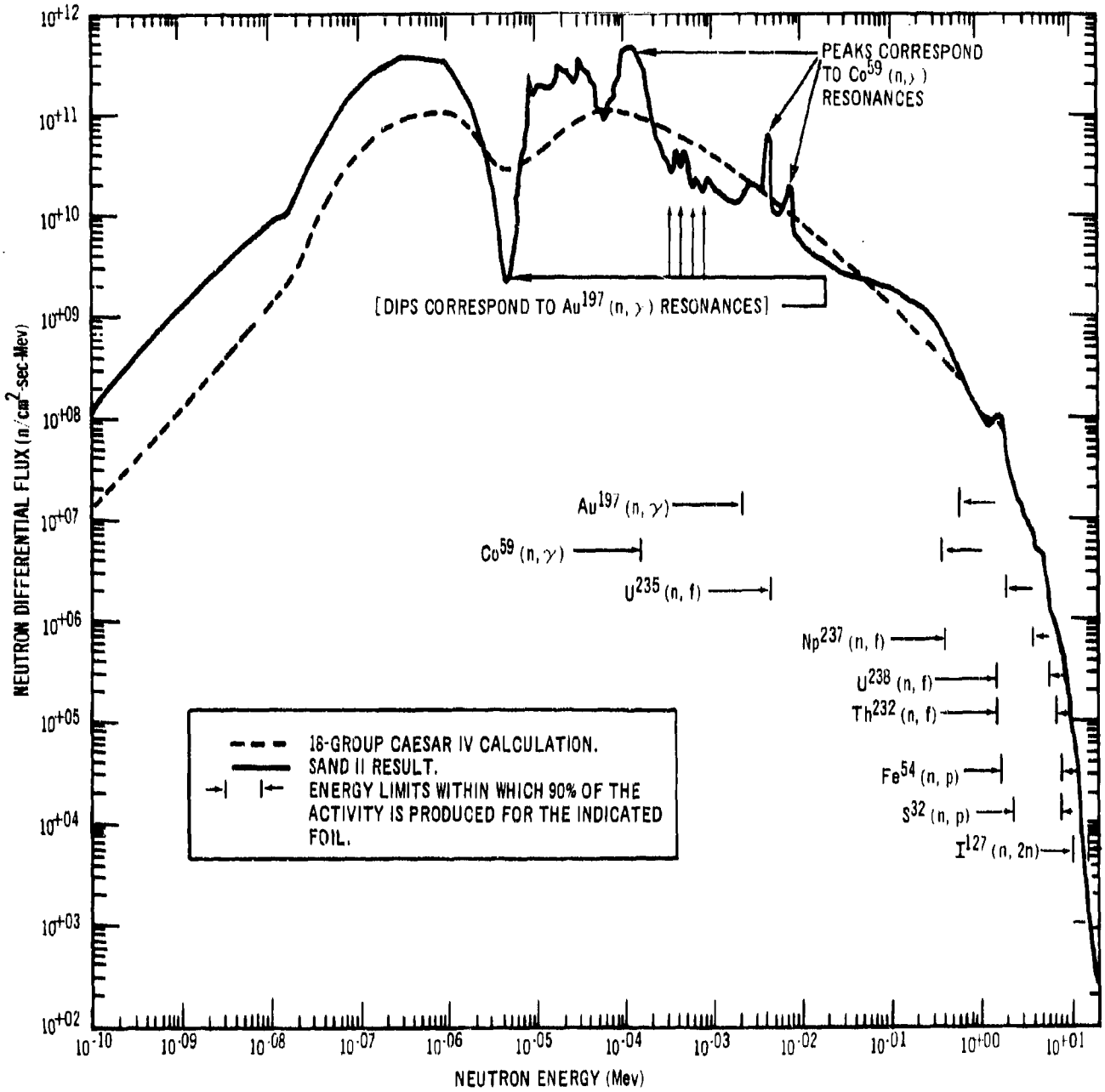

Figure 19. SAND II Solution Spectrum After 18 Iterations for ECEL Test, +Y Boron 10-Covered Location

Table XXVI

ECEL CORE 14-13,18-GROUP CALCULATIONS

(NORMALIZED INTEGRAL FLUX ABOVE THE SPECIFIED ENERGY)

Energy (Mev)	CAESAR IV[(a)]	S-XIII[(b)]	S-XIII[(c)]	Ratio[(d)] IV/XIII
3.0	0.02534	0.02260	0.02552	1.121
1.4	0.1130	0.09665	0.09289	1.169
0.9	0.1688	0.1448	0.1444	1.166
0.4	0.3029	0.2607	0.2343	1.162
0.1	0.5282	0.4628	0.4101	1.141
1.70×10^{-2}	0.7344	0.6715	0.6926	1.094
3.35×10^{-3}	0.8779	0.8379	0.8414	1.048
4.54×10^{-4}	0.9657	0.9548	0.9571	1.011
6.14×10^{-5}	0.9955	0.9956	0.9934	1.000
2.26×10^{-5}	0.9989	0.99935	0.99933	0.999
8.315×10^{-6}	0.99960	0.999918	0.999895	1.000
3.059×10^{-6}	0.999764	0.999983	0.999930	1.000
1.125×10^{-6}	0.999893	0.999989	0.999959	1.000
4.14×10^{-7}	0.9999728	0.9999956	0.999989	1.000
1.52×10^{-7}	0.9999952	0.9999979	0.9999988	1.000
5.60×10^{-8}	0.99999955	0.9999988	0.9999989	1.000
2.52×10^{-8}	0.99999996	0.9999994	0.9999995	1.000
9.26×10^{-9}	1.00000000	1.0000000	1.0000000	1.000

(a) Calculated at Atomics International (Ref. 30), Jan., 1967 (Diffusion code results).
(b) Calculated at Battelle Northwest (Ref. 32), April, 1967 (Transport code results, Program S-XIII using cross sections from reference 34.)
(c) Same as (b), but using the cross sections for Hanford revised Gam (Ref. 32).
(d) Ratio of the 2nd and 3rd columns.

given in Fig. 20. The structure shown in Fig. 20 is not evident in the SAND II solutions, Figs. 17, 18 or 19.

The SAND II solution values of absolute integral flux ($\Phi > 10^{-10}$ Mev) for the +Y Cd-covered, -Y Bare, and +Y B 10-covered locations are 1.17×10^9, 1.12×10^9, and 1.18×10^9 n/cm^2-sec respectively, at a power of 150 watts. (As previously indicated, these results are based on sets of 12, 11, and 9 foil reactions respectively.) An initial estimate based on other data yielded a value of $\sim 3 \times 10^9$ n/cm^2-sec. The theoretical and measured normalized integral flux results at energy points used for the 35-group calculation are presented in Table XXVII. As previously stated, the agreement between measurement and theory is within $\sim \pm 20\%$ at all energy points.

For the +Y B 10-covered test, the boron 10 carbide sphere would be expected to cause a flux depression that would reduce the ECEL core fission rate in its immediate vicinity. The integral flux results presented in Table XXVII do show such an effect. The SAND II code calculates the attenuation effect of the boron 10 carbide sphere only approximately (and results would therefore not be expected to be extremely accurate), because of approximations required regarding geometry, scattering equilibrium, etc. Nevertheless, the -Y B 10-covered results appear to be very consistent with the +Y Cd-covered and -Y bare results.

In Table XXVII, Tuttle's 35-group CAESAR IV results are used as the theoretical spectrum. In addition, the SAND II results are given for seven energy points that are not included in the 35-group results, but were used for the 18-group calculations of Tuttle and Dahl. The SAND II results at those seven points may therefore be compared with the corresponding values from the 18-group calculations, given in Table XXVI. It is noted that these latter calculations are for a radius of 0 cm (i.e., the core center), whereas the 35-group calculation is for a radius of 10 cm, which corresponds to the actual location of the foil sets; however, because of the homogeneous nature of the core region, the normalized results should not be significantly different.

In selection of individual foils for flux measurements in a given environment, the energy sensitivity limits in the anticipated spectrum are very important. The SAND II results, Tables XXIII, XXIV, and XXV, and Figs. 17 and 19 illustrate this fact well; for the ECEL solution spectrum in Cd (or bare), the $Co^{59}(n,\gamma)$

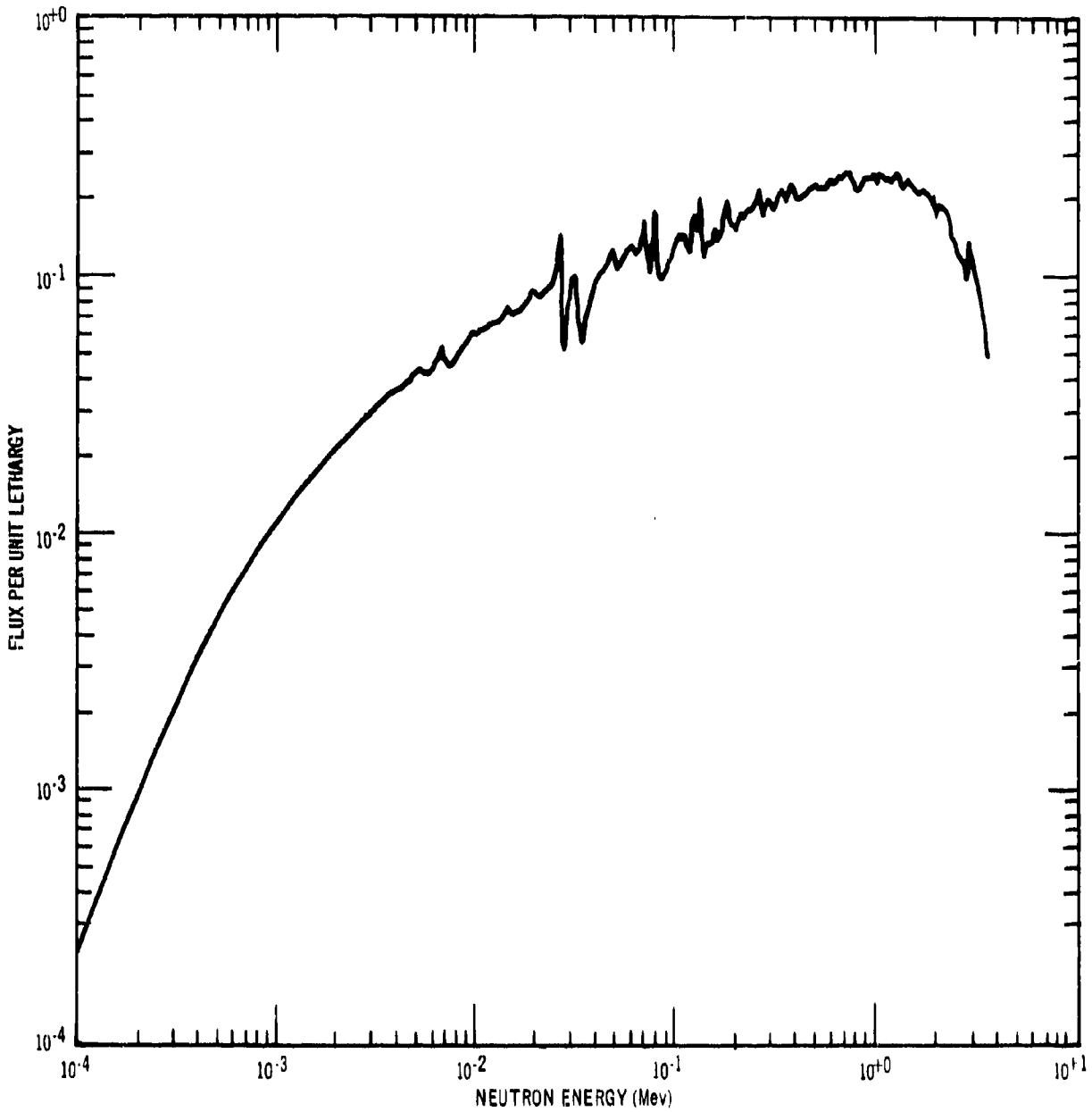

Figure 20. AILMOE Calculated Spectrum for ECEL Core 14-13

Table XXVII

ECEL CORE 14-13 INTERLABORATORY REACTOR TEST INTEGRAL FLUX COMPARISON

(SAND II 20th, 7th, and 18th Iteration Normalized Integral Flux Comparison For the +Y Cadmium-Covered, -Y Bare, and +Y Boron 10-Covered Locations Respectively)

(Page 1 of 2)

Energy (Mev)	Theoretical (a)	Experimental			Ratio (b) Exp. /Theo.
		+Y Cd	-Y Bare	+Y B 10	
9.26×10^{-9}	1.0000000	1.0000	1.0000	1.0000	1.000
4.14×10^{-7}	0.9999828	1.0000	1.0000	1.0000	1.000
6.83×10^{-7}	0.999876	1.0000	1.0000	1.0000	1.000
1.13×10^{-6}	0.999724	0.9999	0.9999	0.9997	1.000
1.86	0.999527	0.9998	0.9998	0.9996	1.000
3.06	0.99935	0.9997	0.9996	0.9995	1.000
5.04	0.99924	0.9996	0.9994	0.9995	1.000
8.32	0.99915	0.9995	0.9992	0.9994	1.000
1.37×10^{-5}	0.9989	0.9992	0.9990	0.9985	1.000
2.26	0.9986	0.9986	0.9985	0.9965	1.000
3.73	0.9977	0.9978	0.9973	0.9930	1.000
6.14	-	0.9944	0.9939	0.9895	-
8.14	0.9956	0.9928	0.9914	0.9874	0.997
1.01×10^{-4}	0.9915	0.990	0.989	0.983	0.998
1.67	0.9849	0.982	0.980	0.957	0.997
2.75	0.9745	0.974	0.970	0.947	0.999
4.54	0.9593	0.959	0.950	0.941	0.9999
7.49	0.9396	0.943	0.928	0.934	1.004
1.23×10^{-3}	0.9148	0.922	0.900	0.926	1.008
2.04	0.8838	0.897	0.867	0.918	1.015
3.35	0.8468	0.869	0.831	0.894	1.026
5.53	0.8050	0.833	0.794	0.828	1.035
9.12	0.7662	0.801	0.757	0.794	1.045
1.50×10^{-2}	0.7152	0.761	0.717	0.768	1.064
1.70	-	0.751	0.706	0.760	-

Table XXVII

ECEL CORE 14-13 INTERLABORATORY REACTOR TEST INTEGRAL FLUX COMPARISON

(SAND II 20th, 7th, and 18th Iteration Normalized Integral Flux Comparison For the +Y Cadmium-Covered, -Y Bare, and +Y Boron 10-Covered Locations Respectively)

(Page 2 of 2)

Energy (Mev)	Theoretical (a)	Experimental			Ratio (b) Exp. / Theo.
		+Y Cd	-Y Bare	+Y B 10	
2.48	0.6589	0.717	0.670	0.735	1.088
4.09	0.6049	0.669	0.620	0.698	1.106
6.74	0.5399	0.612	0.564	0.645	1.134
1.00×10^{-1}	-	0.5574	0.512	0.587	-
1.11×10^{-1}	0.4755	0.543	0.500	0.570	1.142
1.83	0.4073	0.459	0.422	0.467	1.127
3.02	0.3311	0.364	0.337	0.338	1.099
4.00	-	0.309	0.292	0.263	-
4.98	0.2514	0.267	0.256	0.213	1.062
8.21	0.1724	0.187	0.186	0.138	1.085
9.00	-	0.176	0.175	0.128	-
1.35×10^{0}	0.1031	0.130	0.125	0.0900	1.261
1.40	-	0.123	0.120	0.0867	-
2.23	0.04545	0.0393	0.0422	0.0314	0.865
3.00	-	0.0197	0.0213	0.0166	-
3.78	0.01504	0.0160	0.0126	0.0102	1.064
6.07	0.002737	0.00244	0.00273	0.00219	0.891
1.00×10^{1}	0	0.000206	0.000209	0.000108	-

a) 35-Group CAESAR IV Calculation (Ref. 30).
These results are for a radial distance of 10 cm, which corresponds to the actual location of the foil sets for the X, Y, and Z locations.

b) The ratios given are for the +Y Cd location. The ratios for the -Y bare location are closer to unity, in general, than for the +Y Cd location.

reaction behaves in the same manner as does $Au^{197}(n,\gamma)$ in a 1/E environment; i.e., 90% of the activity is produced by a very narrow energy region around the major resonance.* This behavior makes it clear that resonance detectors cannot be used indiscriminately as flux monitors, without knowledge of the energy sensitivity range of the detector in question, in the particular environment in which it is to be used.

It is instructive to examine some additional observations regarding the dips and peaks in the three ECEL solution spectra:

a) For the SAND II data reduction, the fission foil results of Armani (Ref. 18) for the +Y Cd-covered and -Y bare locations, and those of Tochilin (Ref. 19) for the +Y B 10-covered locations, were included as input data. Armani's results are based on counting of reaction products, while Tochilin's are based on counting of fission tracks. The high value of the integral spectrum ratio (Table XXVII) at 1.35 Mev and the spectral peaks indicated by the arrows in Figs. 17 and 18 at that energy, appear to be due to the $Th^{232}(n,f)$ reaction, which has high ratios of measured to calculated activity for both the +Y Cd-covered and -Y bare locations (see Tables XXIII and XXIV).

This same type of behavior was observed in the previous GMRW test, as seen in Fig. 1. The $Th^{232}(n,f)$ results for this test also were provided by Armani by radioactivity counting. When the $Th^{232}(n,f)$ reaction was omitted from the GMRW test results, the SAND II solution flux spectrum changed, the peak was greatly reduced, and the spectral dip on the low energy side of the original peak shifted up in energy, as shown in Fig. 21. The peak observed in each of the spectra of Figs. 17 and 18 (shown by the arrows) does not appear in Fig. 19 at the same energy, but is shifted up in energy as in Fig. 21. (It is again noted that the $Th^{232}(n,f)$ results for the +Y B 10 test (Fig. 19) were provided by Tochilin by counting fission tracks.)

*Regarding the behavior of the gold detector in a spectrum such as the ECEL, it might be noted that in the +Y Cd-covered location, a gold covered gold (sandwich) detector was used (Table XXIII), but the relative hardness of this environment caused the gold-covered, cadmium-covered, and bare gold detectors to have essentially the same energy response range. Since the flux at and below the major gold resonance ($\sim 5 \times 10^{-6}$ Mev) is relatively small compared to a 1/E spectrum, the cadmium cover (which attenuates the thermal neutrons preferentially) and the gold cover (which attenuates preferentially in the region of the gold resonance) had relatively little effect.

These observations, as well as subsequent discussion with the participants, suggest that the $Th^{232}(n,f)$ fission rates as determined by the counting of reaction products may be excessively high compared with those determined by fission track counting, probably due to the uncertainty in the fission yield of the Mo^{99} reaction product that is counted. The possibility of cross section error, however, cannot entirely be ruled out.

b) Examination of the input spectrum used, shown in Figs. 17 and 19 as the dashed curve, may raise conjecture that the peak discussed above is possibly caused by the fact that the input spectrum includes a small peak in that energy region. This is most definitely not the case, however. A repeat SAND II run was made for the +Y Cd-covered location, using a smooth input form with no structure in this region; the peak produced in the solution for this run was essentially the same as that shown in Fig. 17 in magnitude and only very slightly different in shape. The results of this comparison are shown on an expanded scale in Fig. 22. It can be seen that the difference in shape consists of the presence or absence of the remnant of the small input peak at about 1.7 Mev, but that the generation of the solution peak (at 1.35 Mev) is independent of the input peak.

Since the activity results for the $Na^{23}(n,\gamma)$, $In^{115}(n,n')$, $In^{115}(n,\gamma)$, $Fe^{56}(n,p)$, $Al^{27}(n,\alpha)$ and $Mg^{24}(n,p)$ were not available for the current computer runs, the energy region from $\sim$ 1 to 8 Mev did not have proper foil coverage. Additional structure in the solution differential spectra in this energy region may be detected when these reactions are used. There is no doubt as to whether such structure could actually exist. The plausibility of the SAND II solution for the GMRW test, shown in Fig. 21, is strongly supported by the representative spectra shown in Fig. 11 (which show the effects different materials actually do have in causing spectral depressions). Further, there is no question about the ability of the SAND II code to detect such structure if accurate cross sections, accurate activities, and sufficient foil coverage are obtained. The current problem is rather, with existing uncertainties, to properly analyze SAND II solution spectra to determine whether the structure produced is real or is the result of errors in cross sections, measured activities, foil self-shielding effects, or inadequate foil coverage of the entire energy range.

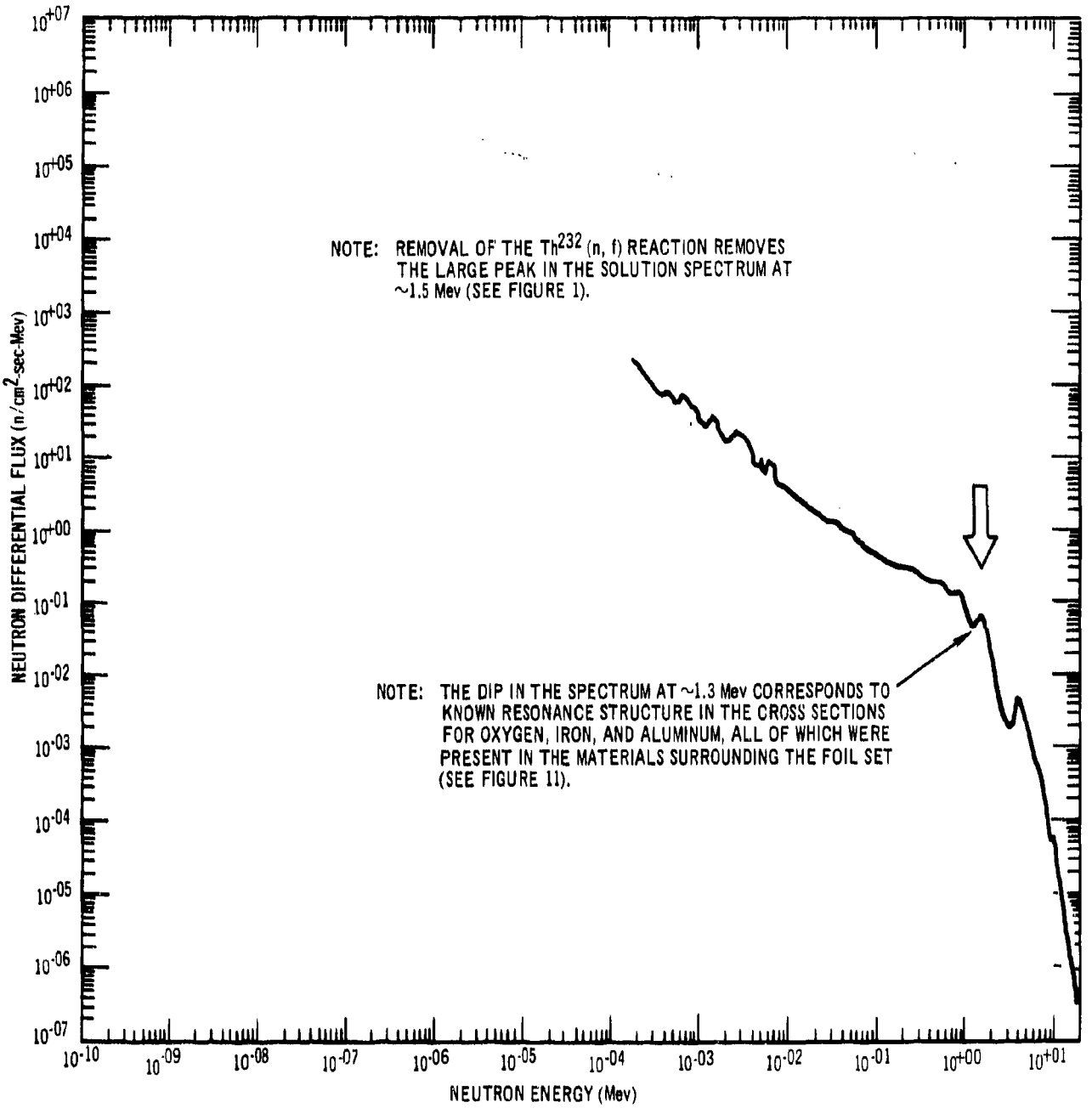

Figure 21. SAND II Differential Flux Results for the GMRW Test with the $Th^{232}(n,f)$ F. P. Reaction Removed

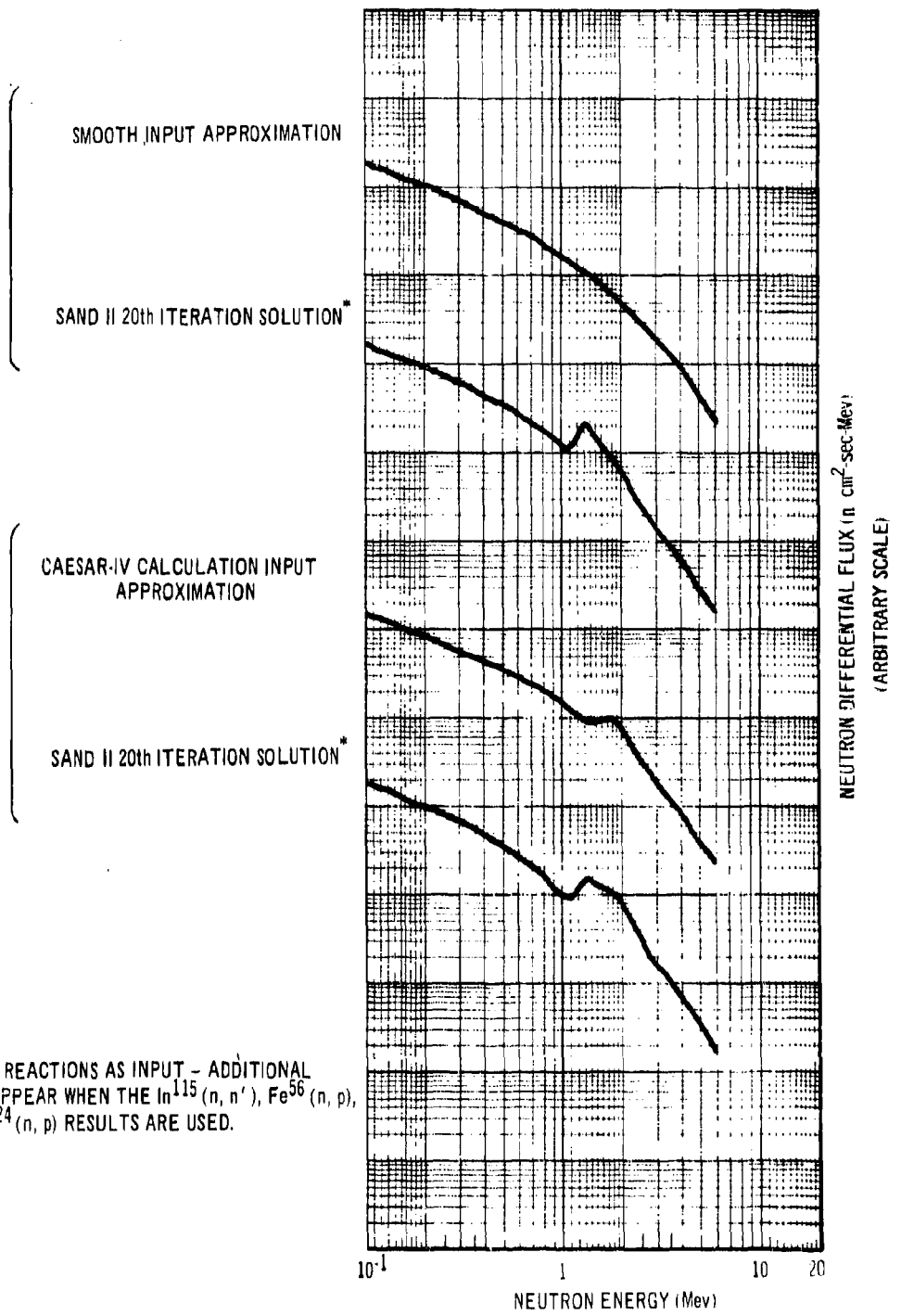

Figure 22. Input Dependence of ECEL Core 14-13 i Y Cadmium-Covered Spectral Solution

c) In Fig. 17, two small dips in the 10^{-3} Mev decade (one between 4 and 5 and one between 7 and 8) very closely coincide with two $Co^{59}(n,\gamma)$ resonances. (Figure 19 shows the artificial peaks produced by these resonances in the +Y B 10-covered test very clearly.) It might appear on first examination, therefore, that these two dips are caused by the $Co^{59}(n,\gamma)$ reaction -- i.e., by a negative error in the measured activity for that foil. This is implausible, however, for two reasons. Firstly, the flux at the major $Co^{59}(n,\gamma)$ resonance (between 1 and 2×10^{-4} Mev) shows no such behavior, whereas any error in the measurement would be propagated most strongly at the major resonance. Secondly, the 90% activity limits plotted in Fig. 17 show that the $Co^{59}(n,\gamma)$ reaction has negligible sensitivity in the 10^{-3} Mev decade, and could therefore not be expected to have any effect on the solution spectrum in that region.

Further examination shows that the dips in question are only two of five that coincide with $Cu^{63}(n,\gamma)$ resonances. The fact that all five dips are quantitatively similar strongly suggests that these dips are indeed caused by a somewhat low activity for the $Cu^{63}(n,\gamma)$ foil and are not real. This is another example of how the generation of structure in the solution differential spectrum can be used to advantage to evaluate the reliability of foil activity measurements.

d) In discussions with Armani (Ref. 18), it was learned that the U^{238} foil used was $\sim$ 240 mg/cm^2 thick. In the GMRW test, Armani had experimentally determined that, in a 1/E environment, the self-absorption correction factor for such a foil is 3.3. Therefore, the measured activity for a 240 mg/cm^2 $U^{238}(n,\gamma)$ foil, without self-absorption correction, will be substantially too low to be consistent with the other foils used (although not necessarily by a factor of 3.3 in the ECEL test, since it is not a 1/E environment). In striking agreement with this prediction is the observation that nearly all the dips in the solution spectrum between 6×10^{-6} Mev and 3×10^{-4} Mev in both Fig. 17 and Fig. 18 correspond to resonances for the $U^{238}(n,\gamma)$ reaction. (This reaction was not included in the +Y B 10-covered test of Fig. 19.) In an environment such as the ECEL (in which U^{238} is uniformly distributed), it is to be expected that some portion of all these dips is real, caused by the resonances in the U^{238} present in the environment.

A very interesting hypothesis emerges from this observation: if the measured activity for the $U^{238}(n,\gamma)$ reaction is carefully determined for a given

thickness of foil in any environment where U^{238} is not in the immediate vicinity of the foils, it is possible (starting with the measured activity) to simply increase the SAND II input activity for that reaction until all the dips due to its resonance disappear in the solution spectrum; the ratio of input activity to measured activity needed to accomplish this would then be the self-shielding correction factor for $U^{238}(n,\gamma)$ for the environment under consideration. Obviously, for an environment where U^{238} is present, only an upper limit for the self-shielding correction factor can be obtained in this manner. (This technique was used to determine a self-shielding correction factor upper limit of $\sim$ 1.45 for the $U^{238}(n,\gamma)$ foil in the +Y cadmium-covered location.)

This method of studying and/or determining self-shielding factors for a given environment can, at least in principle, be extended to any resonance detector reactions, thereby greatly reducing a very important source of uncertainty in thick resonance foil activiation techniques. One obvious requirement for this method is that enough other foils be used which are largely redundant in energy range of sensitivity with the foil under investigation so that determination of the true spectral shape is not strongly dependent on that foil. (Whether or not this latter condition is satisfied can be tested by making a SAND II run with the foil in question removed -- except for the dips corresponding to the resonance structure of the foil being studied, the solution spectrum should be the same with and without the foil.)

e) There is a large peak in the Fig. 17 solution spectrum after 20 iterations (and only an incipient one after 7 iterations in Fig. 18) that coincides in energy with the main $Au^{197}(n,\gamma)$ resonance. In this case, the appearance of a peak would tend to suggest a positive error in the measured activity, since the energy sensitivity region for this reaction does extend over the peak for this solution spectrum.* On the other hand, in Fig. 19, the large dip in the solution spectrum at this same $Au^{197}(n,\gamma)$ resonance energy is of negligible significance with respect to the measured activity, since the energy sensitivity region for $Au^{197}(n,\gamma)$ in that spectrum does not extend below $\sim 2 \times 10^{-3}$ Mev. In fact, the entire solution spectrum below $\sim 1 \times 10^{-4}$ Mev in Fig. 19 should be considered

*The peak may, however, be due to a problem in the SAND II code's approximate calculation of the attenuation for the gold-covered gold sandwich detector.

to be largely meaningless since, for this particular spectrum in the region of the boron 10 carbide sphere, none of the reactions used were significantly sensitive below that energy. It is thus seen to be very important to consider the reaction energy sensitivity limits (for the solution spectrum) tabulated by the SAND II code in evaluating solution spectral structure.

f) Additional structure was introduced into the ECEL solution flux spectra for the +Y Cd-covered and the -Y bare locations by the $Cl^{35}(n,\alpha)$ and $Zn^{64}(n,p)$ reactions; however, the SAND II code discarded both reactions for both locations because of excessive deviation (>1.96 standard deviations high) from consistency with the solution spectrum (results for these reactions were not yet available for these runs for the +Y B 10-covered test). Subsequent checks showed the presence of an impurity in the Cl^{35} samples, which justified the discarding of this reaction. Because of the very low activity of the Zn samples and problems associated with measuring the Cu^{64} activity (see Section V-A-2), the $Zn^{64}(n,p)Cu^{64}$ results were not considered to be very accurate, which justified the discarding of this reaction also.

3. Flux Depression Effects

Because of a suspected flux depression in the GMRW test (due to the presence of 1/4" thicknesses of aluminum and stainless steel, as well as water, around the foil set used), a test was performed in the ECEL minus Z location with $Fe^{54}(n,p)Mn^{54}$, $Ni^{58}(n,p)Co^{58}$, and $Fe^{56}(n,p)Mn^{56}$ foil detectors sandwiched between two 1/2" total thicknesses of aluminum and stainless steel (1/4" x 2" x 2" pieces each of Al and SS) to ascertain the degree of flux depression. Measured activities for these sandwiched foils relative to foils located at the center of the outside surfaces of the 1/2" thick aluminum and stainless steel sandwich, were reduced by 8.4 (±6)% for $Fe^{56}(n,p)$, 7.8 (±3)% for $Fe^{54}(n,p)$, and 7.1 (±3)% for $Ni^{58}(n,p)$. Relative to the average of activities for these reactions previously measured in the center of 2" x 2" x 2" voids (with no aluminum and stainless steel sandwich), the measured reductions were 25.6* (±15)%, 10.5 (±5)%, and 12.6 (±3)% respectively. The more pronounced effect for the $Fe^{56}(n,p)$* may be

*Part of this larger difference for $Fe^{56}(n,p)$ can be attributed to the presence of manganese impurity in the iron foil (see Section V-A-2).

consistent with the fact that it is the most abundant of these three isotopes in stainless steel. That is, the presence of a flux depressant material might be expected to have the strongest effect on a detector of the same material.

Davey and Amundson have made somewhat analogous measurements for ~ 1/4" thick spherical shells of graphite, sodium, aluminum, iron, stainless steel, lead, and depleted uranium around fission chambers (Ref. 35). They report changes in fission count rate ratios, on adding the different shells, of ~ 1.0 to 6.6%; the low and high values correspond to sodium and depleted uranium shells respectively. The high value for the uranium is again consistent with the expectation that the fission chamber (back-to-back halves coated with U^{238} and U^{235}, respectively) will be most strongly affected by the presence of uranium. Comparison of the spherical shell results with those of the ECEL test sandwiched foils is limited by the important difference in geometrical arrangement of the scattering/absorption material. For elastic scattering by an idealized thin shell surrounding a point detector, the neutrons scattered in are exactly compensated by those scattered out. Thus, although the shells used by Davey and Amundson are not thin, their results would not be expected to show as large flux depression effects from elastic scattering as would the ECEL results using plane foil sandwiches.

Davey and Amundson's shell measurements were also made in a fast reactor somewhat similar to the ECEL. These shell measurements and the ECEL test were both conducted in a core region already containing large quantities of aluminum, carbon, stainless steel, uranium, etc. It is likely that measured flux depressions caused by materials placed adjacent to a foil packet might be more pronounced in environments not containing as much of these materials; that is, in an initially unperturbed spectrum.

4. Cross Section Re-Evaluation

In he course of the data analysis from the six tests studied, it became evident that effects of the $Fe^{54}(n, p)Mn^{54}$ foil activity measurements were substantially inconsistent with those of all other foils used. This was also found to be the case for the $Ni^{58}(n, p)Co^{58}$ and $S^{32}(n, p)P^{32}$ reactions, but to a lesser degree. It was further found that the S^{32} and Ni^{58} results were mutually inconsistent independently of the Fe^{54} measurements. Figures 12 and 14, and Tables XIV and XVIII, which show the WMGR and GMRW results, respectively,

are cited as examples of the kind of effect observed. The large peak (in the WMGR result) and dip (in the GMRW result) at 1.7 Mev in the spectrum obtained with the "old" cross section evaluation are due to what can be considered an inappropriate curve drawn through available differential cross section data, especially in a region near the reaction threshold, where the curve is quite steep.*

A comprehensive investigation of these inconsistencies, involving many computer runs not reported here, resulted in a substantial re-evaluation of the $Fe^{54}(n,p)Mn^{54}$ cross section data. This investigation is reported in reference 36. Figure 23 shows the "old" evaluation used (solid curve) as well as the new one obtained from this comprehensive cross comparison of all tests involved (dot-dash curve).** The difference between the two curves does not appear, perhaps, to be significant near the threshold because of the low magnitude; it was seen, however, to be much more significant than the apparently larger difference between about 6 and 13 Mev, because of its much greater effect on the sensitivity curve (product of cross section and differential flux).

Figures 12 and 14 compare the solution spectra resulting from the newer evaluation (top curve in each figure) with the original results, for these two tests. In both cases, the newer results are seen to be much more reasonable.

The newer $Fe^{54}(n,p)Mn^{54}$ evaluation is currently used in SAND II (see Volume III); it is not presented as being correct, but only less incorrect than the "old" one (more properly, it gives more nearly consistent results with different kinds of spectra). This reaction certainly still requires further re-evaluation.

*After the completion of this report, it was found that a narrow peak had been inadvertently introduced into the KAPL evaluation at 1.75 Mev and was the cause of the sharp peak and dip in the WMGR and GMRW solution spectra respectively. The presence of this peak in the KAPL cross section, however, would not be expected to significantly alter the conclusions reached about the $Fe^{54}(n,p)$ cross section.

**The new evaluation is a modification of that reported in reference 17, based on a heavier weighting of the experimental data of Salisburg and Chalmers (see Figure 23). It should be noted that the reference 17 evaluation was originally replaced by the "old" (KAPL) evaluation (solid curve in Figure 23). The KAPL evaluation was based on a Hauser-Feshbach calculation up to 5.8 Mev normalized to fit the data of Carroll and Smith, and an extrapolation to higher energies through 14 Mev data, and had originally been thought to be more accurate than the reference 17 evaluation.

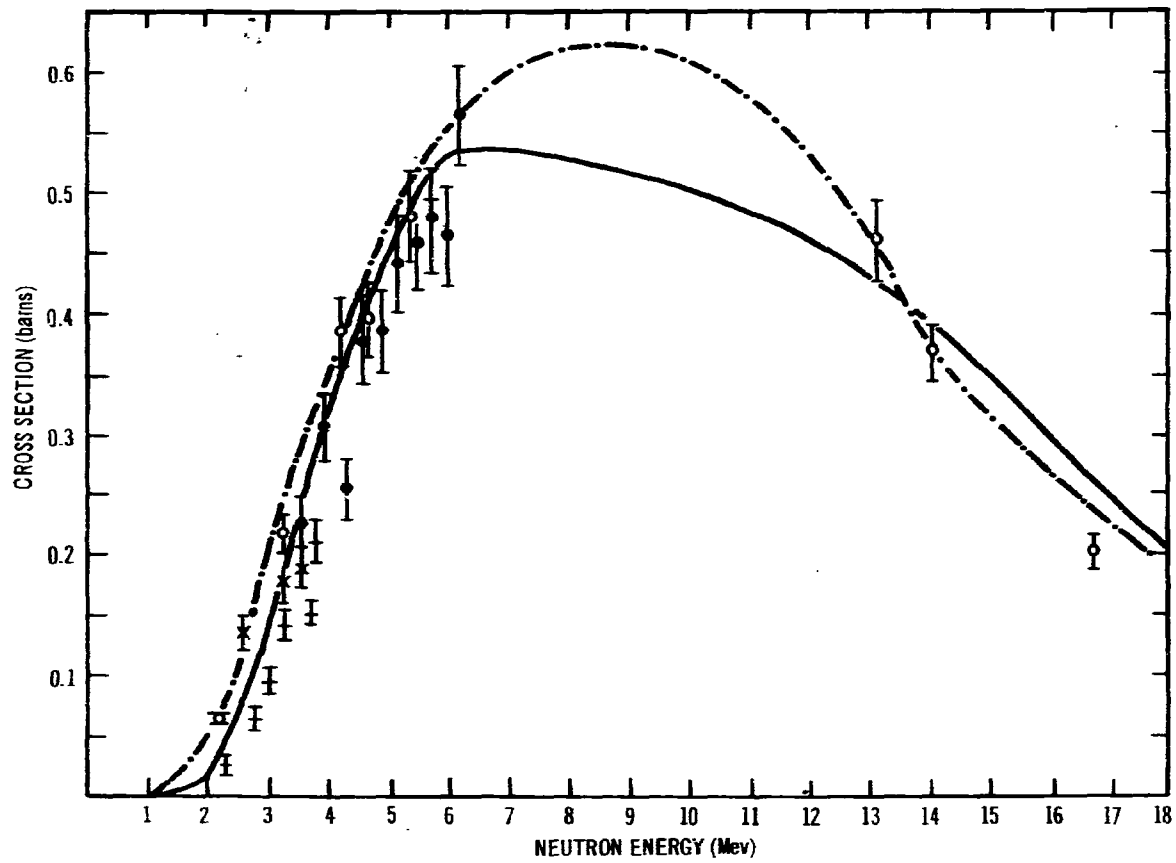

- ● CARROLL AND SMITH, NSE, 22, 411 (1965).
- \+ LAUBER AND MALMSKOG, NUCLEAR PHYS. 73, 234 (1965).
- × VAN LOEF, NUCLEAR PHYS. 24, 340 (1961).
- o SALISBURY AND CHALMERS, PHYS. REV. 140, B305 (1965).
- ——— KAPL EVALUATION, PAPER CN-23-47 CONF. ON NUCLEAR DATA, PARIS (1966) - CALLED THE "OLD" EVALUATION THROUGHOUT THIS REPORT.
- —·—·— RE-EVALUATION USING REFERENCE (17), THIS WORK.

Figure 23. $Fe^{54}(n,p)Mn^{54}$ Measured and Evaluated Cross Section

SECTION VI
ERRORS IN FLUX SPECTRAL DEFINITION

A. Summary Discussion

With substantial errors in cross section and measured activities, an exact solution to Eqs. (38) is likely to yield values of $\varphi^{[k]}(E)$ that contain large errors, because the experimental input errors can cause ill-conditioning in the system of equations. Gold (Ref. 8), DiCola and Rota (Ref. 11), and McElroy (Ref. 1) have investigated the propagation of these experimental errors and their effect on the accuracy of different types of exact solutions for neutron spectra. Grundl (Ref. 10), DiCola and Rota (Ref. 11), and Greer and Walker (Ref. 4) have investigated methods which involve approximate solutions for the neutron energy region above a few hundredths of an Mev, while McElroy, Berg and Gigas (Ref. 3) have considered the same problem, but for the entire neutron energy region. Gold (Ref. 9) has studied the problem from a more fundamental point of view by investigating an approximating, but general, iterative "unfolding" method. These latter studies have shown that the use of an approximate technique for obtaining an appropriate solution to the system of equations minimizes the effects of the propagation of experimental errors. The SAND II iterative procedure was designed to accomplish this type of minimization.

As part of the error analysis study, the SAND II code was used to analyze available data for several different types of neutron environment, as discussed in Section V. The results of these tests as well as the analytical tests discussed in Section IV indicate that the code is capable of producing a solution with reasonably correct envelope of the differential structure. The accuracy with which this can be done depends strongly on several factors; principal among these are

1) adequacy of energy range coverage by the foil set used,

2) accuracy of foil activity measurements (including self-absorption and scattering effects),

3) accuracy of the differential cross section evaluations included in the cross section library, and

4) aptness of initial spectral approximation.

In ill-conditioned cases (in the sense of any of the four items above), the code appears to introduce somewhat unreasonable perturbations in the flux spectrum over certain energy regions. A good deal of cross comparison among all the tests analyzed showed that it is often possible to distinguish among the various possible causes of the ill-conditioning, when such unreasonable structure occurs. For example, anomalous structure in a solution spectrum can probably be attributed to inadequate foil coverage if it occurs in an energy region not well within the sensitivity limits of more than one foil reaction used; this can be determined by examining the list of energy limits within which 90% of the activity is produced for each foil (included in the printed output of each run). Such an examination might result in a decision to irradiate additional foils, to help fill in the energy "gaps".

An ill-chosen initial approximation can, on the other hand, result in sensitivity limits for certain foils which are very much displaced in energy (for the approximation spectrum) from their true location; this can cause iterative corrections to be made in inappropriate energy regions resulting, in turn, in approach to an incorrect, although arithmetically reasonable, solution. This effect is especially obvious in the case of resonance detectors; if, for example, the true spectrum includes a substantial flux in the region of a major resonance, and the initial approximation does not, the calculated sensitivity limits can be shifted upwards as much as several decades in energy to a region of very small cross section, to compensate for the loss of calculated activity under the resonance. Depending on the particular set of foils used, this may cause foils which in fact did overlap in energy regions of sensitivity to appear to be affected by separate regions, or vice versa; this can sharply change the correction factor averaging among the various foils, and produce artificial spectral structure.

An inaccurate foil activity measurement (outside of the bounds of acceptable experimental error in a particular case) can usually be identified by standard statistical techniques, as a result of examining the difference between calculated and measured activities for all foils used for the solution spectrum. Experience to date suggests that errors in activity measurements, particularly with threshold detectors (or, in general, with detectors which overlap strongly in energies of sensitivity), usually result in perturbations much less severe and broader in energy than those caused by, say, inaccuracies in differential cross section.

Inaccurate differential cross section data evaluation for a particular reaction causes unreasonable structure which is not specific to any one test. Evaluation of a large body of data can identify a reaction which results in systematically perturbed solution spectra, or for which a correlation is recognizable between the nature of the perturbation and, perhaps, the kind of environment (thermal, fission, fusion, etc.). The appearance of such unreasonable perturbations in the spectrum is, then, actually an important advantage, since it can be used to adjust currently used cross section evaluations in the SAND II code to provide more consistent results for all kinds of spectra.

It is recognized that this discussion of distinguishing among various causes of ill-conditioning is over-simplified for the sake of illustration. In practice, combinations of difficulties are generally in effect, and require more careful and studious interpretation. It may be difficult to specify the error in a solution spectrum resulting from inadequate foil coverage and/or aptness of the initial spectral approximation. In general, some knowledge about the anticipated form of the environment under study will be required to make a proper assessment of such errors.

Errors associated with cross sections and foil activities are discussed, in somewhat more detail, in the following two sections.

B. Evaluated Cross Sections

Studies have been made of the accuracy of foil detector cross section data by Grundl (Ref. 10), Beauge (Ref. 37), Liskien and Paulsen (Ref. 38), Barrall and McElroy (Refs. 17, 39), Parker (Ref. 40), Boldeman (Ref. 12), Zijp (Refs. 6, 7) and others. A review of the results of the more recent of these studies supports the conclusion that the integrated accuracy of present evaluated cross section data is within ± 10% for many foil detector reactions in current use, particularly resonance and fission reactions.* It is much more difficult, however, to assign limits of accuracy to the differential data; accurate differential cross section evaluations are essential to determining neutron flux spectral shape,

*This means that errors in the cross section data for many of the foil detector reactions used do not result in more than ± 10% errors in the activation integrals (over the pertinent energy ranges) for a neutron spectrum such as 1/E or fission. (See references 10, 17, and 39.)

since this requires independence of the response functions for the various foil reactions used.

As indicated in Section V-B, erroneous (or, more properly for these purposes, inconsistent) cross section evaluations can lead to important spectral structural anomalies. It is important, therefore, that currently used cross section evaluations be surveyed to determine which contain errors that contribute to erroneous spectral structure in iterative solutions, and that these errors be eliminated by further studies and/or re-evaluation. The multiple foil iterative technique may be applied as mentioned in Section V-B, to unfolding the relative shape and absolute magnitude of differential cross section functions.

Dierckx (Ref. 41) has stated that an error of ± 5% to ± 10% in the measurement of cross sections is sufficient for measuring fluxes to ± 1%, when the measurement is done by comparing the unknown spectrum with a known spectrum which is only slightly different. Grundl (Ref. 10) has used this comparison procedure in studying fission type spectra, and suggests that spectral analysis with activation detectors always involves a spectral comparison. The iterative perturbation technique is essentially a comparison procedure, since its initial step is the selection of an input spectral approximation, which may be based on theoretical predictions. Dierckx's comment may therefore be taken to apply to the iterative perturbation technique to some degree, depending on the accuracy of the initial approximation.

C. Activity Measurements

Few statements on the accuracy of the measurement of foil detector activities have appeared in the literature (Ref. 24). For many reactions accuracies to within ± 5% are obtainable. It appears that for other reactions, however, an accuracy to within ± 10% is more realistic. In the multiple foil irradiations discussed in Section V, such accuracy was more often the exception than the rule.

Measurements of activity are often affected by such factors as impurity materials which contribute interfering decay products, incomplete knowledge of decay schemes, uncertainties in half-life and inconsistencies in half-life values used among various laboratories, and the lack of readily available standards for products with short half-lives.

One example of the importance of establishing better information on foil measurement reliability is given in the results of the WMGR test (Fig. 12). Table XIV shows the measured and calculated activity results for this test. It is evident that the magnitude of uncertainty in the measured $Fe^{54}(n,p)Mn^{54}$ activity is of the same order as the magnitude of inconsistency of the ratio of the measured to calculated activities for that foil with the others. Conclusions reached about the particular structure introduced in the solution spectrum at 1.7 Mev (regarding the inaccuracy of the cross section evaluation for this reaction) would become, therefore, questionable to the degree to which these conclusions were unsubstantiated by other results. Obviously, a more careful attempt to achieve accuracy in activity measurement in this case would have been extremely valuable. (It should be pointed out that, in the actual execution of this test, there was no intent to use the measurements as they have subsequently been used; the test was, rather, initially only a check for material impurities in the foils.)

It is possible to improve the reliability of activity measurements by careful interlaboratory comparison and cooperation. The round robin study of three reactions conducted by the ASTM in which eight laboratories participated is a good example of how this can be accomplished (see Table XIII). For the $Ni^{58}(n,p)Co^{58}$ and $Fe^{54}(n,p)Mn^{54}$ reactions, agreement among all the laboratories was within a spread of 4-1/2% of the average; for the $Co^{59}(n,\gamma)Co^{60}$ reaction, the spread was 10% of the average; except for one laboratory, however, this reaction also had a 4-1/2% spread. Improvements in foil activity measurement reliability are necessary and, as this round robin study shows, are possible.

SECTION VII
CONCLUSIONS

The analytical and experimental results presented in this report have provided an indication of the degree to which the SAND II multiple foil iterative method may be useful in achieving the immediate and long-range objectives of this work, as stated in Section II-A. The experimental tests have been particularly valuable, because they have involved different laboratories and have

helped to establish a true measure of the current state-of-the-art. The results of these tests, when viewed as a uniform body of information, strongly support the anticipated accuracy of the multiple foil iterative method. The method can be expected to give integral neutron flux results over the energy range from 10^{-10} to 18 Mev that are accurate to within 10 to 30% at all energies, and is rather uniquely suited for the determination of total absolute integral flux. Differential flux spectra are also obtained which reflect true structure as well as fluctuations resulting from errors in foil reaction cross sections and activities. The method is such that the use of a large number of foils with overlapping energy regions of sensitivity, and subsequent examination of the solution differential spectral structure, can be used to help distinguish the true structure from that which may be caused by cross section, activity, and foil self absorption/scattering errors.

For some tests, the foil activation results have been compared with time-of-flight spectrometer measurements and Monte Carlo calculations, while for others the comparison has been with reactor physics calculations, using diffusion and transport theory. These comparisons indicate that the multiple foil integral flux results are in good agreement with the time-of-flight measurements and Monte Carlo calculations at most energy points, and that some of the disagreement that does exist can be attributed to positioning and/or neutron absorption and scattering effects. In general, the agreement with reactor physics calculations is not as good, except for those cases in which the "real" environment can be represented by an appropriate mathematical model. It is concluded that these studies have yielded quite credible integral flux results, which have increased confidence in (1) the accuracy of current cross section evaluations and (2) the ability of the iterative method to be used to determine the reliability of theoretical predictions.

The addition of gold as the third cover material in the SAND II code has permitted a partial study of the effectiveness of using self-sandwiched resonance detectors, by allowing calculations involving self-sandwiched gold. Results indicate that this stratagem is quite practicable; the effect is to alter the response of the resonance detectors so that their behavior is more nearly like that of integrating threshold detectors. The self-sandwiching technique is limited, however, by the approximations made in calculating attenuation by the sandwich

material; the degree to which these approximations are acceptable depends strongly on the geometry of a particular case. Careful study must be made of the characteristics of the materials used as resonance detectors in the particular environment in which they are used.

The authors have concluded from results of analyzing spectra that, in addition to providing experimental measurement of neutron flux spectra, the iterative method employed affords a procedure for experimental evaluation of foil reaction differential cross section data. Studies are reported in which the authors used the code to re-evaluate the differential cross section data for the $Fe^{54}(n, p)Mn^{54}$ reaction. (Because of its long product half-life, this reaction is often used for long-term irradiations to measure fluence [time-integrated neutron exposure] and is, therefore, of considerable theoretical as well as practical interest.) It is not suggested that the re-evaluation is correct in either absolute magnitude or differential form; it is, after all, without detailed structure, and somewhat arbitrarily drawn in several energy regions. This evaluation is offered as the best currently available, only in the sense that it seems to produce the most nearly self-consistent results in the tests to which it has been applied.

Because of the presence of structural materials in a neutron environment, flux depressions can exist which affect such reactions as $Fe^{56}(n, p)Mn^{56}$, $Fe^{54}(n, p)Mn^{54}$, and $Ni^{58}(n, p)Co^{58}$; results reported here indicate that current differential cross section evaluations for these and other reactions are not sufficiently detailed to allow the SAND II code to "unfold" these depressions properly, and require more detailed study.

REFERENCES

1. McElroy, W. N., Generalized Foil Activation Method of Determining Neutron Flux-Spectra for Radiation Effects Studies, (Thesis), IITRI-A947-3, IIT Research Institute, January 1965.

2. McElroy, W. N., Barrall, R. C., and Ewing, D., An Advanced Foil Activation Method of Determining Neutron Flux Spectra for Radiation Effects Studies, AFWL-TR-65-34, Vol. I, Air Force Weapons Laboratory, August 1965.

3. McElroy, W. N., Berg, S., and Gigas, G., "Neutron-Flux Spectral Determination by Foil Activation," Nuclear Science and Engr., Vol. 27, 533-541, March 1967.

4. Greer, C. and Walker, J., "A Procedure for the Computation of Neutron Flux from Foil Activation Data - SPECTRA Code," Proceedings of the International Conference on Radiation Measurements in Nuclear Power, Paper No. 24, Session 5, 12-16 September 1966.

5. American Society for Testing and Materials, Tentative Methods of Test: Measuring Neutron Flux by Radioactivation Techniques (E261); Measuring Thermal Neutron Flux by Radioactivation Techniques (E262); Measuring Fast-Neutron Flux by Radioactivation of Sulfur (E265); Measuring Fast-Neutron Flux by Radioactivation of Nickel (E264); Measuring Fast-Neutron Flux by Radioactivation of Iron (E263); Measuring Fast-Neutron Flux by Radioactivation of Aluminum (E266).

6. Zijp, W. L., Review of Activation Methods for the Determination of Fast Neutron Spectra, RCN-37, Reactor Centrum Nederland, May 1965.

7. Zijp, W. L., Review of Activation Methods for the Determination of Intermediate Neutron Spectra, RCN-40, Reactor Centrum Nederland, October 1965.

8. Gold, R., "Limitations in the Orthonormal Expansion of Neutron Spectra with Activation Measurements," Nuclear Science and Engr., Vol. 20, 493, December 1964.

9. Gold, R., An Iterative Unfolding Method for Response Matrices, ANL-6984, Argonne National Laboratory, December 1964.

10. Grundl, J. A., Study of Fission Neutron Spectra with High Energy Activation Detectors, LAMS-2883, Los Alamos Scientific Lab., May 1963.

11. DiCola, G., and Rota, A., "Calculation of Differential Fast-Neutron Spectra from Threshold-Foil Activation Data by Least-Squares Series Expansion Methods, Nuclear Science and Engr., Vol. 23, 344, 1965.

12. Boldeman, J. W., "Fission Spectrum Averaged Cross Sections of Threshold Reactions," Journal of Nuclear Energy, Parts A/B, Vol. 18, 417, 1964.

13. Biggers, W. A., Private communications, Los Alamos Scientific Laboratory, 1966-1967.

14. Biggers, W. A. and Mehl, C., Private communications, Los Alamos Scientific Laboratory and Sandia Corporation, 1966-1967.

15. Profio, A. E., et al, Fast Neutron Spectrum of the AFRRI TRIGA Reactor, GA6465, June 1965.

16. Fulmer, R. H., and Ruane, T. F., "A Technique to Determine Slow Neutron Spectra from Foil Activation," Nuclear Applications, Vol. 3, 191, March 1967.

17. Barrall, R. C., and McElroy, W. N., Experimental and Evaluated Cross Section Library of Selected Reactions, AFWL-TR-65-34, Vol. II, August 1965.

18. Armani, R., Private communications, Argonne National Laboratory, 1966-1967.

19. Tochilin, E., Private communications, U. S. Naval Radiological Defense Laboratory, 1966-1967.

20. Walker, J., and Morrison, L., Private communications, Sandia Corporation, 1965-1967.

21. Dahl, R. and Zimmer, W., Private communications, Battelle Northwest and Iso-Chem Corporation, 1965-1967.

22. Barrall, R., Private communications, Stanford University and IIT Research Institute, 1964-1967.

23. Bingham, C. D., Private communications, ASTM E-10, Sub-Committee V, Neutron Dosimetry Task Group, 1966.

24. Yoshikawa, H. H., and Zimmer, W. H., Fast-Neutron Dosimetry: Inter-Calibration of Counting Facilities, HW-81871, Hanford Laboratories, April 1964.

25. Mountford, L. A. and Morewitz, H. A., "The Advanced Epithermal Thorium Reactor (AETR) Critical Experiments," Nuclear Science and Engr. Vol. 21, 421-428, 1965.

26. NARF Facilities Handbook, FZK-185, March 1964.

27. Krumbein, A. D. and O'Reilly, B. D., Engineering Compendium on Radiation Shielding, Section 5.23, p. 81-88, to be published.

28. Siik, M. G., The Determination of the Fast-Neutron Spectrum in Thermal Reactors by Using Lithium-6 and Helium-3 Semiconductor Spectrometers, AERE-R-5183, September 1966.

29. Courtney, J. C., Fast-Neutron Scattering from Small Cylinders of Steel, Aluminum, and Graphite, ORNL-TM-1156, July 1965.

30. Tuttle, R., Private communications, Atomics International, 1966-1967.

31. Otter, J. and Beller, L., Private communications, Atomics International, 1966.

32. Dahl, R. and Ulseth, J., Private communications, Battelle Northwest, 1966-1967.

33. McElroy, W. N., Barrall, R. C. and Smiley, D., Tory II-C Flux Spectral Measurements Using an Advanced Foil Activation Method, AFWL-TR-65-34, Vol. IV, August 1965.

34. Tuttle, R. J., A Summary of the Calculated Characteristics of the Epithermal Critical Assemblies 1 through 13, NAA-SR-TDR-11799, January 1966.

35. Davey, W. G. and Amundson, P. I., "Inelastic Scattering Measurements in a Fast Reactor by the Spherical Shell Method," Nuclear Science and Engr. Vol. 28, 111-123, 1967.

36. McElroy, W. N., et al, "Investigation of the Accuracy of $Fe^{54}(n, p)Mn^{54}$ Evaluated Differential Cross Section Data by a Multiple Foil Activation Method," to be published.

37. Beauge, R., Sections Efficaces Pour Les Detecteurs De Neutrons Par Activation, Recommandees Par Le Groupe De Dosimetrie D'Euratom, Euratom Report DEP/SEPP-148, 1963.

38. Liskien, H. and Paulsen, A., Compilation of Cross Sections for Some Neutron Induced Threshold Reactions, EUR 119.e, Presses Academiques Europeennes, Brussels, 1963.

39. Barrall, R. C. and McElroy, W. N., "Nuclear Reactions for Determining Neutron Spectrum and Dose: A World Literature Search," Symposium on Personnel Dosimetry for Radiation Accidents, International Atomic Energy Agency, Vienna, March 1965.

40. Parker, K., A Review of Evaluations of Neutron Cross Sections Available at November 1964, British Report AWREO-13/65, March 1965.

41. Dierckx, R., Private communication to J. Comera, Maximum Error in Threshold Reaction Cross Section Measurements, with a View to Their Use in Fast Neutron Spectrum Measurements, EANDC (E) 51 "L", European American Nuclear Data Committee, June 1964.

DISTRIBUTION

No. cys

HEADQUARTERS USAF

Hq USAF, Wash, DC 20330

1 (AFRDQ)
1 (AFTAC/TD-3, Capt Herman)
1 (AFMSG, Biomedical Science Branch)
1 (AFRSTG, Maj Brunson)
1 (AFRDP-F)
1 USAF Dep, The Inspector General (AFIDI), Norton AFB, Calif 92409
1 USAF Directorate of Nuclear Safety (AFINS), Kirtland AFB, NM 87117

MAJOR AIR COMMANDS

AFSC, Andrews AFB, Wash, DC 20331

1 (SCOP)
1 (SCOTR)
1 (SCTSW)
1 (SCTL)
1 (SCTT)
1 (SCTS)
1 ATC (S-W), Randolph AFB, Tex 78148
1 AUL, Maxwell AFB, Ala 36112

USAFIT, Wright-Patterson AFB, Ohio 45433

1 (Library)
1 (Capt R. Murfitt, NETF)
1 (A. Fasano, NETF)
2 (Capt Jerry McKenzie, NETF)
1 USAFA (DFLBA), Colo 80840

AFSC ORGANIZATIONS

1 AFSC STLO, R&T Div, AFUPO, Los Angeles, Calif 90045
1 FTD (TDBTL), Wright-Patterson AFB, Ohio 45433
1 AF Materials Laboratory, Wright-Patterson AFB, Ohio 45433
1 AF Avionics Laboratory, Wright-Patterson AFB, Ohio 45433
1 AF Flight Dynamics Laboratory, Wright-Patterson AFB, Ohio 45433
1 AF Aero-Propulsion Laboratory, Wright-Patterson AFB, Ohio 45433
1 ASD (ASAPR), Wright-Patterson AFB, Ohio 45433
1 ORA (RRRD), Holloman AFB, NM 88330

UNCLASSIFIED

Security Classification

DOCUMENT CONTROL DATA - R&D

(Security classification of title, body of abstract and indexing annotation must be entered when the overall report is classified)

1. ORIGINATING ACTIVITY (Corporate author)

Atomics International, A Division of North American Aviation, Inc.
Canoga Park, California 91304

2a. REPORT SECURITY CLASSIFICATION: UNCLASSIFIED

2b. GROUP:

3. REPORT TITLE

A COMPUTER-AUTOMATED ITERATIVE METHOD FOR NEUTRON FLUX SPECTRA DETERMINATION BY FOIL ACTIVATION, Vol I, A Study of the Iterative Method

4. DESCRIPTIVE NOTES *(Type of report and inclusive dates)*

April 1966-July 1967

5. AUTHOR(S) *(Last name, first name, initial)*

McElroy, W. N.; Berg, S.; Crockett, T.; Hawkins, R. G., Lt, USAF

6. REPORT DATE	7a. TOTAL NO. OF PAGES	7b. NO. OF REFS
September 1967	122	41

8a. CONTRACT OR GRANT NO. AF 29(601)-7196 and AF 29(601)-6780	9a. ORIGINATOR'S REPORT NUMBER(S)
b. PROJECT NO. 1831 and 5710	AFWL-TR-67-41, Vol I
c. Task No. 183108 Subtask No. 06.514	9b. OTHER REPORT NO(S) *(Any other numbers that may be assigned this report)* Contractor's report No. AI-67-90, Volume I
d.	

10. AVAILABILITY/LIMITATION NOTICES This document is subject to special export controls and each transmittal to foreign governments or foreign nationals may be made only with prior approval of AFWL (WLDN), Kirtland AFB, NM, 87117. Distribution is limited because of the technology discussed in the report.

11. SUPPLEMENTARY NOTES	12. SPONSORING MILITARY ACTIVITY
	AFWL (WLDN) Kirtland AFB, NM 87117

13. ABSTRACT (Distribution Limitation Statement No. 2)

A multiple foil activation iterative method has been developed to determine neutron flux spectra. A computer code (SAND II) has been written which provides a "best fit" neutron differential flux spectrum for a given input set of infinitely dilute foil activities. The results of experimental and analytical studies for a wide variety of neutron environments strongly suggest that, in addition to determining neutron flux spectra, the multiple foil activation iterative method can be helpful in (1) the validation and improvement of calculational techniques used to predict neutron flux spectra, (2) upgrading of confidence in neutron spectrometer measurements, (3) determining the reliability of foil activity measurementsmethods, (4) assessing material scattering/absorption effects, and (5) examining current foil detector cross section evaluations to provide guidance for re-evaluation for these data, and eventual "unfolding" of the absolute differential form of cross sections for any foil reactions producing a detectable product.

DD FORM 1 JAN 64 1473

UNCLASSIFIED

Security Classification

14. KEY WORDS	LINK A		LINK B		LINK C	
	ROLE	WT	ROLE	WT	ROLE	WT
Neutron flux spectral measurements Foil activation Neutron activation cross sections Activation data reduction code						

INSTRUCTIONS

1. ORIGINATING ACTIVITY: Enter the name and address of the contractor, subcontractor, grantee, Department of Defense activity or other organization *(corporate author)* issuing the report.

2a. REPORT SECURITY CLASSIFICATION: Enter the overall security classification of the report. Indicate whether "Restricted Data" is included. Marking is to be in accordance with appropriate security regulations.

2b. GROUP: Automatic downgrading is specified in DoD Directive 5200.10 and Armed Forces Industrial Manual. Enter the group number. Also, when applicable, show that optional markings have been used for Group 3 and Group 4 as authorized.

3. REPORT TITLE: Enter the complete report title in all capital letters. Titles in all cases should be unclassified. If a meaningful title cannot be selected without classification, show title classification in all capitals in parenthesis immediately following the title.

4. DESCRIPTIVE NOTES: If appropriate, enter the type of report, e.g., interim, progress, summary, annual, or final. Give the inclusive dates when a specific reporting period is covered.

5. AUTHOR(S): Enter the name(s) of author(s) as shown on or in the report. Enter last name, first name, middle initial. If military, show rank and branch of service. The name of the principal author is an absolute minimum requirement.

6. REPORT DATE: Enter the date of the report as day, month, year; or month, year. If more than one date appears on the report, use date of publication.

7a. TOTAL NUMBER OF PAGES: The total page count should follow normal pagination procedures, i.e., enter the number of pages containing information.

7b. NUMBER OF REFERENCES: Enter the total number of references cited in the report.

8a. CONTRACT OR GRANT NUMBER: If appropriate, enter the applicable number of the contract or grant under which the report was written.

8b, 8c, & 8d. PROJECT NUMBER: Enter the appropriate military department identification, such as project number, subproject number, system numbers, task number, etc.

9a. ORIGINATOR'S REPORT NUMBER(S): Enter the official report number by which the document will be identified and controlled by the originating activity. This number must be unique to this report.

9b. OTHER REPORT NUMBER(S): If the report has been assigned any other report numbers *(either by the originator or by the sponsor)*, also enter this number(s).

10. AVAILABILITY/LIMITATION NOTICES: Enter any limitations on further dissemination of the report, other than those imposed by security classification, using standard statements such as:

(1) "Qualified requesters may obtain copies of this report from DDC."

(2) "Foreign announcement and dissemination of this report by DDC is not authorized."

(3) "U. S. Government agencies may obtain copies of this report directly from DDC. Other qualified DDC users shall request through _____."

(4) "U. S. military agencies may obtain copies of this report directly from DDC. Other qualified users shall request through _____."

(5) "All distribution of this report is controlled. Qualified DDC users shall request through _____."

If the report has been furnished to the Office of Technical Services, Department of Commerce, for sale to the public, indicate this fact and enter the price, if known.

11. SUPPLEMENTARY NOTES: Use for additional explanatory notes.

12. SPONSORING MILITARY ACTIVITY: Enter the name of the departmental project office or laboratory sponsoring *(paying for)* the research and development. Include address.

13. ABSTRACT: Enter an abstract giving a brief and factual summary of the document indicative of the report, even though it may also appear elsewhere in the body of the technical report. If additional space is required, a continuation sheet shall be attached.

It is highly desirable that the abstract of classified reports be unclassified. Each paragraph of the abstract shall end with an indication of the military security classification of the information in the paragraph, represented as *(TS)*, *(S)*, *(C)*, or *(U)*.

There is no limitation on the length of the abstract. However, the suggested length is from 150 to 225 words.

14. KEY WORDS: Key words are technically meaningful terms or short phrases that characterize a report and may be used as index entries for cataloging the report. Key words must be selected so that no security classification is required. Identifiers, such as equipment model designation, trade name, military project code name, geographic location, may be used as key words but will be followed by an indication of technical context. The assignment of links, rules, and weights is optional.

SUPPLEMENTARY

INFORMATION

IDENTIFICATION	FORMER STATEMENT	NEW STATEMENT	AUTHORITY
AD-820 556 Atomics International, Canoga Park, Calif. Technical rept. Apr 66-Jul 67. Rept. no. AI-67-90-Vol-1, AFWL-TR-67-41-Vol-1 Sep 67 Contract AF 29(601)-7198	No Foreign without approval of Air Force Weapons Lab., Attn: WLDN, Kirtland AFB, N. Mex.	No limitation	AFWL notice, 23 Oct 69